University of Stavanger

Faculty of Science and Technology

MASTER'S THESIS

Study program/ Specialization: Engineering Structures and Materials - Civil engineering structures	Spring semester, 2018 Open / ~~Restricted access~~
Writer: Thomas Ødegaard	…… (Writer's signature)
Faculty supervisor: Samindi Samarakoon External supervisor(s): Jan Fredrik Rambech	
Title of thesis: Seismic performance assessment of reinforced concrete structures: a case study of Kanti Children's Hospital, Kathmandu, Nepal	
Credits (ECTS): 30	
Key words: Performance based seismic design Eurocode 8 IS-1893 Time-history analysis Pushover analysis	Pages: 120 + enclosure: 43 Stavanger, 15-6-2018 Date/year

ABSTRACT

Structures should be ensured good structural performance in the event of high magnitude earthquakes. This thesis is built around a case study of Kanti Children's Hospital, Kathmandu, Nepal where there is a history of high magnitude earthquakes. A seismic performance assessment was performed for the structural system of Kanti Children's Hospital as a measure of quality assurance.

The theory chapter of thesis will provide the underlying theory for seismic hazards, structural modelling and analysis, and seismic code applications.

For the structural analyses of the case study, a combination of linear (lateral force, response spectrum and modal time-history) and nonlinear (pushover and direct integration time history) analyses were performed.

While the structural design of the case study complies with the Indian seismic code (IS1893), with a few limitations, the difference is seismic demand compared to the European seismic code (EC8) is substantial. The structure is not expected to comply with the criteria of Eurocode 8.

The performance assessment was conducted after a *performance based seismic design* approach, with acceptance criteria from FEMA 356 and ASCE 41-13. The structure was subjected to seismic loading equivalent of earthquakes with 50%-, 10%- and 2% probability of occurrence in 50 years. The following results were obtained:

	Operational (O)	Immediate Occupancy (IO)	Life Safety (LS)	Near Collapse (NC)
50% / 50 years				
10% / 50 years				
2% / 50 years				

The stairway tower is considered to be the weak-point of the structure. To increase the performance the focus should be put into reducing the overall torsional irregularity and strengthening the stairway.

ACKNOWLEDGEMENTS

"There is no such thing as a 'self-made man. We are made up of thousands of others. Everyone who has ever done a kind deed for us, or spoken one word of encouragement to us, has entered into the make-up of our character and of our thoughts, as well as our success."
- George Matthew Adams

First and foremost, I would like to thank Anne Asselin at Engineers Without Borders for providing the subject of the thesis, coordinating the supervision, and for making the field in Nepal visit a possibility. For the technical part of thesis, I would like to thank my school supervisor, Samindi Samrakoon, and my supervisor at Norconsult, Jan Fredrik Rambech. Lastly, my wife Enya deserves a huge thanks for coping with through all of my studies.

NOMENCLATURE

Latin letters

Chapter 2

$\boldsymbol{M_W}$	**Moment magnitude**
$\boldsymbol{M_s}$	Surface wave magnitude
P-Δ	Second order effect

Chapter 3

M	Mass matrix
C	Damping matrix
K	Stiffness matrix
$\boldsymbol{u}$	Displacement
$\dot{\boldsymbol{u}}$	Velocity
$\ddot{\boldsymbol{u}}$	Acceleration
$\boldsymbol{\omega}$	Mode of vibration
$\boldsymbol{\zeta}$	Damping ratio
$\boldsymbol{e_0}$	Accidental eccentricity
r	Torsional radius
l_s	Radius of gyration
$\boldsymbol{\Omega}$	Diagonal matrix of eigenvectors
$\boldsymbol{\Phi}$	Mode-shape

Chapter 4

I	Importance factor (EC8 and IS1893)
q	Behavior factor (EC8)
R	Behvaior factor (IS1893)
$\boldsymbol{\alpha_u/\alpha_1}$	Overstrength factor (EC8)
$\boldsymbol{T}$	Period of vibration

Abbreviations

OMRF	Ordinary Moment Resisting Frame (IS1893)
SMRF	Special Moment Resisting Frame (IS1893)
PGA	Peak ground acceleration
EC8	Eurocode 8
FEMA	Federal Emergency Management Agency
ASCE	American Society of Civil Engineers
PSHA	Probabilistic Seismic Hazard Analysis
DSHA	Deterministic Seismic Hazard Analysis
NL	Nonlinear
L	Linear
SDOF	Single degree of freedom
MDOF	Multiple degree of freedom
HHT	Hilber-Hughes-Taylor
FEM	Finite Element Method
SPT	Standard Penetration Test (Geotechnical)
SSI	Soil-Structure-Interaction
DCH – DCM – DCL	Ductility Class High – Medium – Low
SRSS	Square Root of sum of squares
CQC	Complete Quadradic Combination
FNA	Fast Nonlinear Analysis (Nonlinear Modal Time-History)
Mumty	Stairway-tower

CONTENTS

LIST OF FIGURES

LIST OF TABLES

1 INTRODUCTION

1.1 Background

The Norwegian non-profit organization FORUT is sponsoring an extension of Kanti Children's Hospital in Kathmandu, Nepal as shown in Figure 1-1. The building consists of four floors, with a total height of 18.2 meters. Detailed drawings are found in Appendix A.

Through Engineers Without Borders (EWB), Norconsult has been involved to perform quality assurance of the structural system. Furthermore, EWB provided the opportunity to have a master thesis with a case study of Kanti Children's Hospital, as an extended quality assurance.

The work in this thesis is thereby a collaboration between EWB, Norconsult, and FORUT, with the aim of providing quality assurance of the structural performance for the structural system with regards to seismic loading.

Figure 1-1 - Kanti Children's Hospital - Ref. Team Consultants

1.2 Problem formulation

Is the structural design complying with the Indian Standard for seismic design (IS 1893), and how does this compare to a seismic analysis after Eurocode 8? Regardless of code, what is the structural performance be, e.g. is it possible to maintain operationality in the event of significant earthquakes?

This thesis will provide insight to the process of seismic performance assessment of concrete structures. With every step of the assessment, the underlying theory found relevant for structural engineers to preform similar assessments is presented. It will also compare the different methods given in standards to assess seismic performance.

1.3 Limitations

The theory of this thesis is limited to theory relevant for concrete structures. The reader is expected to have basic knowledge of structural dynamics.

For the case study, the performance assessment is limited to displacement-based analyses approaches. Individual structural members are therefore not evaluated, only the global structural performance.

1.4 Structure of the report

Chapter 2 – Seismic Hazard:
This chapter provides an overview of definitions relating to seismic hazards.

Chapter 3 – Structural modelling and analysis:
This chapter highlights the underlying theory of computational structural analysis, from modelling to analysis

Chapter 4 – Code application
This chapter provides an overview the seismic codes relevant for case study. This includes Eurocode 8, IS1839 (Indian code of seismic design), NBC105 (Nepali code of seismic design), and highlight subjects of *Performance Based Seismic Design* with a basis in ASCE 41-13 and FEMA 356.

Chapter 5 – Case specific structural analysis
This chapter presents the seismic analysis and results for the case study, with a focus on overall structural performance. This includes analysis for Eurocode 8, IS1893, and structural performance assessment with basis in ASCE 41-13 and FEMA 356.

Chapter 6 – Discussion
In this chapter the assumptions and uncertainties of the case study is highlighted, the differences in seismic codes is evaluated, and the verdict of the seismic performance assessment of case study discussed.

Chapter 7 – Conclusion
This chapter provides conclusions regarding code application of the case study, presents the final results of the structural performance assessment, provides recommendations to improve seismic performance of the case study, and suggests some measures to ensure good seismic performance in future projects.

2 SEISMIC HAZARD

This chapter aims to give a theoretical background for seismic hazards, and its application to structural analysis and seismic design codes. It is in large parts based on theory from the book *Basic Earthquake Engineering* [1].

2.1 Earthquakes

Earthquakes occur when energy stored in the earth's crust is suddenly released. The main source of earthquakes of significance originates from tectonic plate movement.

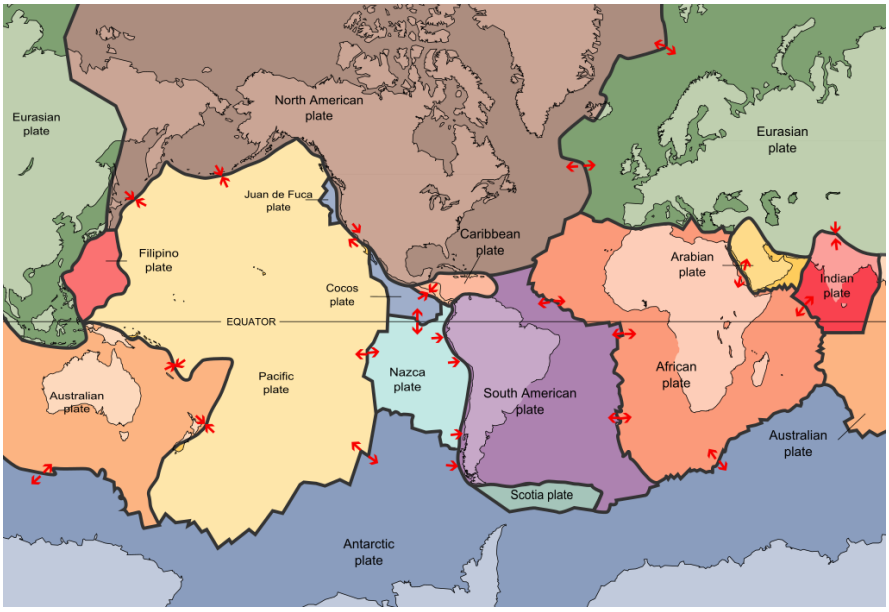

Figure 1 - Tectonic plate theory (From USGS [2])

Energy builds up in the earth's crust as the tectonic plates converge, diverge, or transform, and when the stresses of plate movement exceed the strength of the rocks of the earth, earthquakes occur. These areas of plate collision are referred to as faults.

2.2 Faults

There are three main types of faults; normal-, reverse-, and strike-slip fault. Normal faults occur in areas where the tectonic plates are moving apart, reverse faults occur when the tectonic plates converge, and strike-slip faults occur when the tectonic plates shear.

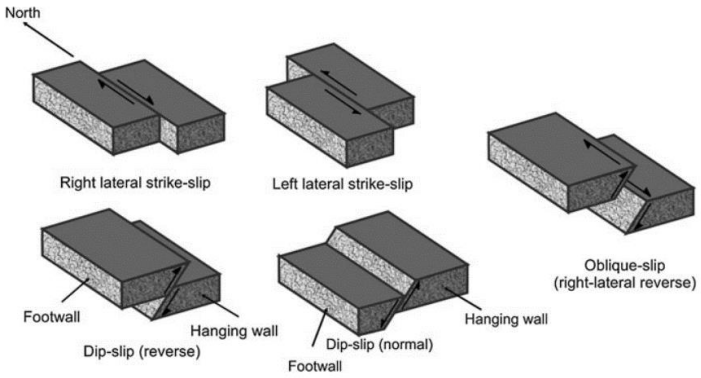

Figure 2-1 - Fault mechanisms (From *Basic Earthquake Engineering* [1])

Earthquakes are triggered by sudden raptures of these faults and are affected by combination fault mechanisms. For practical reasons, the earthquakes are classified by the main contributing fault mechanism. As the characteristics of the earthquake depend on the contributing fault mechanism, this is considered in the selection of ground motions for use in time-history analysis.

2.2.1 Seismic waves

When faults rupture, seismic waves are discharged. These seismic waves have been classified into four types:

Table 2-1 - Characteristics of seismic waves

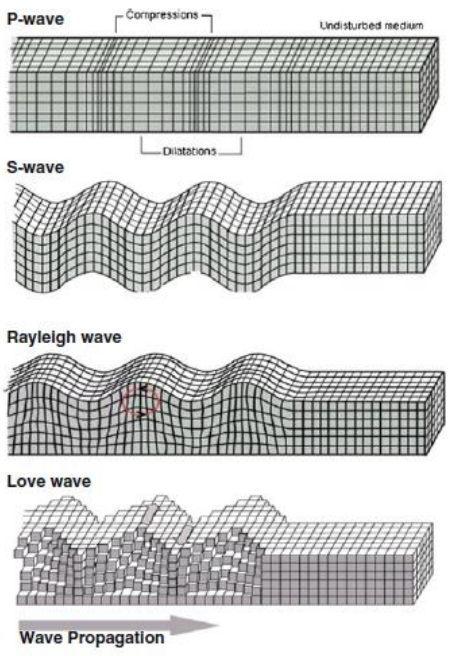	**Ground waves**	**Pressure waves (P-waves)** Approximately moving $\sqrt{3}$ times than surface waves. Arrives first, but usually yield a comparatively small contribution to the overall ground motion. Moves with compression and dilatations. Can travel through solids, water and gass.
		Shear waves (S-waves) Moderate speed, arrives secondly. Moves with a shearing body motion. Comparative contribution to overall ground motion depends on focal distance. Can only travel through solids
	Surface waves	**Surface waves:** Surface waves move the slowest and arrives last. Travels long distances, making the comparative contribution to ground motions large for sites with long focal distance. **Rayleigh wave** Movement similar to water-waves, which induces vertical effect on structures. **Love waves** Movement in the horizontal directions, which contributes largely to the horizontal effect on structures.

Figure 2-2 - Seismic waves (From Basic Earthquake Engineering **[1]**)

The properties defined for the different wave classifications are exemplified in the following figure:

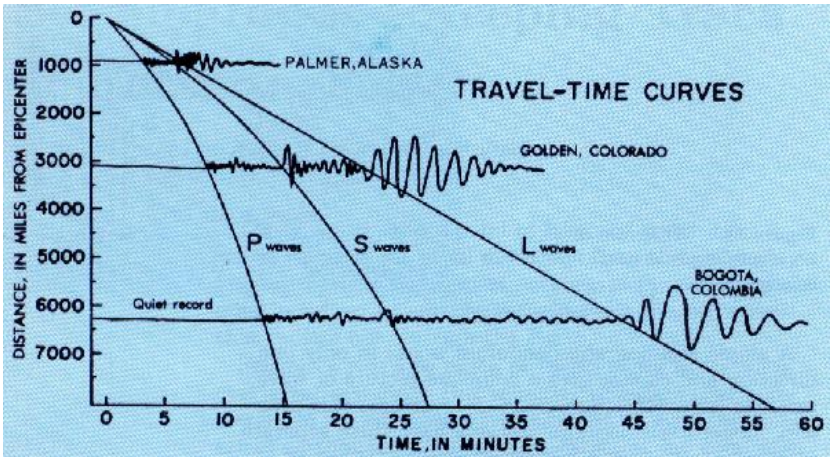

Figure 2-3 - Seismic waves - speed and magnitude correlation (From USGS [3])

2.3 Classification of earthquakes

With the focus of this thesis being on seismic design after Indian and European seismic design codes, the classification relevant for these codes are discussed in this chapter.

The Eurocode is based on the moment- and surface wave magnitude scale, while the Indian standard is based on the MSK-64 scale.

2.3.1 Moment- and surface wave magnitude

The moment- and surface wave magnitude scales are modifications to the Richter's magnitude scale. All are calculated from the energy dissipated during an earthquake, with measurements from seismographs.

Moment magnitude, denoted $M_{w,}$ is calculated from the seismic moment M_o. The seismic moment is further a function of fault rapture area and average slip between the moving blocks. Moment magnitude is then defined:

$$M_W = \frac{2}{3} log_{10}(M_0) - 6 \tag{2.1}$$

There have been developed many formulations for calculating the surface wave-magnitude. A commonly used formulation by Vanêk (1962 [4]) depend on amplitude of the surface waves (A), the dominant period of vibration (T) and the distance from epicenter (Δ).

$$M_s = log_{10}\left(\frac{A}{T}\right)_{max} + 1.66\, log_{10}\,\Delta + 3.33 \tag{2.2}$$

2.3.2 MSK-64

The MSK-64 (Medvedev-Sponheuer-Karnik) scale is an intensity scale defined by the observed effects near the epicenter of an earthquake. It is very similar to the MMI (Modified Mercalli Intensit) scale.

Table 2-2 - Comparison of MSK-64 and MMI classification

	MSK-64 [5]	**MMI [6]**
I	Not noticable	Not fealt
II	Scarcely noticable	Weak
III	Weak, partially observed	Weak
IV	Largly observed	Light
V	Awakeniing	Moderate
VI	Frighenin|g	Strong
VII	Damage of buildings	Very strong
VIII	Destruction of buildings	Severe
IX	General damage of buildings	Violent
X	General destruction of buildings	Extreme
XI	Destruction	Extreme
XII	Landscape changes	Extreme

As the MSK-64- and moment magnitude scales are based on different earthquake characteristics, no accurate comparison can be made between the two. With this mentioned, USGS has made a typical observed correlation of intensities and magnitudes:

Tabell 1 - Magnitude & Intensity comparison (From USGS [6])

Magnitude (Richter)	**Intensity (MMI)**
1.0 – 3.0	I
3.0 – 3.9	II – III
4.0 – 4.9	IV – V
5.0 – 5.9	VI – VII
6.0 – 6.9	VII – IX
7 and higher	VIII or higher

2.4 Seismic Hazard Assessment

To determine the seismic hazard of any area, site or region, seismic hazard analysis is conducted. These are mainly divided into two categories; deterministic (DSHA) and probabilistic (PSHA).

2.4.1 Probabilistic (PSHA)

In a PSHA, all earthquake scenarios that can be generated from a seismic source is considered for the site in question. The seismic sources (faults) are characterized after the maximum moment magnitude. Seismic hazard is then normally calculated with respect to PGA with a defined probability of exceedance, e.g. PGA with 10% probability of exceedance in 50 years (475year return period).

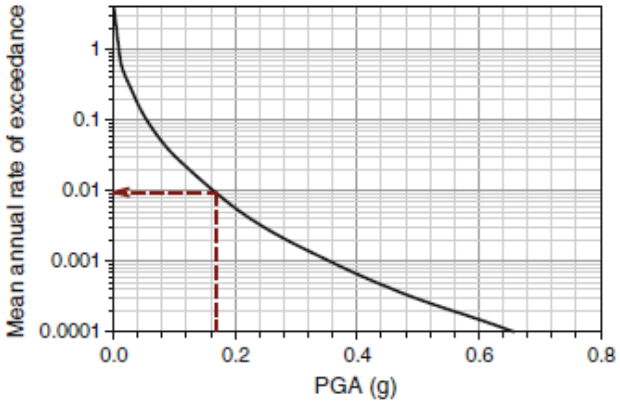

Figure 2-4 - Typical results of a PSHA (From *Basic Earthquake Engineering* [1])

2.4.2 Deterministic (DSHA)

In a DSHA, the seismic hazard is defined on the least favorable earthquake scenario for the project site. All earthquake scenarios, with characteristics as source-to-site distance and magnitude, should be evaluated. This approach will yield a more conservative representation for seismic hazard as it does not reflect likelihood of seismic activity, only the possibility.

2.5 Seismicity in Nepal

Nepal lies right on the collision boundary of the Indian- and Eurasian plate, in the Himalaya region. The Himalaya region is geologically divided into the Higher Himalaya, sub-Himalaya, lesser Himalaya, and Tethyan Himalaya. On the border of these geological divides you find the following geological structures; the Main Frontal Thrust (MFT), Main Boundary Thrust (MBT), Main Central Thrust (MCT), and South Tibet Detachment (STD). These are presented in Figure 2 - Geological map of Nepal (From

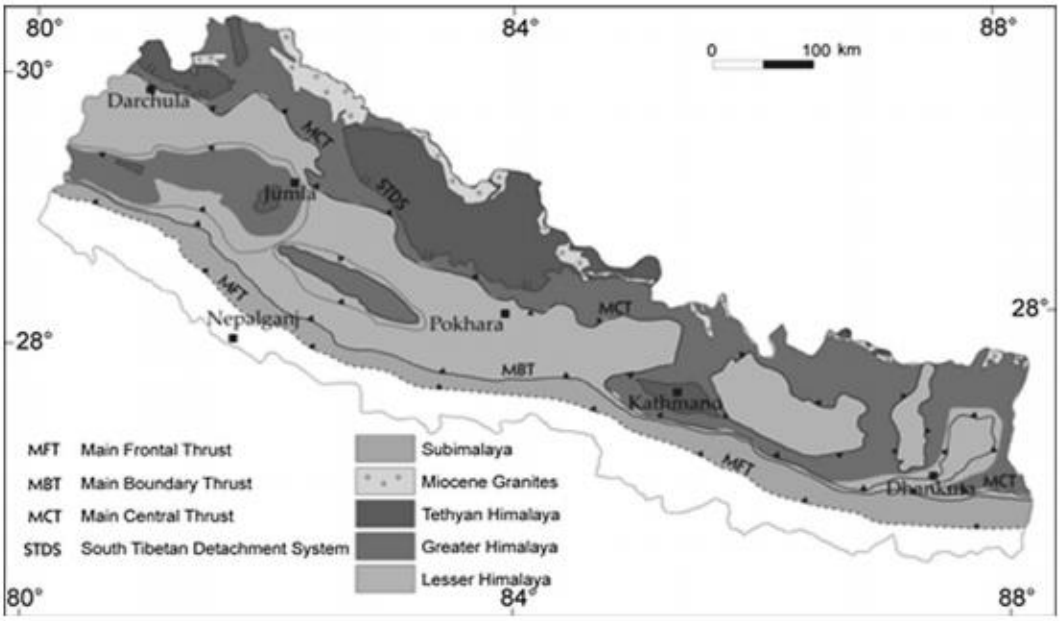

Figure 2 - Geological map of Nepal (From *Seismic risk assessment and hazard mapping in Nepal* [7])

Earthquakes form in these thrust systems, and among these the most active faults lie in the MBT and MCT. As the tectonic plates are converging, the most typical faulting mechanism of earthquakes is reverse faulting.

The region is very seismic, with a number of significant earthquakes in the last century. A list compiled of earthquakes with a magnitude of over 6.5 within the last century is presented in Table 2-3, with data from *National Center of Environmental Information (NCEI)* [8].

Table 2-3 - Earthquakes (>6.5Mw) in Nepal in the last century (From *NCEI* [8])

Year	Month	Magnitude	Intensity (MMI)	Fatalities
1916	August	7.7M_w	No data	No data
1934	January	8.0M_w	XI	10 600
1980	July	6.5M_w	No data	200
1988	August	6.6M_w	VIII	1 091
2015	April	7.8M_w	VIII	8 857
2015	May	7.8M_w	VII	117

Further, the seismic hazard for Kathmandu for use in the case study is based on the conference paper *Comparative study of seismic hazard of Kathmandu valley, Nepal with other seismic prone cities* [9]. The paper suggests the following PGA-values based on PSHA:

Table 2-4 - PGA with probabilities of exceedance for Kathmandu, Nepal [9]

Probability of exceedance in 50 years		**PGA [g]**
(PV)	50%	0.26
(DCE)	10%	0.49
(MCE	2%	0.76

The results presented in the study show a prominent correlation to other seismic prone cities, such as Los Angeles, USA and Sendai, Japan.

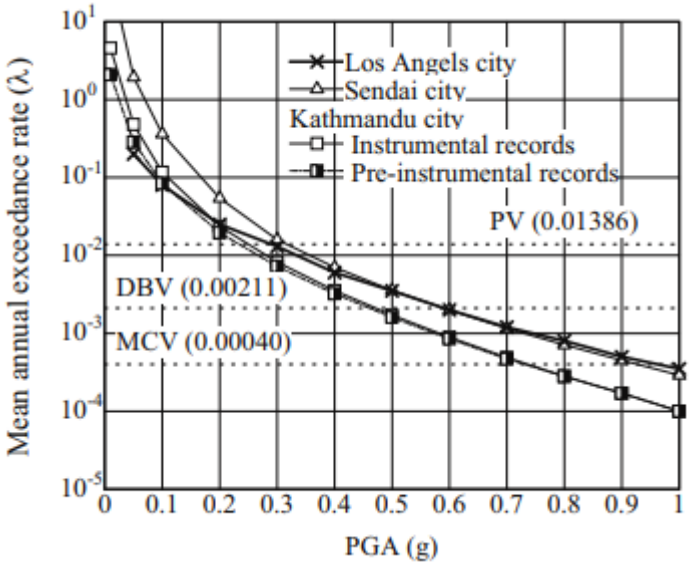

Figure 2-5 - Comparison of PGA for Kathmandu city (Sunuwar 2005 [9])

3 STRUCTURAL MODELLING AND ANALYSIS

This chapter will describe and discuss the process of modelling and analyzing concrete structures using computer software. For the case study of this thesis the structural analysis software SAP2000 was used so the theory is focused towards this software but will most likely be applicable for similar software.

3.1 Structural analysis elements

To perform a structural analysis all the structural elements needs to be idealized using elements based on mathematical models. These elements are based finite element formulation. Represented here are the elements that are necessary to model concrete structures. The theory in this chapter is obtained from the *CSI Analysis Reference Manual* [10].

3.1.1 Frame elements

The frame elements are based on 3D finite elements beam formulation.

$$[F] = \begin{bmatrix} X & 0 & 0 & 0 & 0 & 0 & -X & 0 & 0 & 0 & 0 & 0 \\ & Y_1 & 0 & 0 & 0 & Y_2 & 0 & -Y_1 & 0 & 0 & 0 & Y_2 \\ & & Z_1 & 0 & -Z_2 & 0 & 0 & 0 & -Z_1 & 0 & -Z_2 & 0 \\ & & & S & 0 & 0 & 0 & 0 & 0 & -S & 0 & 0 \\ & & & & Z_3 & 0 & 0 & 0 & Z_2 & 0 & Z_4 & 0 \\ & & & & & Y_3 & 0 & -Y_2 & 0 & 0 & 0 & Y_4 \\ & & & & & & X & 0 & 0 & 0 & 0 & 0 \\ & & & & & & & Y_1 & 0 & 0 & 0 & -Y_2 \\ & & & & & & & & Z_1 & 0 & Z_2 & 0 \\ & & & & & & & & & S & 0 & 0 \\ & & & & & & & & & & Z_3 & 0 \\ & & & & & & & & & & & Y_3 \end{bmatrix} \cdot \begin{bmatrix} u_1 \\ v_1 \\ w_1 \\ \theta_{x,1} \\ \theta_{y,1} \\ \theta_{z,1} \\ u_2 \\ v_2 \\ w_2 \\ \theta_{x,2} \\ \theta_{y,2} \\ \theta_{z,2} \end{bmatrix} \tag{3.1}$$

This means that the element can describe displacements and rotations in x-, y-, and z-axis. Using compatibility relations, bending-, axial- and torsional stresses and forces can be calculated. This element is applicable to analyze three-dimensional columns and beams and are modeled as lines, either straight or curved, between two points and can have properties that vary within its length.

3.1.2 Shell elements

The shell elements are finite element area elements that can be used to model membrane, plate and shell behaviors. In SAP2000 shell elements can either follow the four-node quadrilateral (Q4), or the triangular finite element definition.

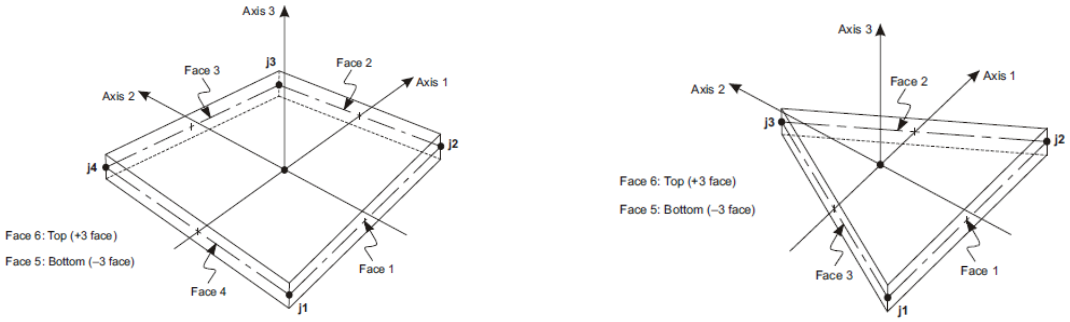

Figure 3-1 – Q4- and triangular shell elements in SAP2000 (From CSI Analysis Reference manual [10])

To gain accuracy in shell elements, meshing is applied to the shells. Again, the challenge is to find the optimal balance between computational efficiency and accuracy of the results. This was exemplified in the case study while modelling shear walls.

	No meshing				Max mesh size 800x800mm			
Mode	**Period [s]**	U_x	U_y	R_z	**Period [s]**	U_x	U_y	R_z
1	0.32	4%	27%	22%	0.43	0%	46%	23%
2	0.27	14%	27%	0%	0.33	61%	0%	4%
3	0.23	31%	6%	24%	0.30	0%	22%	30%
4	0.20	14%	0	11%	0.22	7%	0%	10%

Figure 3-2 - Comparison of meshing options effect on modal analysis

Where U_x is displacement in x-direction, U_y is displacement in y-direction and R_z is torsional rotation.

3.2 Diaphragm

The theory in chapter is obtained from the *CSI Analysis Reference Manual* [10].

The term *diaphragm* describes a structural element that transfers lateral loads to the vertical structural-system and is thereby a very important modelling tool in seismic design of buildings. In most structural systems the floors and roofs are designed to act as diaphragms, either rigid- or semi-rigid, with provisions in the code on how to classify the diaphragm.

A rigid diaphragm assumes that in-plane stiffness of a structure is infinite. This assumption is based on the notion that with sufficient in-plane stiffness, the in-plane deflection of floor is neglectable. A typical rigid diaphragm consists of a concrete floor system with large in-plane stiffness.

With semi-rigid diaphragms the in-plane stiffness is smaller comparatively to the lateral force-resisting system. The in-plane stiffness must then be calculated by the software, which makes it more computational expensive. Examples of semi-rigid diaphragm are; light-weight floors of thin concrete slabs, wood-frame floors, metal sheet roofing.

In SAP2000, diaphragm is assigned as joint constraints and can automatically be assigned for each leap in elevation. It is important to only assign these constraints to joints that are connected by the diaphragm component.

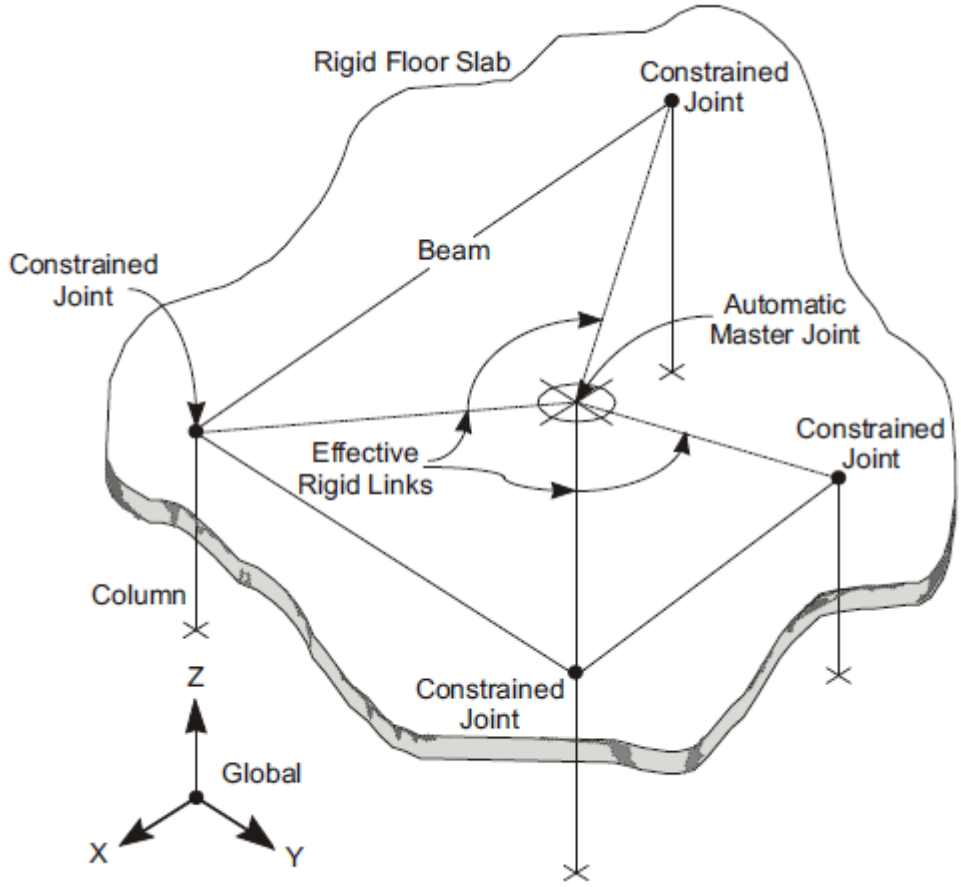

Figure 3-3 - Diaphragm behavior (From CSI Analysis Reference manual [10])

3.3 Nonlinear behavior

The nonlinear behavior of structural components is defined as the behavior of which the change of input is not proportional to the change of the output. In structural analysis this behavior is mostly considered as being related to material- or geometrical properties.

The theory in this subchapter is obtained from the *CSI Analysis Reference Manual* [10], *Theory of Nonlinear Structural Analysis: The Force Analogy Method for Earthquake Engineering* [11] and *NIST – Guidelines for Nonlinear Structural Analysis for Design of Buildings* [12] [13].

3.3.1 Geometric nonlinearity

Geometric nonlinearity occurs when the displacement-strain relation behaves nonlinearly. This results in changes to the stiffness matrix depending on the deflection of either the globally for the whole structure (Large P-Delta – P-Δ), or locally for each member (Small P-Delta – P-δ).

The two main computation methods for computing geometric nonlinearity are the P-Delta-, and the geometric stiffness approach. The main difference of the two is that the P-Delta approach neglects small P-Delta, the geometric approach includes it. This makes the P-Delta approach more computational efficient for analysis of overall structural stability, while the geometric stiffness approach is more precise and more suitable for design and verification of structural members. The latter approach is implemented in SAP2000

For nonlinear analysis in SAP2000 three options when considering geometric nonlinearity;

- P-Delta plus large displacements:
  Deformed shape is fully implemented in the equilibrium equations. The loading is applied stepwise, and for each step the stiffness matrix is recalculated.
- P-Delta:
  Deformed shape is partially implemented in the equilibrium equations.
  The initial stiffness matrix is modified depending the initial deformation, making the P-Delta procedure a one-step procedure.
- Not considered:
  Undeformed configuration of structure and initial stiffness matrix is used in analysis

According to the reference manual, the P-Delta option is recommended for most cases of nonlinear analysis, as the displacement range of geometric nonlinearity covered by this approach usually is well within the limit of acceptable material nonlinearity.

3.3.2 Material nonlinearity

There are several ways to analyze the non-linear behavior of concrete frames in the state of the art software. The balance between computational efficiency and precision is an important measure to consider, and so there have been developed several idealizations analysis models depending on where the balance is put.

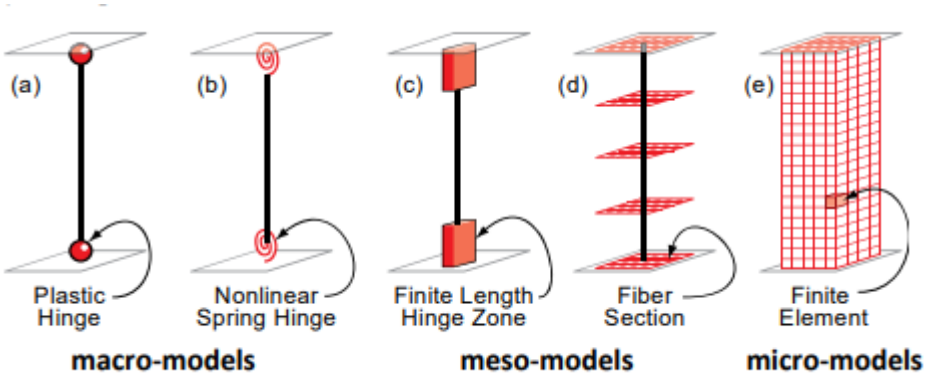

Figure 3-4 - Section material nonlinearity models (From *Guidelines for Nonlinear Structural Analysis for Design of Buildings* [12])

In the case study of this thesis, there were used both concentrated plastic hinge and fiber hinges, depending on the type of non-linear analysis performed. These are further discussed:

3.3.2.1 Concentrated plastic hinge

When using concentrated plastic hinges, the nonlinear behavior is idealized to appear in zero-length rotational springs. These hinges should be assigned to the points of the members most likely to experience plastic deformation.

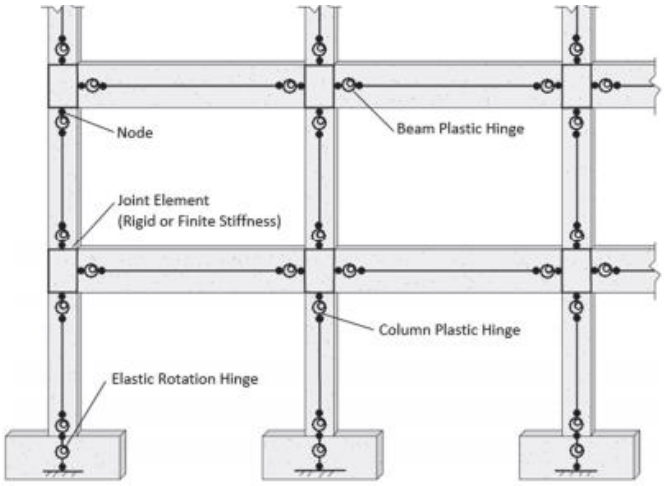

Figure 3-5 - Concentrated plastic hinges (From *Guidelines for Nonlinear Structural Analysis for Design of Buildings* [12])

The hinge-properties are most commonly defined as either M3 or P-M2-M3. M3-hinges are used for elements for which plastic mechanism is mainly contributed by the bending moment along the dominant axis, and so is typically used for beams in which axial force and sideways bending moment can be neglected. P-M2-M3 are used for elements for which the plastic mechanism is contributed by the interaction of axial force, and bending moment about both longitudinal axis, and so is typically used columns.

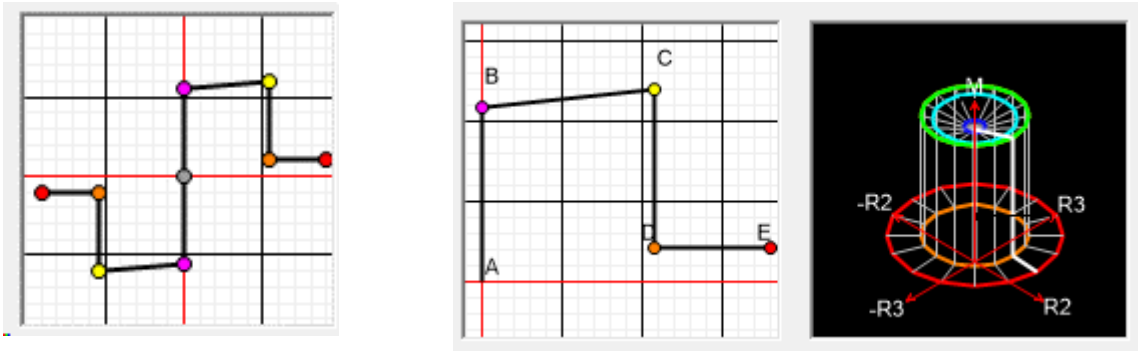

Figure 3-6 - Moment-curvature (y-,x-axis) relation for plastic hinges in SAP2000. L.S M3-hinge, R.S P-M2-M3 Hinge

As the moment-curvature relation is well defined, the hinge states can easily be obtained. And, if acceptance criteria for hinge rotation is defined, structural performance assessment on the basis of hinge rotation can be efficiently performed.

In SAP2000 such hinge properties can be automatically defined on the basis of ASCE 41-13. These hinges are created with an isotropic hysteresis model, which is found applicable for pushover analysis. For nonlinear time history analysis, this hysteresis model is not recommended to use, and either user-defined hinges or fiber hinges should be used in these instances.

3.3.2.2 Fiber hinges

Fiber hinge idealization reduces the section into a number of *fibers*, each with its own nonlinear parameters. Hinge properties can therefore automatically be defined on the basis of section properties and material properties. This eliminates the uncertainties of selection of hysteresis model for the hinge, making it a more suitable selection for use in time history analysis.

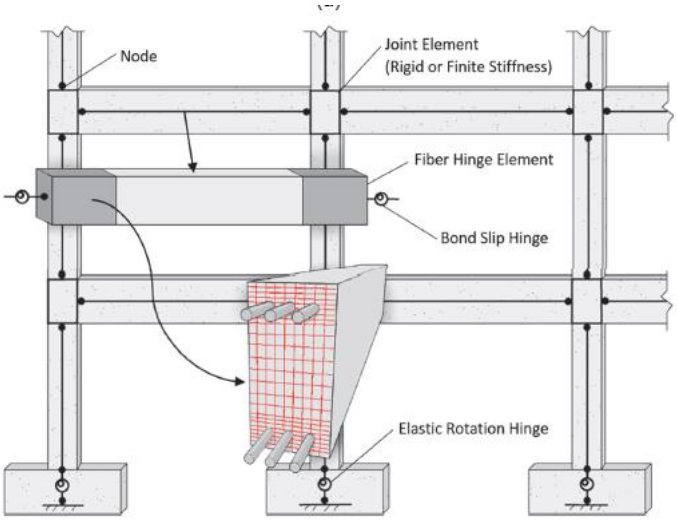

Figure 3-7 - Fiber type hinges - Conectrated plastic hinges (From Guidelines for Nonlinear Structural Analysis for Design of Buildings [3])

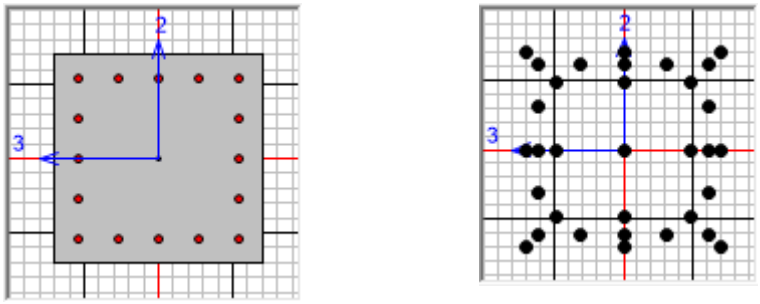

Figure 3-8 - L.S Column section, R.S generated fiber hinge

Fiber hinges though, are more computational expensive, both in analysis and in obtaining results. In SAP2000 acceptance criteria based on hinge rotation cannot be assigned directly to the elements and must evaluated in the post-processing of the results. Fiber hinges provides the option of evaluating the stress and strain of each defined fiber, providing the possibility of thoroughly evaluating the state of both the concrete rebar separately. This method of evaluating the hinge is more accurate, but proves significantly more time-consuming, making it not as suitable for more complex analytical models.

3.3.2.3 Nonlinear layered shell elements

SAP2000 also allows for material-nonlinear modelling of shells, by the use of nonlinear layered shell elements. The shell element is defined and built up by layers of selected material properties and thickness. Further it can be selected which layers, and in which directions (longitudinal, horizontal, and transversal) that should be considered as nonlinear. This option provides the choice of accuracy versus computational efficiency.

These elements are useful for modelling shear walls. The CSI analysis reference manual recommends the following two nonlinear configurations for modelling of shear walls:

Table 3-1 - Nonlinear shear wall modelling

		"Realistic"			*"Practical"*		
	Type	σ_x	σ_y	σ_{xy}	σ_x	σ_y	σ_{xy}
Concrete	Membrane	NL	NL	NL	L	NL	L
Rebar Top Vert.	Membrane	NL	-	NL	NL	-	-
Rebar Top Hor.	Membrane	NL	-	NL	NL	-	-
Rebar Bot. Vert.	Membrane	NL	-	NL	-	-	-
Rebar Bot. Hor.	Membrane	NL	-	NL	-	-	-
Concrete	Plate	-	-	-	L	L	L

In the case study the shear walls were modelled after the *realistic* approach:

Table 3-2 - Shear wall model used in case study

	Type	**Thickness**	σ_x	σ_y	σ_{xy}
Concrete	Membrane	230mm	NL	NL	NL
Rebar Top Vert.	Membrane	0.753mm	NL	-	NL
Rebar Top Hor.	Membrane	0.753mm	NL	-	NL
Rebar Bot. Vert.	Membrane	0.753mm	NL	-	NL
Rebar Bot. Hor.	Membrane	0.753mm	NL	-	NL

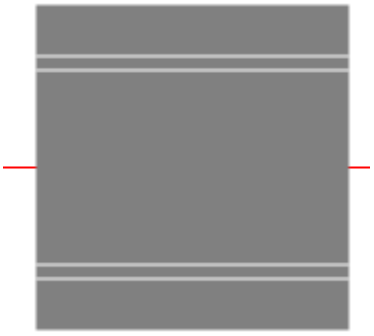

Figure 3-9 - Shear wall model used in case study

3.4 Damping

The damping effect in structural dynamics is defined as *the process by which free vibration steadily diminishes in amplitude* (p.12, [14]). In the equation of motion, damping coefficient *C* is linked to the velocity.

$$M\ddot{u}(t) + \boldsymbol{C\dot{u}} + Ku(t) = F(t) \tag{3.2}$$

Where *M* is the mass matrix, *C* is the damping matrix, *K* is the stiffness matrix, *F(t)* is the loading functions, and $u, \dot{u}$ and $\ddot{u}$ is displacement, velocity and acceleration.

For structural dynamic purposes, the dissipation of energy is usually idealized as equivalent viscous damping.

To idealize the viscous damping acting in a structure, there are generally two options:

3.4.1 Modal damping

A modal damping ratio, which is defined as the fraction of critical damping ζ/ζ_{crit}, is assigned to designated modes. Damping is therefore not implemented directly into the equation of motion but

assigned to results of a modal analysis. This approach is mostly used or analysis methods which rely on modal analysis, e.g. response spectrum and modal time history.

3.4.2 Rayleigh damping

Damping is calculated as a mass- and stiffness-proportional damping, and unlike the modal damping approach a full damping matrix is calculated for the equation of motion. This enables a more accurate description of damping, as coupling between modes can be considered. Mass- and stiffness proportional damping is combined in *Rayleigh damping*, which is defined as

$$C = a_0 M + a_1 \mathrm{K} \tag{3.3}$$

Where *C* is the damping matrix, *M* is the mass matrix, and *K* is the stiffness matrix.

The coefficients a_0 and a_1 can be calculated on the basis of predefined modes and designated damping ratios:

$$\frac{1}{2}\begin{bmatrix} 1/\omega_i & \omega_i \\ 1/\omega_j & \omega_j \end{bmatrix}\begin{Bmatrix} a_0 \\ a_1 \end{Bmatrix} = \begin{Bmatrix} \zeta_i \\ \zeta_j \end{Bmatrix} \tag{3.4}$$

Where ω is mode of vibration and ζ is damping ratio.

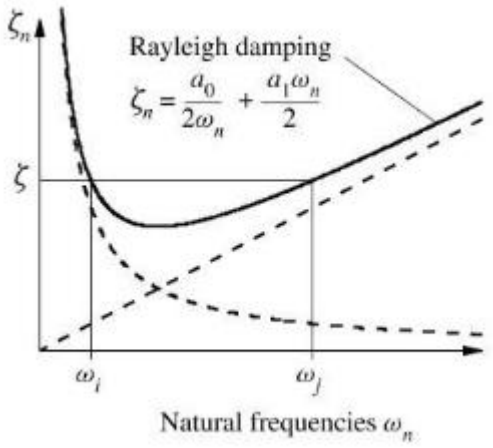

Figure 3-10 - Rayleigh damping (from Chopra [14])

3.5 Torsion

In dynamic earthquake loading, torsional force can be quite significant, and is often the source of damage in the perimeter of the structure. In both Eurocode 8 and IS1893 the torsional rigidity is classified on the basis of *center of mass, center of rigidity, torsional radius,* and *radius of gyration*. This subchapter introduces procedures to obtain these values from a structural analysis model:

Center of mass:

$$[x_m, y_m] = \frac{\sum_{i=1}^{n}([x_i, y_i] \cdot m_i)}{\sum_{i=1}^{n}(m_i)} \tag{3.5}$$

Center of rigidity

$$[x_r, y_r] = \frac{\sum_{i=1}^{n}([x_i, y_i] \cdot k_i)}{\sum_{i=1}^{n}(k_i)} \tag{3.6}$$

Where *x* and *y* are node coordinates, *m* is node mass, and *k* is lateral stiffness for the node.

If using a spatial model in analysis software that doesn't provide automatic definition of center of rigidity, the following procedure can be used:

Apply three load cases with point loads at the center of mass $[x_m, y_m]$.

Case 1: $F_x = 1kN$
Case 2: $F_y = 1kN$
Case 3: $M_z = 1kNm$

From the analysis results the eccentricities to the center of rigidity is found by the following expression:

$$e_{0x} = -\frac{M_{z,case\ 2}}{M_{z,case\ 3}} \tag{3.7}$$

$$e_{oy} = \frac{M_{z,case\ 1}}{M_{z,case\ 3}} \tag{3.8}$$

The coordinates to the center of rigidity is then $[x_m + e_{0x}, y_m + e_{0y}]$.

From the same analysis result the torsional radius can be obtained. The torsional radius is defined by:

$$[r_x, r_y] = \left[\sqrt{\frac{K_M}{K_{Fy}}}, \sqrt{\frac{K_M}{K_{Fx}}}\right] \tag{3.9}$$

Where:

$$\mathrm{K_{Fx}} = \frac{1}{U_x(x_m, y_m)_{Case\ 1}} \tag{3.10}$$

$$K_{Fy} = \frac{1}{U_y(x_m, y_m)_{Case\ 2}} \tag{3.11}$$

$$K_M = \frac{1}{R_z(x_m, y_m)_{Case\ 3}} \tag{3.12}$$

Where U and R is the deflection and rotation of the node at center of mass.

To classify the structure according to Eurocode 8, the radius of gyration (l_s) of the floor mass in plan must be determined. The radius of gyrations is determined by the expression:

$$l_s = \sqrt{\frac{I}{M}} \tag{3.13}$$

With a spatial analysis model, the radius of gyration can be determined by the assembled joint masses by:

$$l_s = \sqrt{\frac{\sum_{i=1}^{n}\left(m_i \cdot \sqrt{(x_i - x_m)^2 + (y_i - y_m)^2}\right)}{\sum_{i=1}^{n}(m_i)}} \tag{3.14}$$

3.6 Modal

The modes of vibration of a structure provides much information about its behavior during seismic action. To obtain these modes, a modal analysis is performed. The number of vibration modes depends on the number degrees of freedom of the structural system, so for a spatial model the number of mode is quite substantial. When performing modal analysis for use in response spectrum or modal time history analysis, its therefore interesting to find the necessary amount of modes to gain sufficient accuracy.

The parameter used to evaluate the accuracy of the modal analysis is the *modal mass participation ratio*. This value represents the ratio of modal mass that is active in a deflection or rotation for a given mass. When considering the amount of modes needed, the accumulated modal mass participation ratio in the relevant directions is evaluated. Both IS1893 and Eurocode 8 sets demand for minimum modal mass participation ratio.

For finding the modes, there are several approaches. The two most prominent, and which are available in SAP2000 is further discussed:

3.6.1 Eigenvectors

When performing a modal-eigenvector analysis, the modes of vibration are found for the undamped free vibration, i.e. natural modes, of the structural system:

$$M\ddot{u}(t) + Ku(t) = 0 \tag{3.15}$$

$$[K - \Omega^2 M]\Phi = 0 \tag{3.16}$$

Where Ω is the diagonal matrix of eigenvectors and Φ is the corresponding mode-shape.

3.6.2 Ritz-vectors

When preforming a modal-ritz-vector analysis, the modes of vibration are found by seeking the modes the modes that are excited by a set loading scheme:

$$M\ddot{u}(t) + Ku(t) = R(t) \tag{3.17}$$

To find the modes of vibration, dependent on the Ritz-loading, an algorithm is applied, presented Table 15.4.1 of *Dynamics of Structures* [14].

This approach to modal analysis is especially beneficial for response spectrum and time history analysis, as it considers the spatial distribution of dynamic loading. Modes that is not affected by the chosen loading scheme, with no modal mass participation in relevant directions, are not captured by the modal analysis, resulting in fewer modes to reach a target mass participation.

The main drawback of using Ritz-vectors is that the modes of vibration are only approximates of the real eigenvectors

For modal analysis for use in response spectrum analysis, the loading used may be acceleration forces in x-, y-, and z-direction.

3.7 Response spectrum analysis

Theory for response spectrum analysis is obtained from *Dynamics of Structures* [14].
As the peak force and displacements occur in the modes of vibration of the structure, these points will be of particular interest in dynamic analyses. With response spectrum analyses, the spectral acceleration is assigned the modes of vibration, from a modal analysis, and further combines the peak values to obtain the seismic design forces and displacements.

3.7.1 Modal combination

If the peak modal responses are combined by simply adding all the peak response, the results will be very conservative. From both Eurocode 8 and IS1893 it is recommended to either use SRSS- or CQC-modal combinations to obtain seismic design forces.

3.7.1.1 SRSS

SRSS – square root of sum of squares – uses the following combination to obtain design forces:

$$r_o = \sqrt{\sum_{n=1}^{N} r_{no}^2} \tag{3.18}$$

Where r_o is the total response and r_{no} is the induvial peak modal response.

This approach is sufficient for cases where modes of vibration are separated, and not closely space. For cases of closely spaced modes, the CQC-combination should be used.

3.7.1.2 CQC

CQC – complete quadratic combination – uses the following combination to obtain design forces:

$$r_o = \sqrt{\sum_{i=1}^{N}\sum_{n=1}^{N} \rho_{in} \cdot r_{io}^2 \cdot r_{io}^2} \tag{3.19}$$

Where ρ_{in} is a correlation coefficient between 0 and 1.

This approach considers the effect of closely space modes of vibration, and is therefore often considered the most accurate approach.

3.8 Nonlinear static analysis

As the name indicates, in these analyses nonlinear behavior is analyzed using static forces. With regards to seismic analysis, there are two main procedures that uses nonlinear static analysis; P-Delta- and pushover analysis.

3.8.1 P-Delta

For seismic analysis the vertical loads/weights, which are defined for as the seismic weigh, are applied in a static analysis. The purpose of such analysis is to determine the reduced stiffness with the seismic weight applied.

In SAP2000 other nonlinear analysis can be conducted to start from the end state of a P-Delta analysis. With this approach, the reduced stiffness and the vertical force from the P-Delta analysis is incorporated in to the analysis of choice.

3.8.2 Pushover analysis

A pushover analysis is performed by incrementally applying a lateral static load which is controlled by the displacement of an assigned control node, commonly assigned at roof level. The lateral load pattern depends on the procedure chosen for the analysis, e.g. modal- or gravity load pattern.

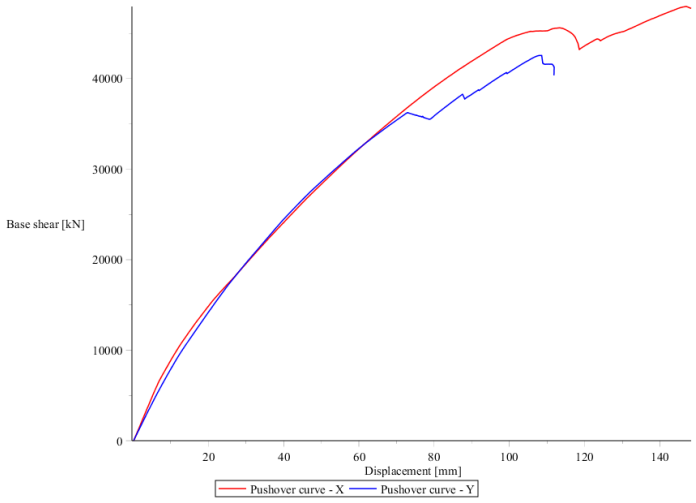

Figure 3-11 - Pushover curve

In the case study, a gravity lateral load pattern was used. This way the lateral force is applied at each node depending only on the seismic mass. This will usually replicate the main mode of vibration for the two horizontal axis.

With the pushover analysis performed, the displacement of the control node is plotted against the base shear to create the *pushover curve*. From the pushover curve the behavior of the structure can be interpreted, i.e. in what range does it behave linearly and when does the plastic mechanisms begin. With a seismic demand set, there can also be determined target displacements for a given seismic hazard.

3.9 Time History Analysis

The theory of this chapter is obtained from Selection and Scaling Time History Records for Performance-Based Design [15] and Guidelines for Nonlinear Structural Analysis for Design of Buildings [13].

In a time-history analysis, the earthquake loading is represented in the form of accelerograms. When performed correctly, it is considered the most accurate approach to determine seismic forces.

The accelerograms used in the analysis can either be recordings of real earthquakes, artificially created to be compatible with design response spectrums, or synthetic records obtained from seismological models. As large databases of ground motions from real earthquakes are readily available, e.g. PEER Ground motion database [16], it is the type further considered and used in the case study.

To get a good representation of the seismic forces expected to be prevalent at the project site, there should be defined some criteria for selection of ground motions based on geological and seismological conditions. The following characteristics should be considered, according to *Fahjan* [15]*:*

- Magnitude
- Faulting mechanism
- Distance to fault
- Rupture directivity
- Site conditions (e.g. shear velocity)
- Spectral content

As the point of obtaining several ground motions is to provide variation, it is further recommended to only use on set of ground motion per earthquake.

With the ground motion obtained, they need to be scaled or spectral matched to match the seismic hazard level of the project site. This can either be obtained through the response spectrum from the relevant code, or though site-specific PSHA. A common approach is to scale spectral acceleration of the suite of ground motions to the spectral acceleration seismic demand at the most prominent mode(s) of vibration of the structure.

With a suite of ground motions selected and scaled, the can be performed. In SAP2000 there are two categories of time-history analysis; modal and direct integration, both of which can be analyzed either linearly or nonlinearly.

3.9.1 Modal time-history analysis

Modal time-history is by far the most computational efficient approach. It uses the same theoretical background as the response spectrum analysis, while instead of calculating peak modal responses, the modal response is calculated for each time step (Chapter 13.1 Chopra [14]).

In SAP2000 there is the possibility of nonlinear modal time-history analysis, referred to as *Fast Nonlinear Analysis (FNA).* This approach is suitable for load cases which is primarily linearly, and

only a small degree of nonlinearity is expected. The nonlinear behavior is lumped into link-elements, which simplifies the nonlinear relation of the equation of motion to:

$$M\ddot{u}(t) + C\dot{u}(t) + K_L u(t) + r_N(t) = r(t) \tag{3.20}$$

Where K_L is the stiffness matrix for linear elastic elements, and r_N is the vector forces from the nonlinear behavior of the link-elements.

3.9.2 Direct integration time-history analysis

In direct integration procedures the linear equations of motion are fully integrated:

$$M\ddot{u}(t) + C\dot{u}(t) + Ku(t) = F(t) \tag{3.21}$$

Direct integration methods are very computational expensive, as for each step. The results obtained are very accurate.

To perform the direct integration several algorithms can be used, among these the Newmark and Hilbert-Hughes-Taylor (HHT) algorithms is available in SAP2000. The main difference between the two is that HHT allows for additional damping of high frequency modes. This comes in handy when using unprocessed ground motion, as the noise in high frequencies can be damped out in the analysis.

4 ANALYSIS AND DESIGN GUIDELINES TO EVALUATE SEISMIC ACTION

This chapter provides an overview of regulations regard seismic design for Eurocode 8, IS1893, and PBSD methodology following guidelines from FEMA and ASCE.

As earthquake force are so significant, and with long return periods, the probability of a large earthquake to occur in the lifespan of a structure is low. It is therefore normal practice to allow for some damages to the structure in these rare events. The degree of allowable damage depends mostly on the importance of building, as a hospital should remain operational in larger earthquake.

4.1 Eurocode 8-1

This chapter contains the requirements and recommendations to perform seismic analysis following Eurocode 8 [17]. In the cases that it can be chosen between values recommended by the code, or values regulated by the national annex, the code recommendations are followed.

Eurocode 8 does, to a small degree, implement PBDS methodology in its criteria. For a seismic design to comply with the code, it has to fulfill both its *Damage limitation* and *No collapse* requirements. The degree of implementation of the *damage limitation* limit is dependent on the national authorities, for instance in Norway this limit state is not considered.

4.1.1 Seismic Hazard

In the Eurocode, the seismic hazard is defined on the basis of peak ground acceleration, the ground type, and the surface wave magnitude of the earthquakes considered in a probabilistic seismic hazard analysis.

The seismic hazard considered for the limit states of Eurocode is set by the national authorities, while the recommended seismic hazard is:

Damage limitation	10% in 10 years	95year return
No collapse	10% in 50 years	475year return

To account for the difference in importance of buildings, an importance factor is implemented in the peak ground acceleration. This way, the PGA with return period considered to fulfill the *damage limitation* requirements are higher for hospitals than for houses. The following approximation can be done according to clause 2.1(4) for an area of high seismicity (k=4).

Table 4-1 - Design ground accelerations correlated to return period

	PGA	**I=0.7**	**I=1**	**=1.2**	**I=1.4**
Damage limitation	$a_{g,95year}$	$\sim a_{g,50year}$	$a_{g,95year}$	$\sim a_{g,225year}$	$\sim a_{g,365year}$
No collapse	$a_{g,475year}$	$\sim a_{g,50year}$	$a_{g,475year}$	$\sim a_{g,50year}$	$\sim a_{g,2000year}$

An elastic horizontal design spectrum is then established on the basis of design peak ground motion, ground type and seismicity of the region.

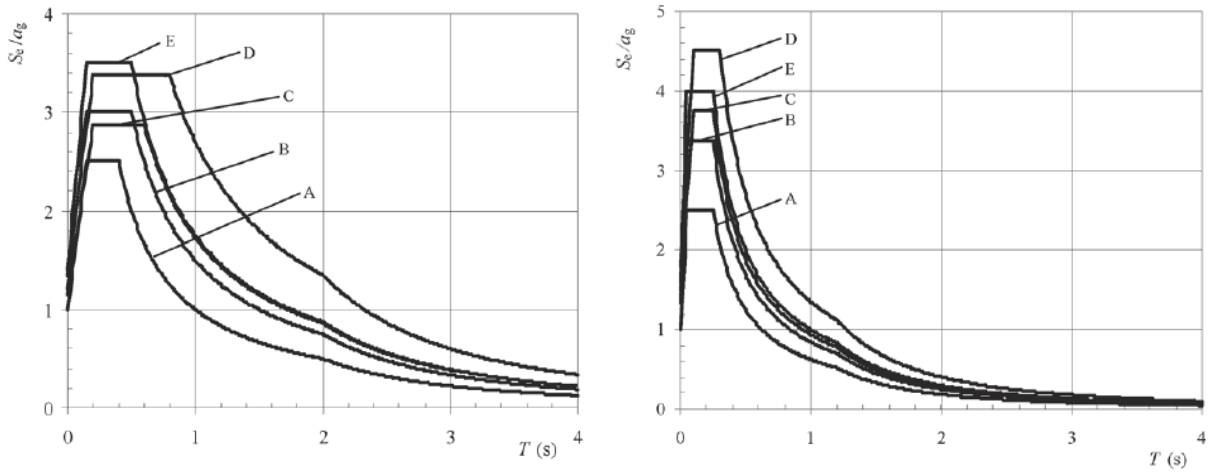

Figure 4-1 - Type 1 & 2 horizontal response spectrum, behavior factor not included (From EC8 [17])

The *Type 1* response spectrum is used in regions of high seismicity(>5.5M_s), while *Type 2* is used in regions with low seismicity (<5.5M_s).

4.1.2 Classifications

Many of the parameters of analysis is dependent on classifications regarding structural system, regularity and ground types. These classifications are further discussed in the following sub-chapters:

4.1.2.1 Structural system

The structural system is classified after the Eurocode as follows:

Frame system	Structural system where 65% of total base shear sustained by a beam- column system
Dual system	Vertical loads mainly supported by columns, lateral loads supported by both columns and structural walls
Wall-equivalent	When the structural walls obtain more than 50% of total shear resistance.
Frame-equivalent	When the frame system obtains more than 50% of total shear resistance
Wall system	Where structural walls resist both lateral- and vertical loads. Walls resist more than 65% of lateral force
Coupled/ Uncoupled	Structural walls are coupled if two more walls are connected by ductile beams, in a regular pattern.
Torsional flexible system	Dual- and wall system which does not provide the minimum torsional rigidity required by the code.
Inverted pendulum system	Structural systems where the upper third of the structure contains over 50% of the total mass

Some of these structural classifications comes with further regulations/benefits. For concrete wall-equivalent dual frame the interaction of masonry infills, which for instance is a component much used in concrete frame structures in Nepal.

To determine if the structure is torsional flexible, it needs to satisfy the following condition, where the eccentricity, radius of gyration, and torsional radius is defined in Chapter 3.5.

$$[r_x, r_y] \geq l_s \tag{4.1}$$

$$[e_{0x}, e_{0y}] \leq [0.3r_x, 0.3r_y] \tag{4.2}$$

4.1.2.2 Regularity

The Eurocode classify structural systems as either regular- or irregular in plan and elevation. The criteria to evaluate structural regularity is well defined in chapter 4.2.3.

The Eurocode rewards buildings with regularity in plan and elevation with greater reduction regarding the buildings ductility, and with simpler forms of dynamic analysis. This is due to the limitation of torsional forces in regular designs, and the mode shape which regularity provides.

For non-linear static analysis, plan regular buildings are also allowed the simplification of planar analysis, while plan irregular buildings must be analyzed by a spatial model.

4.1.2.3 Ground types

The effect of site soil conditions is accounted for by the *ground types.* These are characterized by soil classification, shear wave velocity, SPT value, and the undrained shear strength of the soil. As the geotechnical report provided for the case study only contains SPT values, this is presented in Table 4-2 and further compared to the classes of IS1893. Full list of ground types is found in Table 3.1 in Eurocode 8-1.

Table 4-2 – equivalent SPT values for soil types

		SPT-value
Type A	Rocks	-
Type B	Very dense sand, gravel, or very stiff clay	>50
Type C	Dense sand, gravel, or stiff clay	15-50
Type D	Loose-to-medium cohesionless soil	<15

Per clause 4.3.1(9), soil structure interaction may always be considered even if it will have a beneficial effect, while for situations where SSI it thought to have adverse effect it is required to be included in the analysis model.

4.1.3 Analysis model

On a global level, the Eurocode has a set of requirements for the type analysis model allowed. The analysis model can either be planar or spatial, with the requirement being regularity in plan which is further discussed in chapter.

Table 4-3 - Analysis models depending on structural regularity

Regularity		**Allowed Simplification**		**Behavior factor**
Plan	**Elevation**	**Model**	**Linear-elastic Analysis**	**(for linear analysis)**
Yes	Yes	Planar	Lateral Force	Referenced value
Yes	No	Planar	Modal	Decreased value
No	Yes	Spatial	Lateral Force	Referenced value
No	No	Spatial	Modal	Decreased value

For linear elastic analysis, the flexural and shear stiffness properties should be modified to represent the cracked moment of inertia. The recommended reduction in moment- and shear stiffness is 50% of the corresponding stiffness of the uncracked elements. Reduction of torsional constant to account for cracked torsional stiffness is not included in the code but is a recommended practice in *Seismic Design of Concrete Buildings to Eurocode 8* [18]. The torsional constant is recommended set at 10% of uncracked torsional stiffness. This applies to all beam-, column- and slab sections.

To transfer lateral loads to the vertical structural system, diaphragms should be assigned. Diaphragms may be either rigid, or semi-rigid depending on the ratio between the in-plane stiffness of the diaphragm and the lateral stiffness of the vertical system. The limit of when a diaphragm should be considered semi-rigid or assumed rigid is not defined. For concrete structures, floor slabs of over 70mm can be considered to serve as diaphragms.

When considering the base constraints of the structural model, the foundation of the building and soil properties of the site must be considered. If foundation deformability is thought to have an adverse effect on the building, soil-structure interaction should be included in the model. When this is not the case it is allowed to model with more simplified constraints, for example pinned or fixed.

4.1.4 Behavior Factor

In the Eurocode there are three ductility classes for structural analysis; DCL, DCM, and DCH (DC – Ductility Class). The ductility class of the structure is based on its ability to sustain post-yield loading, i.e strength in the non-linear domain.

For the different ductility classes there are different values for a behavior factor. This behavior factor is used to reduce earthquake force in the linear elastic analysis and sets a limit for what portion of the seismic loading is to be sustain within the linear-elastic domain of the structure. This allows for some permanent deformation and damage to the structure in the event of rare earthquakes.

The behavior factor also considers factors such as:

- Structural classification
- Regularity in plan and elevation
- Multiplication factor (α_u/α_1) based on:
    - Approximate values from the code depending on structure type, and number of bays and stories.

- Overstrength ratio obtained through a nonlinear static procedure (Pushover analysis)

Further details on the use of pushover analysis is discussed in chapter 3.8.2.

Table 4-4 - Initial behavior factor

STRUCTURAL TYPE	q_0 **DCM**	q_0 **DCH**
Frame system, dual system, coupled wall system	3,0 α_u/α_1	4,5 α_u/α_1
Uncoupled wall system	3,0	4,0 α_u/α_1
Torsionally flexible system	2,0	3,0
Invereted pendulum system	1,5	2,0

The behavior factor is further defined as:

$$q = q_0 \cdot k_w \cdot \geq 1.5 \tag{4.3}$$

Where the factor k_w depends on the structural system classification.

4.1.5 Linear elastic analysis

For all linear elastic analysis, a design horizontal response spectrum is established on the basis of the elastic horizontal response spectrum and the behavior factor q.

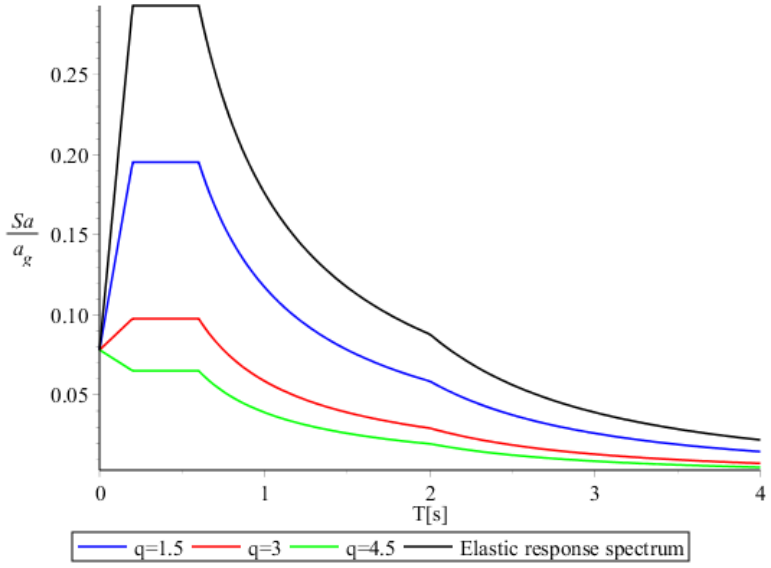

Figure 4-2 - Design horizontal response spectrum

For both methods of analysis, it should be evaluated if P-Δ effect should be considered by the use of inter-story drift sensitivity coefficient:

4.1.5.1 Lateral force method

The simplest seismic analysis form is the lateral force method. For it to be applicable the following criteria must be met:

- The fundamental period of vibration in the two main directions must fulfill:

$$T_1 \leq \begin{Bmatrix} 4 \cdot T_c \\ 2.0s \end{Bmatrix} \tag{4.4}$$

- The structure must be regular in elevation

If these criteria are met, the base shear for each horizontal direction can be determined by:

$$F_b = S_d(T_1) \cdot m \cdot \lambda \tag{4.5}$$

Where $S_d(T)$ is the horizontal design spectrum, m is the total mass of the building above the foundation level and λ is a correction value which considers the effective modal mass of the building depending on its height.

The fundamental period of the structure can either be obtained through a modal analysis, or through simplified approximations provided by the code. These approximations take into consideration the material of the structural system and the height of the building.

Further, the lateral force is distributed to the floors either linearly if the fundamental period is approximated, or dependent on the mode shapes if modal analysis is used:

$$F_i = F_b \cdot \frac{z_i m_i}{\sum z_j m_j} \tag{4.6}$$

$$F_i = F_b \cdot \frac{s_i m_i}{\sum s m_j} \tag{4.7}$$

Where *z* is height from the base of the building, *m* is the mass of the story, and *s* is the displacement off masses in the fundamental mode shape.

4.1.5.2 Modal response spectrum analysis

To conduct a modal response spectrum analysis, a set of requirements are set to the modal analysis:

- The sum of effective modal masses considered must be at least 90%
- All modes with modal mass greater than 5% must be considered

These requirements must be met for all directions considered for the response spectrum analysis. Special conditions apply for structures with significant effects from torsional modes.

The combination of modal response can be obtained either by SRSS or CQC, established in chapter 3.7.1.

4.1.6 Nonlinear Static Analysis (Pushover)

According to EC8, pushover analysis can be used for the following purposes:

- to verify or revise the overstrength ratio values α_u/α_1
- to estimate the expected plastic mechanisms and the distribution of damage
- to assess the structural performance of existing or retrofitted buildings for the purposes of EN 1998-3
- as an alternative to design based on linear-elastic analysis which uses the behavior factor q. In that case, the target displacement indicated in 4.3.3.4.2.6 (1) should be used as the basis of the design.

The lateral load pattern used depends on the procedure used. Assumptions and limitations of the selected procedure should be carefully regarded. In the N2-method proposed by the Eurocode, there is to be made to load cases, one for each direction. The later loading scheme can be defined by a uniform – incrementally increasing – lateral gravity loading. This is further discussed in chapter 3.8.2.

4.1.6.1 N2-method for target displacement

The procedure for determining a target displacement for a pushover analysis is presented in Annex B of EC8. This procedure is otherwise referred to as the N2-procedure (nonlinear analysis in two directions). The basic principle is to transform the structural model (MDOF) in to SDOF so that the elastic response spectrum can be used, develop an idealized elasto–perfect plastic force-displacement relationship from the pushover curve, and use this information to determine a target displacement where analysis results should be collected from.

The following relation between story mass m_i, normalized lateral force $\overline{F_i}$, and normalized displacement Φ_i:

$$\overline{F_i} = m_i \Phi_i \tag{4.8}$$

The displacement pattern is then normalized so that the roof displacement is $\Phi_n = 1$. This relation can either be decided by the engineer or obtained from actual deformation of the pushover analysis.

The mass of equivalent SDOF system is defined as:

$$m^* = \sum m_i \Phi_i = \sum \bar{F}_i \tag{4.9}$$

MDOF structural model results can then transformed to a SDOF by a transformation factor:

$$\Gamma = \frac{m^*}{\sum(m_i \Phi_i^2)} = \frac{\sum(m_i \Phi_i^2)}{\sum(m_i \Phi_i^2)} = \frac{\sum \bar{F}_i}{\sum\left(\frac{\bar{F}_i^{\,2}}{m_i}\right)} \tag{4.10}$$

$$F^* = \frac{F_b}{\Gamma} \tag{4.11}$$

$$d^* = \frac{d_n}{\Gamma} \tag{4.12}$$

With the pushover curve transformed to a SDOF system, the idealized elasto-perfect plastic force-displacement can be determined. The N2-procedure uses bi-linearization to approximate the pushover curve, assuming no stiffness after reaching plastic mechanism (A). The bi-linearization is made so that the area above- is equal to the area below the transformed pushover curve, shown in grey in Figure 4-3 - Bilinearization of the idealized pushover curve (From Annex B of EC8)

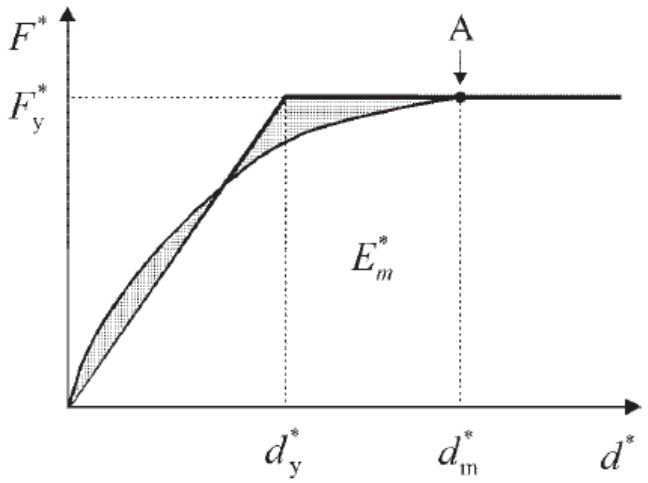

Figure 4-3 - Bilinearization of the idealized pushover curve (From Annex B of EC8 [17])

First, the displacement of which the plastic deformation occurs must be obtained. This point introduces some uncertainty, as most pushover curves will not be as regular as the one in Figure 4-3 - Bilinearization of the idealized pushover curve (From Annex B of EC8).

With the displacement at plastic formation (d_m^*), the yield displacement can be found by the following relation:

$$d_y^* = 2\left(d_m^* - \frac{E_m^*}{F_y^*}\right) \tag{4.13}$$

Where E_m^* is the deformation energy up to displacement $d_m{}^*$. This is defined as:

$$E_m^* = \int_0^{d_m^*} F^*(d^*)\, dd^* \tag{4.14}$$

From software such as SAP2000 the output of pushover analysis is in the form of incremental data points, and not a pure function. The deformation energy can then be found by the trapezoidal method:

$$E_m^* = \sum_{i=d_1}^{d_m^*} \left(\frac{(F_{i-1} + F_i)}{2} \cdot (d_i - d_{i-1}) \right) \tag{4.15}$$

With the yield displacement and base shear determined, the period of the idealized system is determined:

$$T^* = 2\pi \sqrt{\frac{m^* d_y^*}{F}} \tag{4.16}$$

The target displacement for a system assumed to behave purely elastic is given by:

$$d_{et}^* = Se(T^*) \left[\frac{T^*}{2\pi} \right]^2 \tag{4.17}$$

Where $Se(T^*)$ is the elastic response spectra defined in chapter 4.1.1.

Further determination of the target displacement depends on which range – short- or medium-long range – the structural period lies. If in the short range ($T^* < T_c$):

First it's determined if the structural response is elastic or in-elastic by the relation:

$$\frac{F_y^*}{m^*} \geq Se(T^*) \tag{4.18}$$

If the relation is true the structural response is elastic, and the target displacement is equal to eq. (4.17)

$$d_t^* = d_{et}^* \tag{4.19}$$

If the relation is false the structural response is inelastic, and a factor q_u is introduced which represents the ratio between the system of limited strength and the elastic response spectra:

$$q_u = \frac{Se(T^*) \cdot m^*}{F_y^*} \tag{4.20}$$

The target displacement is then defined as:

$$d_t^* = \frac{d_{et}^*}{q_u}\left(1 + (q_u - 1)\frac{T_c}{T^*}\right) \; while \begin{bmatrix} d_t^* \geq d_{et}^* \\ d_t^* \leq 3d_{et}^* \end{bmatrix} \tag{4.21}$$

If the structural period is in medium-long range ($T^* \geq T_c$), the target displacement is defined as:

$$d_t^* = d_{et}^* \tag{4.22}$$

When the proper target displacement is defined it is then transformed back to the MDOF system:

$$d_t = d_t^* \cdot \Gamma \tag{4.23}$$

At the target displacement the result parameters can then be evaluated to see if the structure fulfills the rest of the code, and if performance of the system is acceptable.

4.1.6.2 Overstrength factor

From the pushover analysis you can also obtain a correction to the behavior factor through the overstrength factor. This is described in clause 5.2.2.2 (4) for concrete structures. The overstrength factor consist of the factors α_u and α_1, which are defined as:

α_1 *".. the value by which the horizontal seismic design is multiplied in order to first reach the flexural resistance in any member in the structure, while all other design actions remains constant"*

α_u *".. the value by which the horizontal seismic design action is multiplied in order to form plastic hinges in a number of sections sufficient for the development of overall structural instability, while all other design actions remain constant"*

Both these factors can be obtained by the pushover analysis. α_u can be determined graphically in the same manner as the plastic mechanism defined in chapter 4.1.6.1. There are several ways to determine α_1, a very convenient way in SAP2000 is to determine this through hinge rotation. If fiber hinges are used, a yield rotation must be defined. If lumped plasticity hinges following FEMA 356, the yield rotation can be found automatically and is graphically displayed in the results, making for a much easier procedure.

A preliminary response spectrum analysis must also be completed beforehand, with the original behavior factor. This is done to ensure that the linear elastic analysis is in the elastic region.

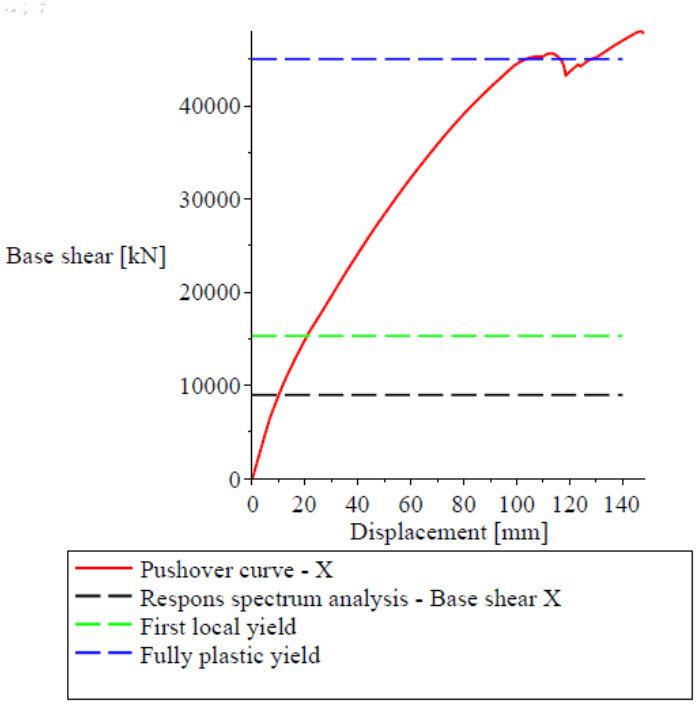

Figure 4-4 - Pushover analysis - overstrength factor

With the base shear from the preliminary response spectrum analysis and the first local- and fully plastic- yield base shear points, the factors can then be calculated:

$$\alpha_1 = \frac{F_{First\ local\ yield}}{F_{response\ spectrum}} \tag{4.24}$$

$$\alpha_u = \frac{F_{Fully\ plastic\ yield}}{F_{response\ spectrum}} \tag{4.25}$$

$$\frac{\boldsymbol{\alpha_u}}{\boldsymbol{\alpha_1}} = \frac{\boldsymbol{F_{First\ local\ yield}}}{\boldsymbol{F_{Fully\ plastic\ yield}}} \tag{4.26}$$

This value can further be used to correct the behavior factor in Table 4-4 - Initial behavior factor.

4.1.7 Time History Analysis

Selection of ground motion should consider the following criteria:

- Fault distance
- Magnitude
- Site ground type

After selecting applicable ground-motions you have the option of either scaling, or spectral-matching, the ground motions to the design response spectrum for the given case. There are here two requirements for the selected records:

- At zero-period, the mean spectral acceleration for all the records must be greater than the value of S (soil amplification factor) $\cdot\ a_g$.
- Between $0.2T_1$ and $2T_1$, where T_1 is the fundamental period in the direction considered, the mean spectral acceleration should not be less than 90% of the design spectrum.

There is the option to either use three- or seven ground motion records for the analysis. If three records are used, the design parameters are taken from the least favorable results. If seven records are use the design parameters is derived from the average of the results.

For linear time history analysis, the ground motions are scaled according to the design horizontal response spectrum, while for nonlinear time history analysis the ground motions are scaled according to the elastic response spectrum.

The results from a linear time history analysis can be used to:

- Determine design forces for section design
- Determine inter-story drift for *damage limitation* demand

The results from a nonlinear time history analysis can be used to:

- Determine true inter-story drifts
- Determine plastic hinge rotation, and subsequently limit states according to EC8-3

4.1.8 Damage limitation – Drift limits

Due to the low seismicity in Norway, the damage limitation limit state is not required. As the case study is located in an area of high seismicity, the requirements of *damage limitation* are therefore relevant.

Per the Eurocode, structures should endure moderate earthquakes with little or no damage. For the overall structural this requirement is met by satisfying the drift limits in clause 4.4.3.2

Table 4-5 - Drift limits - Damage limitation

$\frac{\boldsymbol{d_I}}{\boldsymbol{H_i}} \leq \frac{\mathbf{0.005}}{\boldsymbol{\nu}}$	Structures with brittle non-structural elements
$\frac{\boldsymbol{d_I}}{\boldsymbol{H_i}} \leq \frac{\mathbf{0.0075}}{\boldsymbol{\nu}}$	Structures with ductile non-structural elements
$\frac{\boldsymbol{d_I}}{\boldsymbol{H_i}} \leq \frac{\mathbf{0.01}}{\boldsymbol{\nu}}$	Structures with non-interfering non-structural elements

Where H_i is the story height, ν is a reduction factor to find the equivalent drift for different return periods. The inter-story drifts d_I is calculated as:

$$d_I = q_d(d_{e,i} - d_{e,i-1})$$

Where q_d usually is chosen to be the same as behavior factor q, d_e denotes displacement obtained from linear elastic analysis, and i denotes story.

Further requirements are recommended for buildings of civil importance, per clause 4.4.3.1 (2): "Additional damage limitation verifications might be required in the case of buildings important for civil protection or containing sensitive equipment.". These additional verifications should be incorporated in the national annex of the Eurocode. As there are no requirements provided by the Norwegian national annex, further requirements might be obtained from other codes. For instance, the damage limitation demand coincides with the Operational-performance level from ASCE 41-13 presented in chapter 4.4.2.

4.2 IS1893

In the Nepali Building Code (NBC 105) it is stated that it should be applied in conjunction with the Indian code of seismic design. With only minor differences, it is therefore more practical to use the Indian Code as it is substantially more detailed and is implemented in many commercial software.

4.2.1 Seismic hazard

The peak ground acceleration is determined by the following zone-map in figure #. Per NCB Nepal should be considered as zone 5 after the Indian standard. This map was made on the basis of deterministic seismic hazard analysis.

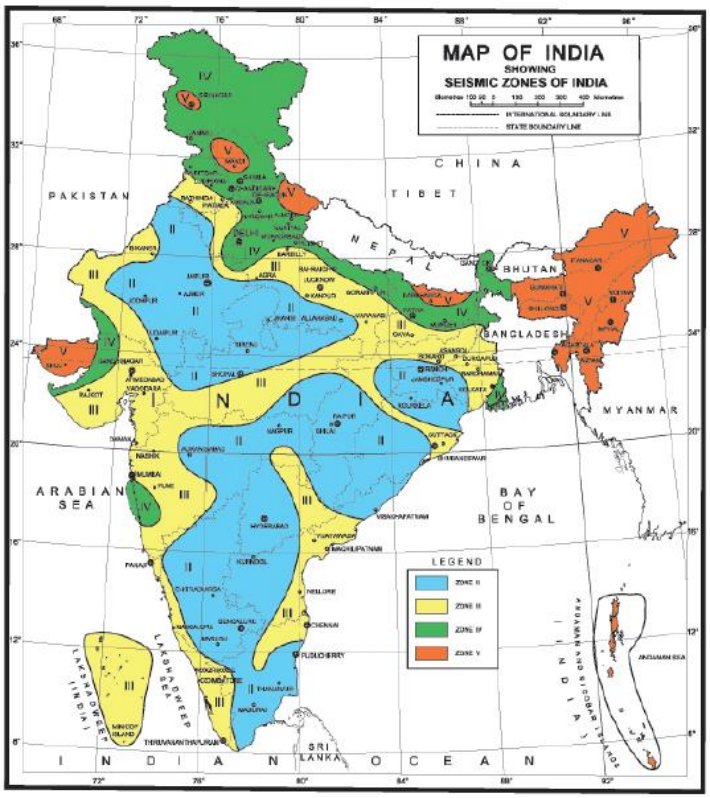

Figure 4-5 - Seismic zone map of India (from IS1893 **[5]**)

Table 4-6 - Zone factors for IS1893

		MSK Intensity	Zone factor (PGA [g])
Zone 2		VI or less	0,10
Zone 3		VII	0,16
Zone 4		VIII	0,24
Zone 5		IX and above	0,36

The PGA is based on the MSK intensity scale and approximates earthquake with 475year return period. In the previous version of IS1893 (2002), it was differentiated between the *design earthquake* (DE – approximately 95-year return) and *maximum considered earthquake* (MCE – approximately 95-year return). This differentiation is left out in the new version of IS1893 (2016), and it is only operated with a design seismic action of Z/2, which approximates a return period of 95-years.

Per clause 6.3.3.1 the vertical effect of earthquakes should be considered if; the building is in seismic zone 4 or 5, the building is irregular in plan or elevation, or the building is rested in soft soils.

4.2.2 Classifications

There is assigned a number of classifications to the structure and site to determine the seismic demand and response of the structure after IS1893

4.2.2.1 Structural system

The structural system is mainly classified into three types; Frame-, wall-, and dual structural systems. Based on the ductility of the chosen structural system, further sub-classifications are made to determine a behavior factor for the structure.

There is made a clear distinction for frame systems between *Ordinary Moment Resisting Frames (OMRF)* and *Special Moment Resisting Frames (SMRF).* To be able to classify the frame-system as *SMRF* it is required that the structure must comply with *IS 13920 – Ductile detailing of reinforce concrete structures subjected to seismic forces* [19]. Ductile shear walls are also required to comply with this standard.

4.2.2.2 Ground Types

In IS1893 soil types are classified into three types, presented in Table 2 in IS1893. When examining the site using standard penetration testing, the classification of the soil material combined with the following SPT-values are used to classify the soil type:

Table 4-7 – equivalent SPT values for soil types

	SPT-value
Type A – Rock or hard soils	>30
Type B – Medium or stiff soils	10-30
Type C – Soft soils	<10

The choice of structural system is limited by the seismic zone.

4.2.2.3 Regularity

The criteria for regularity in plan and elevation is well defined in table 5 and 6 in IS1893. Two criteria are though highlighted, as these differ significantly from Eurocode 8, and are especially relevant for the case study:

Torsional irreguliarty:
Torsional irregularity is classified byc the difference in lateral deflection at of the two sides of the building. Three limits are defined by Table 5 in IS1893. In opposition to Eurocode 8, IS1893 does not allow for significanlty torsional irregular structural configruations:

$$\frac{\Delta_{max}}{\Delta_{min}} \leq \mathbf{1.5}$$ Torsionally regluar

$$\mathbf{2} \geq \frac{\Delta_{max}}{\Delta_{min}} \geq \mathbf{1.5}$$ Complient if; the fundamental torsional mode shall be smaller than the two horizontal, and three dimensional analysis is conducted

$$\frac{\Delta_{max}}{\Delta_{min}} \geq \mathbf{2.0}$$ Not complient, building configuration should be revised.

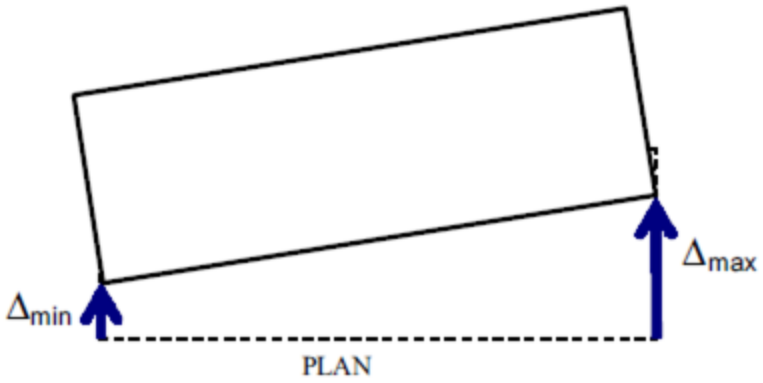

Figure 4-6 - Criteria for torsional regularity

Requirements for seismic zone IV and V:
For structures in seismic zone IV and V, additional criteria are defined. The first three modes of vibration should account for an accumulative 65% modal mass participation in each principle plan direction, and the fundamental periods should differ by at least 10%:

$$T_2 \leq 0.9T_1$$

4.2.3 Analysis model

For linear-elastic analysis the moment of inertia shall be taken as 70% of gross moment of inertia of columns, and 35% for beams.

Soil structure interaction can be included, but in simplification can be made by modelling as fixed constraints if the soil is not thought to have a negative impact on the analysis results. In most cases, the inclusion of soil structure interaction will yield conservative results as the soil will sustain a portion of the dissipated energy in an earthquake.

Regarding the use of spatial or planar analysis model, clause 7.2.2 requires that the analysis model should adequately represent irregularities in the structural configurations. The choice of analysis model is therefore dependent on the interpretation of *adequately*.

4.2.4 Behavior factor

In IS1893 the allowance of nonlinear behavior at design level earthquake is based on the behavior factor *R*, ranging from 1 (brittle) to 5 (highly ductile). In IS1893, this value is solely dependent on the chosen structural system, further explained in chapter 4.2.2.1.

4.2.5 Linear elastic analysis

For the linear elastic analysis, a design horizontal acceleration spectrum is defined on the basis of a horizontal seismic coefficient A_h:

$$A_h = \frac{\left(\frac{Z}{2}\right)\left(\frac{S_a}{g}\right)}{\left(\frac{R}{I}\right)}$$

Where Z is zone factor, R is the behavior factor, I is the importance factor, and S_a/g is the spectral acceleration dependent on the ground type. The linear elastic analysis can either be performed by lateral force method or response spectrum analysis.

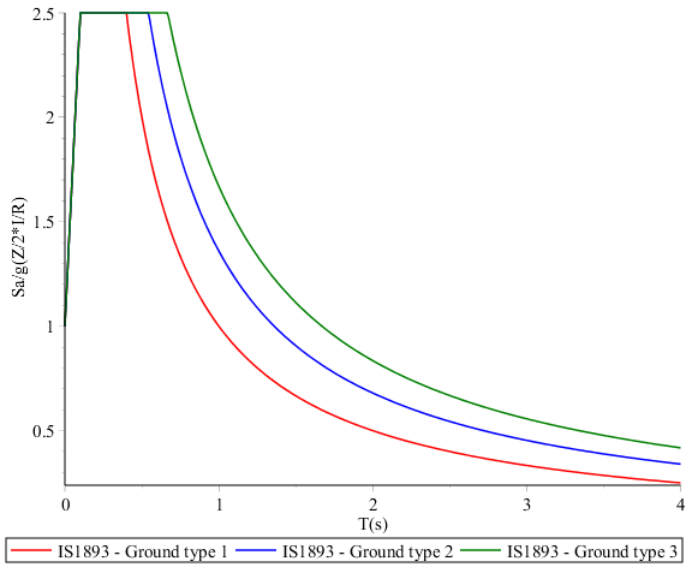

Figure 4-7 - Design horizontal response spectrum for response spectrum analysis - IS1893

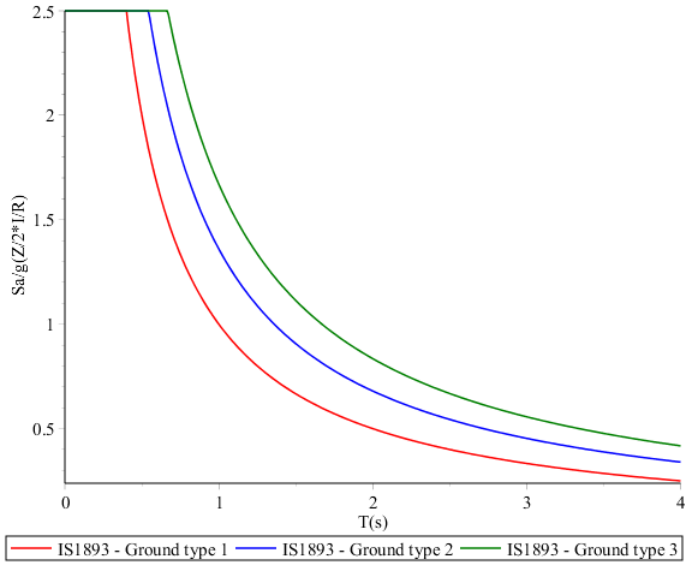

Figure 4-8 - Design horizontal response spectrum for lateral force method - IS1893

4.2.5.1 Lateral force method

In the lateral force method, the total base shear is determined by:

$$V_B = A_H W \tag{4.27}$$

Where A_H is the horizontal seismic coefficient, and W is the seismic weight of the building. The modes of vibration can either be found by a modal analysis, or be approximated in a similar manner of Eurocode, according to clause 7.6.2 of IS1893. The total base shear is to be distributed linearly by the same procedure as in Eurocode 8 (Equation (4.6, chapter 4.1.5.1).

4.2.5.2 Modal response spectrum analysis

The following criteria is set for the modal response spectrum analysis:

- The sum of effective modal masses considered must be at least 90%
- Modes with periods of less than 0.03s can be cut off
- Modes may be combined by CQC
- The response spectrum should be scaled so that base shear is equivalent to that of the lateral force method (Equation (4.27))

4.2.6 Drift limits

Per clause 7.11.1 of IS1893, the interstory drift should be less than 0.4%. The interstory drifts should be obtained by the unscaled service level seismic loading.

$$d_I < 0.4\% \tag{4.28}$$

4.3 NBC 105

As noted in the previous chapter, the Nepali building code for seismic design (NBC105 [20]) is very similar to IS1893. This chapter will highlight some of the differences between the two.

4.3.1 Seismic Hazard

In a different approach than both Eurocode 8 and IS1893, NBC105 does not represent the ground acceleration factor in relation to earthquake intensity directly. Instead, the ground acceleration of Kathmandu is incorporated into the horizontal response spectrum, with the zone-factor functioning as a reduction factor.

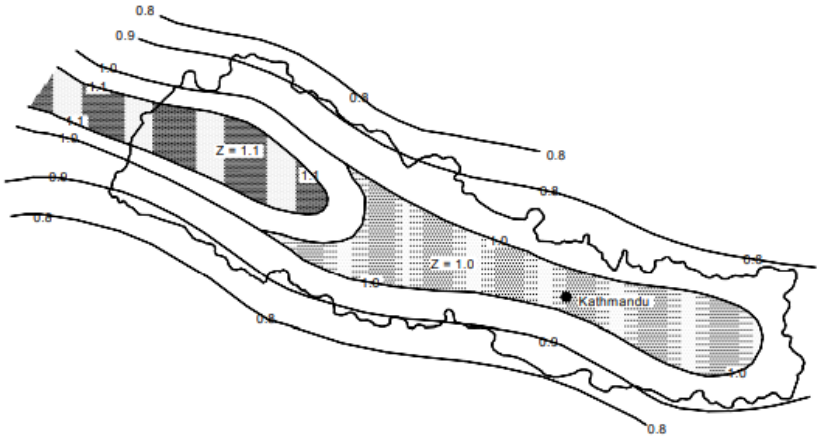

Figure 4-9 - Seismic zones (NBC 105 [20])

When comparing the seismic demand for Kathmandu, NBC105 and IS1893 (seismic zone V) yields nearly identical seismic demands.

4.3.2 Behavior factor

The behavior factor *K*, described as *structural performance factor* by NBC105, is oriented in the opposite order of IS1893 and Eurocode 8. A behavior factor of 1 represents the highest ductility available, and a behavior factor of 5 represents a completely brittle behavior.

4.3.3 Linear elastic analysis

In NBC105 the design horizontal response spectrum is established on the basis of horizontal seismic force coefficient C_d.

$$C_d = C \cdot Z \cdot I \cdot K \tag{4.29}$$

Where *C* is a spectral acceleration function, *Z* is the zoning factor, *I* is importance class and *K* is the behavior/structural performance factor.

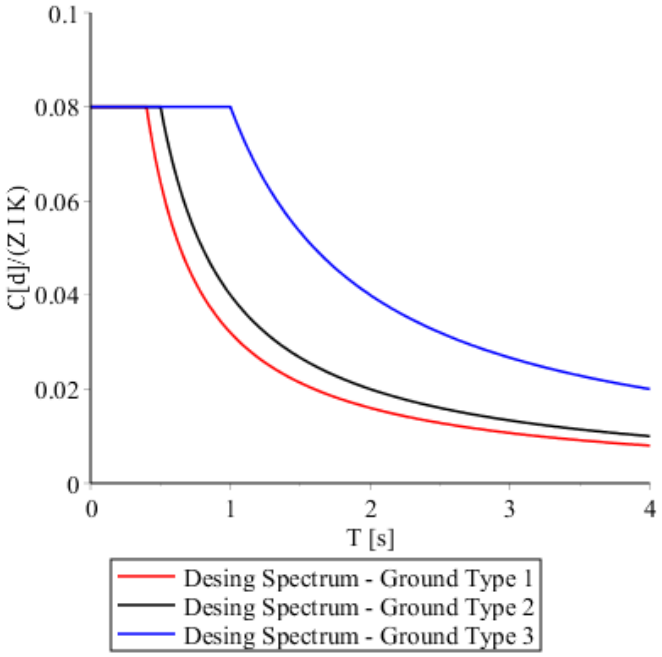

Figure 4-10 - Design spectrum after NBC 105 [20]

Design force can then be obtained either through lateral force- or response spectrum analysis. Both are to be analyzed by the same approach as for IS1893.

4.3.4 Drift limits

All deformations from linear elastic analysis is to be multiplied by a factor of *5/K*. For all structures, the drift limit is set to 1% and should not exceed 60mm.

4.4 Performance based seismic design

With regards to performance based seismic design, the following regulations and guidelines are considered:

- ASCE 41-13 – Seismic Evaluation and Retrofit of Existing Buildings [21]
- FEMA 356 – Pre-standard and Commentary for the Seismic Rehabilitation of Buildings [22]

The main gist of the performance-based seismic design methodology is to determine the structural performance of a structure in accordance with earthquake of different magnitude.

Table 4-8 - PBSD after FEMA 356 with example acceptance criteria

		Target building Performance Level			
		Operational	Immediate Occupancy	Life Safety	Collapse Prevention
Earthquake Hazard Level	50%/50year				
	20%/50year				
	10%/50year				
	2%/50year				

This design philosophy is incorporated into many building codes to a higher or lower degree. In Eurocode 8-1, for design of new buildings, there are defined two performance levels; *Damage Limitation* and *Collapse Prevention*. In Eurocode 8-3, for evaluation of existing buildings, a third performance level is introduced; *Significant Damage*.

Table 4-9 - Approximation of performance levels of ASCE 41-13 and EC8-3

ASCE 41-13	Operational	Immediate occupancy	Life safety	Collapse prevention
EC8-3	Damage limitation	Significant damage		Near Collapse

4.4.1 Seismic Hazard

The definition of seismic hazard levels is not uniform across the codes. FEMA 356 describes four seismic hazard levels, depended on maximum earthquake probabilities. In the case study of this thesis it is chosen to analyze for earthquakes with 50%-, 10%- and 2% probability of occurrence in 50 years.

4.4.2 Performance levels

The performance level is limit states that describes the integrity of a structure. There are many ways in which performance levels are defined, but a common definition used is; Opertaional (O), Immediate occupancy (IO), Life safety (LS) and Near collapse (NC). Per ASCE 41-13 the description of the performance levels are as follows:

Tabell 2 - Decription of performance levels4

Performance Levels (Structural system)	**Description**
S-1 – Immediate Occupancy (IO)	"*Immediate Occupancy* is the post-earthquake damage state in which only very limited structural damage has occurred. The basic vertical- and lateral-force-resisting systems of the building retain almost all of their pre-earthquake strength and stiffness. The risk of life-threatening injury as a result of structural damage is very low, and although some minor structural repairs might be appropriate, these repairs would generally not be required before re-occupancy. Continued use of the building is not limited by its structural condition but might be limited by damage or disruption to nonstructural elements of the building, furnishings, or equipment and availability of external utility services."
S-2 – Damage Control	*"Damage Control,* is defined as a post-earthquake damage state between the Life Safety Structural Performance Level (S-3) and the Immediate Occupancy Structural Performance Level (S-1)."
S-3 – Life safety (LS)	"*Life Safety*, is defined as the post-earthquake damage state in which a structure has damaged components but retains a margin against the onset of partial or total collapse."
S-4 – Limited safety	"*Limited safety* is defined as a post-earthquake damage state between the Life Safety Structural Performance Level (S-3) and the Collapse Prevention Structural Performance Level (S-5)."
S-5 – Collapse Prevention (CP)	"*Collapse prevention* is defined as the post-earthquake damage state in which a structure has damaged components and continues to support gravity loads but retains no margin against collapse."
S-6 – Not considered	"Where an evaluation or retrofit does not address the structure, the Structural Performance Level shall be Structural Performance Not Considered (S-6)."
Performance Level – Nonstructural components	**Description**
N-A – Operational	"Nonstructural Performance Level N-A is the post-earthquake damage state in which the nonstructural components are able to provide the functions they provided in the building before the earthquake."
N-B – Position Retention	"Nonstructural Performance Level N-B is the post-earthquake damage state in which nonstructural components might be damaged to the extent that they cannot immediately function but are secured in place so that damage caused by falling, toppling, or breaking of utility connections is avoided. "
N-C – Life Safety	"Nonstructural Performance Level N-C is the post-earthquake damage state in which nonstructural components may be damaged, but the consequential damage does not pose a life-safety threat"
N-D – Not considered	"Where an evaluation or retrofit does not address all nonstructural components to one of the levels in the previous sections, the Nonstructural Performance Level shall be Nonstructural Performance Not Considered (N-D)."

With a combination of these the following building performance levels are defined:

Building Performance Level	Description
1-A – Operational	Backup utility services maintain function; very little damage (S-1 & N-A).
1-B – Immediate Occupancy	The building remains safe to occupy; any repairs are minor (S-1 & N-B)
3-C – Life Safety	Structure remains stable and has significant reserve capacity; hazardous damage is controlled (S-3 & N-C)
5-E Collapse Prevention	The building remains standing, but only barely; any other damage or loss is acceptable (S-5 & N-E)

4.4.3 Acceptance criteria

There are a lot of different answers as to what parameters of the analysis that will predict the performance level. The limit state set for each performance level is referred to as "acceptance criteria". This section will present the most used

4.4.3.1 Interstory drifts, velocity and acceleration

The interstory drift is a good indicator of the performance level of a structure. It is easily defined as the ratio of displacement of two adjacent floors, divided on the floor height. Usually analyzed in both x-, y- direction:

$$d_I = \frac{u_{floor\ i} - u_{floor\ i-1}}{H_{floor}} = \% \tag{4.30}$$

Transient drift ratio is defined as the maximum resultant interstory drift:

$$d_{I,T} = \sqrt{d_{I,x}^2 + d_{I,y}^2} \tag{4.31}$$

With regards to defining acceptance criteria with drift demands, there is no consensus on what these limits should be. FEMA 356 presents suggested drift limits for the different performance levels, which are used in the case study. With this in mind, the use of drift limits as acceptance criteria on its own is not enough to define the true performance of the building and should be accompanied by other acceptance criteria.

4.4.3.2 Plastic hinge rotation

The acceptance criteria for plastic hinge rotation of beams and columns can be found in table 10-7 and 10-8 in ASCE 41-13.

For beams controlled by flexure, the acceptance criteria depend on the balance of compression and tension rebar in the beam, conformity of transverse reinforcement, shear force at hinge location.

For columns controlled by flexure, the acceptance criteria depend on the axial force ratio of the columns.

4.4.4 Analysis

The perform the seismic performance assessment, several analysis methods can be used.

If the structure is expected to behave linearly, most relevant for earthquakes of 50% in 50 years, linear analysis can be conducted. Here both response spectrum and linear time history analysis can be used, with minor limitation for response spectrum analysis for structures of high complexity. If the other earthquake hazard levels are to be analyzed by time history analysis, then the ground motions can easily be scaled the desired hazard level.

If the structure is expected to behave nonlinearly, which would most likely be the case for earthquakes of 10-2% probability of occurrence in 50 years, either nonlinear static- or nonlinear time history can be used to determine structural performance. ASCE 41-13 does allow for linear analysis approaches nonlinearly behaving structures, but the most accurate approach would be to use nonlinear analysis methods.

5 CASE STUDY

Kanti Children's hospital is situated in the north-eastern part of Kathmandu, Nepal. There is planned an extension to make room for a child-psychiatrics department. The extension is to be built as a separate building on the western part of the hospital site.

Figure 5-1 – North-elevation view (Ref. Team Consultants)

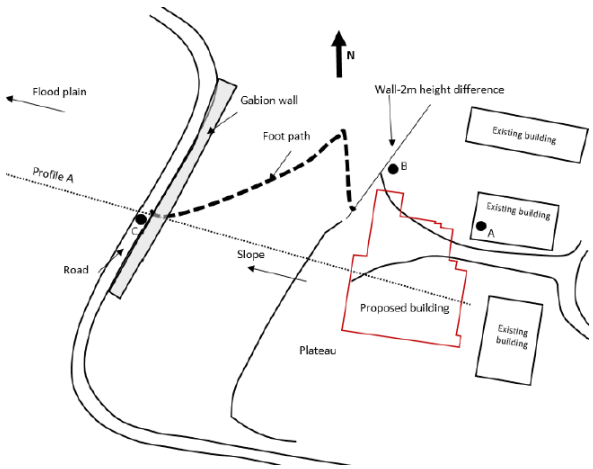

Figure 5-2 - Site plan, Kanti Children's hospital

The building is planned with 4 stories of 492m^2. The structural system consists of concrete moment resisting frames, shear walls, and floor slabs. In the facade there is infill brick walls.

A geotechnical report was conducted for the hospital site. This report concludes that there is no risk of liquefaction, as the waterbed is found to be deeper than 15m. Four standard penetration tests were conducted, with equivalent SPT values at the surface layer ranging from 14-29. There was proposed to use a piled-raft system as the foundation of the building.

The proposed structural design is based on provision from IS1893, and consists of the following column-, beam- and shear wall plan:

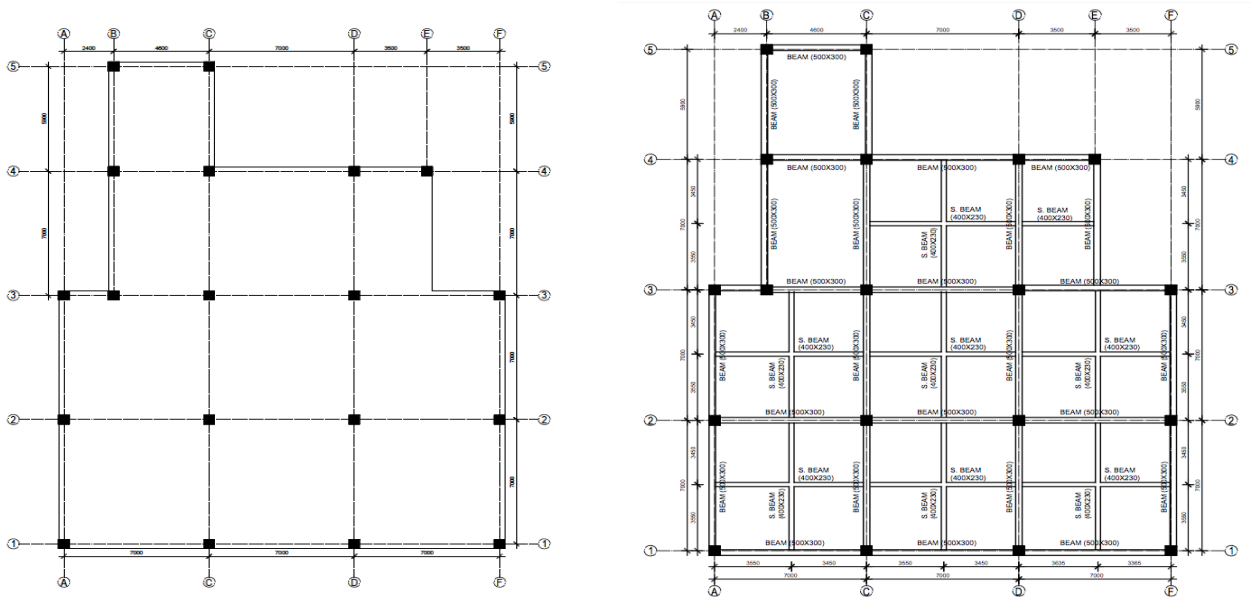

Figure 5-3 – Beam- and column plan for story 1-4

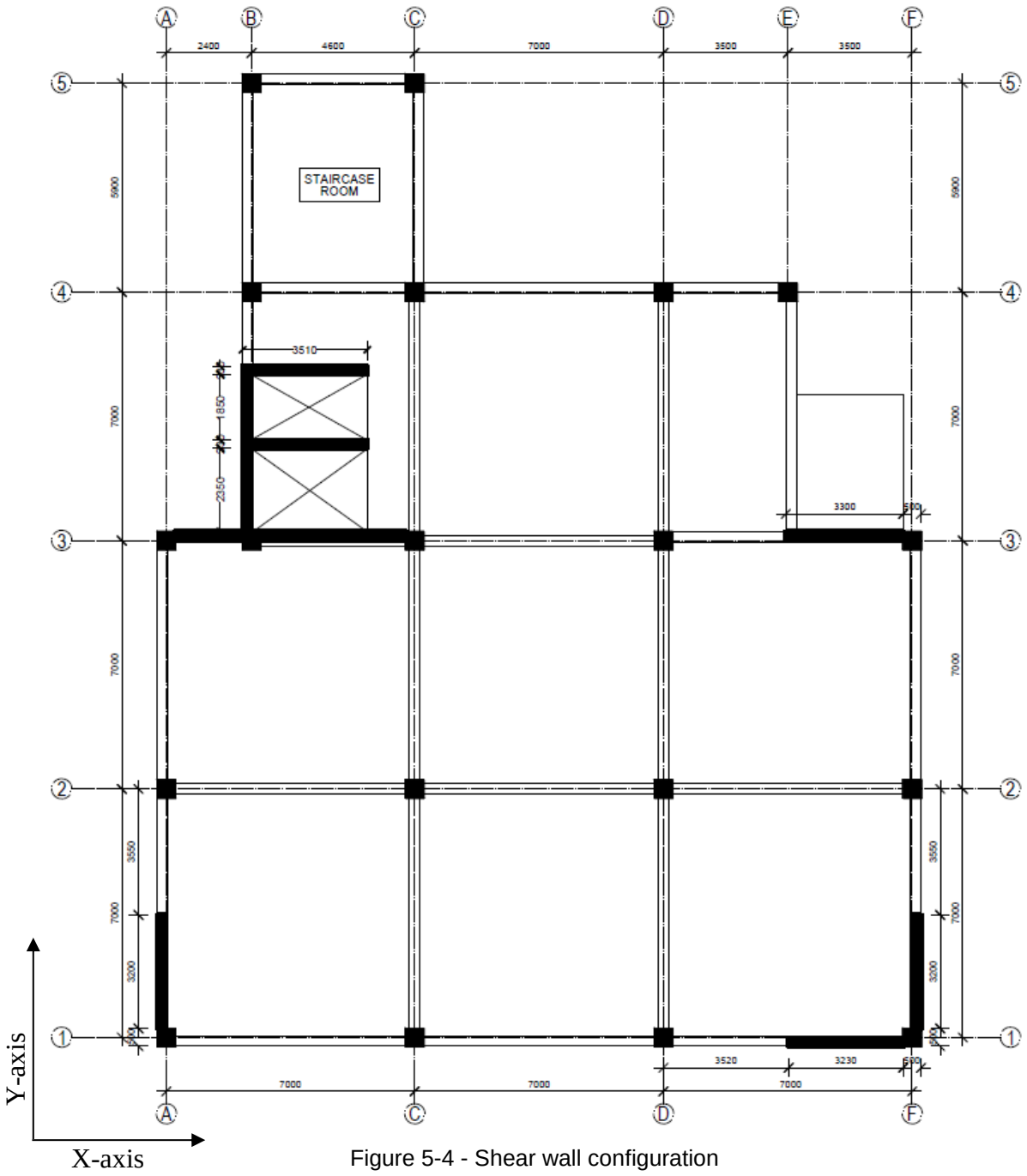

Figure 5-4 - Shear wall configuration

The following sections were used in the analytical model:
For all concrete sections, a 40mm cover is assigned.

Table 5-1 - Beam sections

Beam ID:	AT-1	AT-2	AT-3	AT-4	AT-5	AT-6	AT-7	AT-8	AT-9	AT-10	AT-11	AT-12
Width [mm]	270	270	300	300	300	300	300	300	300	300	300	270
Depth [mm]	400	400	500	500	500	500	500	500	500	500	500	400
Rebar tension	3xØ16	3xØ16	1xØ16 2xØ20	1xØ16 2xØ20	1xØ16 2xØ20	1xØ16 2xØ20	2xØ16 2xØ20	1xØ16 2xØ20	1xØ16 3xØ20	1xØ16 2xØ20	1xØ16 2xØ20	1xØ12 2xØ16
Area [mm^2]	603	603	829	829	829	829	1030	829	1143	1143	1143	515
Rebar compression	4xØ16	2xØ16	3xØ16 2xØ20	2xØ20	2xØ16 2xØ20	3xØ16 3xØ20	3xØ20	3xØ20	4xØ16 3xØ20	2xØ16 3xØ20	4xØ16 3xØ20	3xØ20
Area [mm^2]	803	402	1231	628	1030	1545	942	942	1746	1344	1746	942

Table 5-2 - Column sections

Column ID [500x500mm]	**C1**	**C2**	**C3**	**C4**	**C5**
Rebar configuration	8xØ12 8xØ16	16xØ16	8xØ20 8xØ16	12xØ20 4xØ16	8xØ20 8xØ25
Area [mm^2]	2512	3215	4120	4572	6437

Table 5-3 - Slab sections

Slabs:	**Thickness [mm]**	**Long. rebar**	**Vert. rebar**
Shear walls	230	Ø10/cc150mm 533mm/m	Ø12/cc150mm 753mm/m
Floor slabs	200	Not set/not relevant	Not set/not relevant

5.1 Structural analysis Model

A spatial model was created in SAP2000 based on the initial structural design. Beams and columns were modeled as line elements, floor- and stairway slabs were modeled as thin shell elements, and shear walls were modelled as nonlinear-layered shell elements.

The base of the structural model is assumed fixed constrained. This was done as the foundation consists of a piled raft system, providing moment retention, and since neither IS1893 or Eurocode requires implementation of soil-structure-interaction. For the geotechnical properties of the site, implementation of SSI would most likely provide more liberal results, making it a conservative assumption.

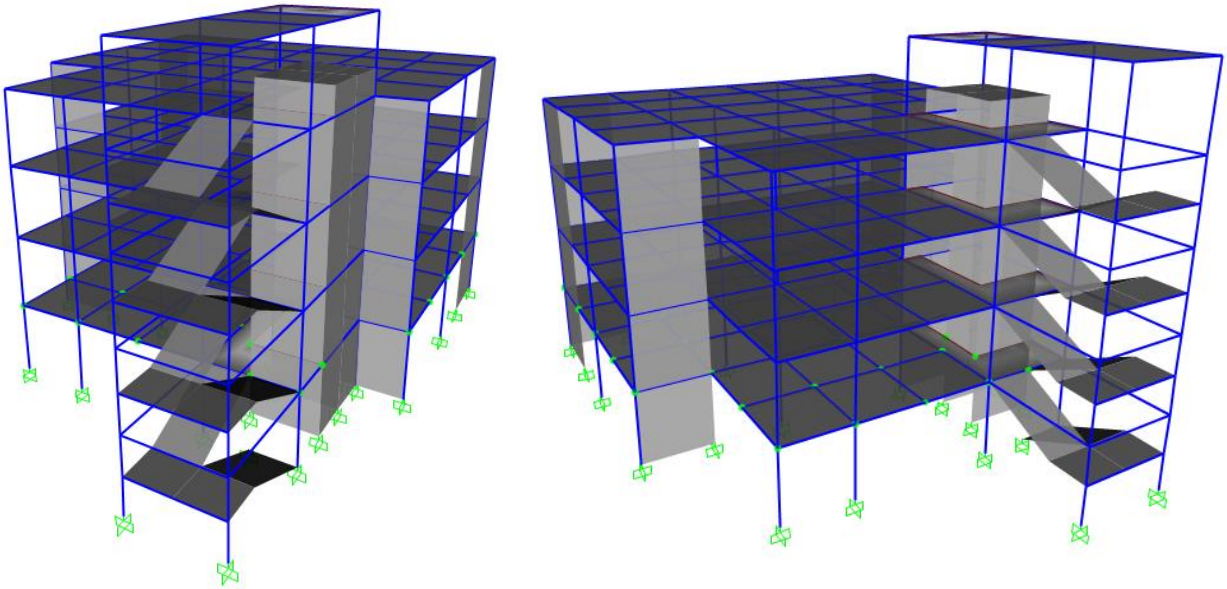

Figure 5-5 - Structural analysis model

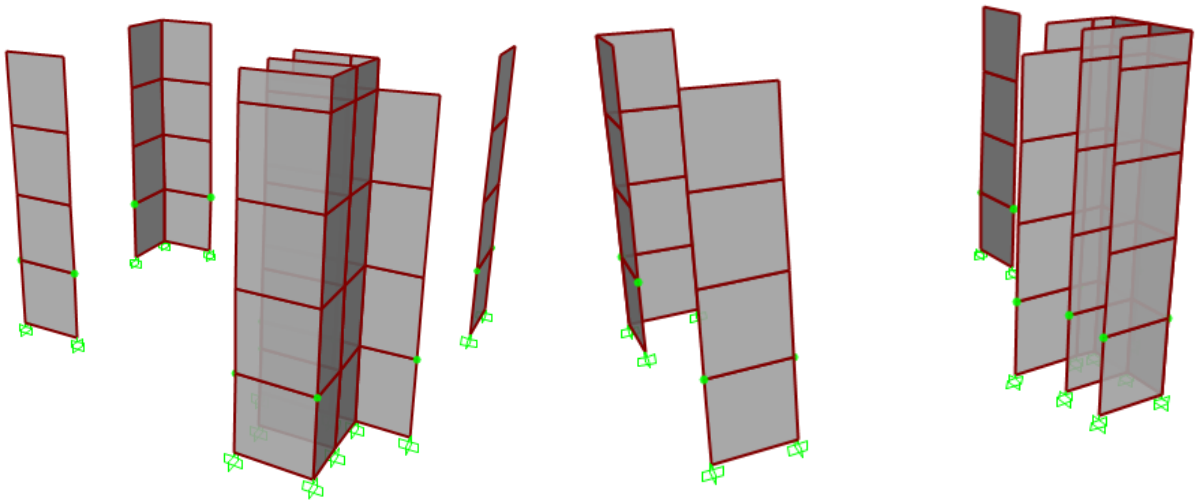

Figure 5-6 - Shear wall configuration

For all structural members, concrete of class M20 and rebar of quality HYSD500 is used:

Table 5-4 - Material properties

Materials	Characteristic strength [MPa]	Modulus of elasticity [MPa]	Poisson ratio [ν]	Weight [kN/m^3]
Concrete - M20	20	22 360	0.3	25
Rebar – HYSD500	500	200 000	0.2	77

The shear walls were modeled as nonlinear layered shell elements. The mesh size was configured to be maximum 800x800mm. The shear walls have the following configuration:

Table 5-5 - Shear wall configuration

	Type	Thickness	σ_x	σ_y	σ_{xy}
Concrete	Membrane	230mm	NL	NL	NL
Rebar Top Vert.	Membrane	0.753mm	NL	-	NL
Rebar Top Hor.	Membrane	0.753mm	NL	-	NL
Rebar Bot. Vert.	Membrane	0.753mm	NL	-	NL
Rebar Bot. Hor.	Membrane	0.753mm	NL	-	NL

Center of mass and rigidity is calculated after procedures presented in chapter 3.5.

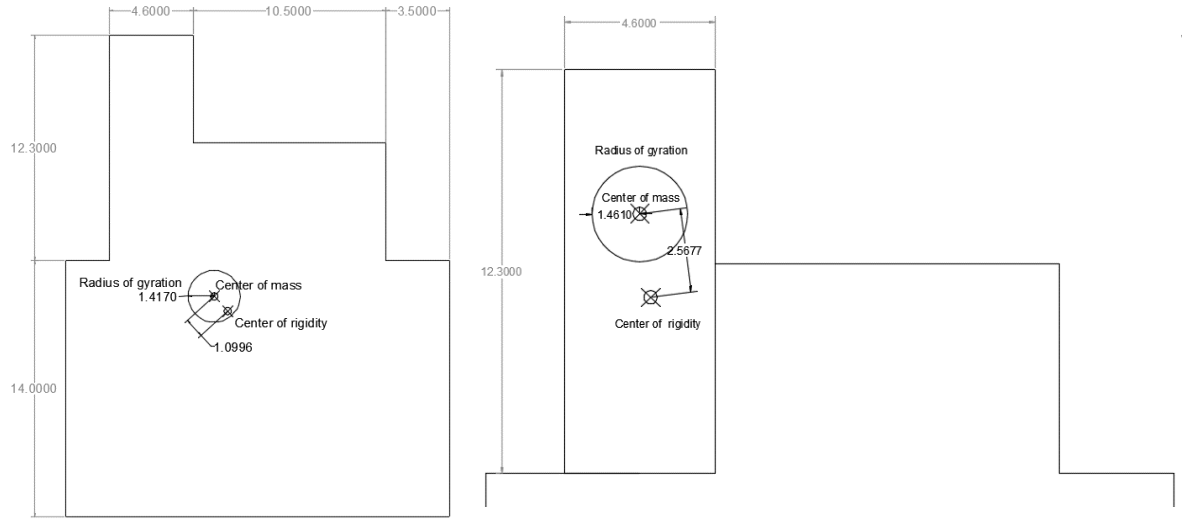

Figure 5-7 - Center of mass- and rigidity, and radius of gyration for main floors and mumty

As the loading schemes according to EC8 and IS1893 were quite similar, calculations for torsional radii were conducted for EC8-model, but deemed applicable for IS1893-model:

Table 5-6 - Torsional parameters

	Center of mass [mm]		**Eccentricity [mm]**			**Torsional radius [mm]**		**Radius of gyration [mm]**
	x	y	e_{0x}	e_{0y}	e_0	r_x	r_y	l_s
Story 2- Roof	8 067	12 030	798	820	1144	11 707	9 946	1 417
Mumty	4 700	20 300	333	935	993	5 339	6 116	1 461

Rigid diaphragm constraints were assigned to all nodes connected to the floor slabs at each story. This is applicable for both EC8 and IS1893 as the depth of the floor slabs is sufficient. The floor mesh size was set to maximum 800x800mm to properly include the interaction between the slab and beams.

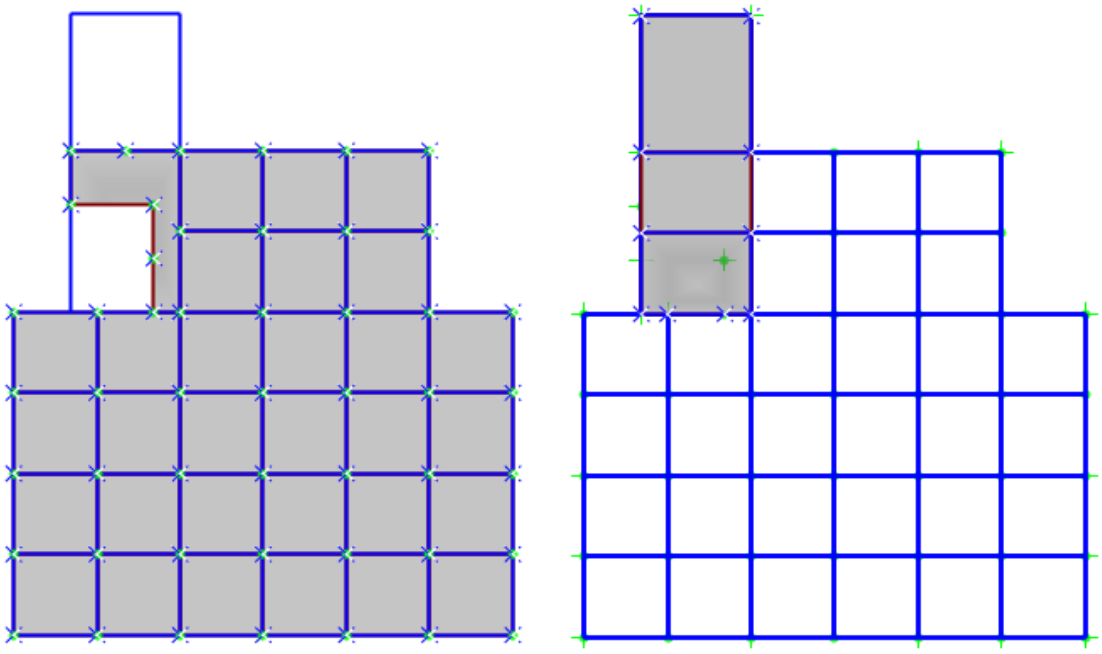

Figure 5-8 - Diaphragm constrains. Left side. floor 1-roof, right side: mumty

As the differences regarding loading and effective stiffness yield quite similar results in a modal analysis, only the modal analysis for EC8 is presented.

A total of 450 modes were used in the analysis, achieving modal load participation of $[u_x, u_y, u_z] \approx 100\%$. The four first, and most prominent modes are:

Table 5-7 - Modal mass participation

Modal mass participation ratio

Mode	Period [s]	U_x	U_y	R_z
1	0.43	0%	46%	23%
2	0.33	61%	0%	4%
3	0.30	0%	22%	30%
4	0.22	7%	0%	10%

Where U_x and U_y is displacement in x-, y-direction and R_z is torsional rotation.

From the results it can be seen that is a significant torsional effect on this building. This is to be expected due its irregular plan structure. The modal analysis also indicates that the mumty seems to be the most fragile part of the structural design.

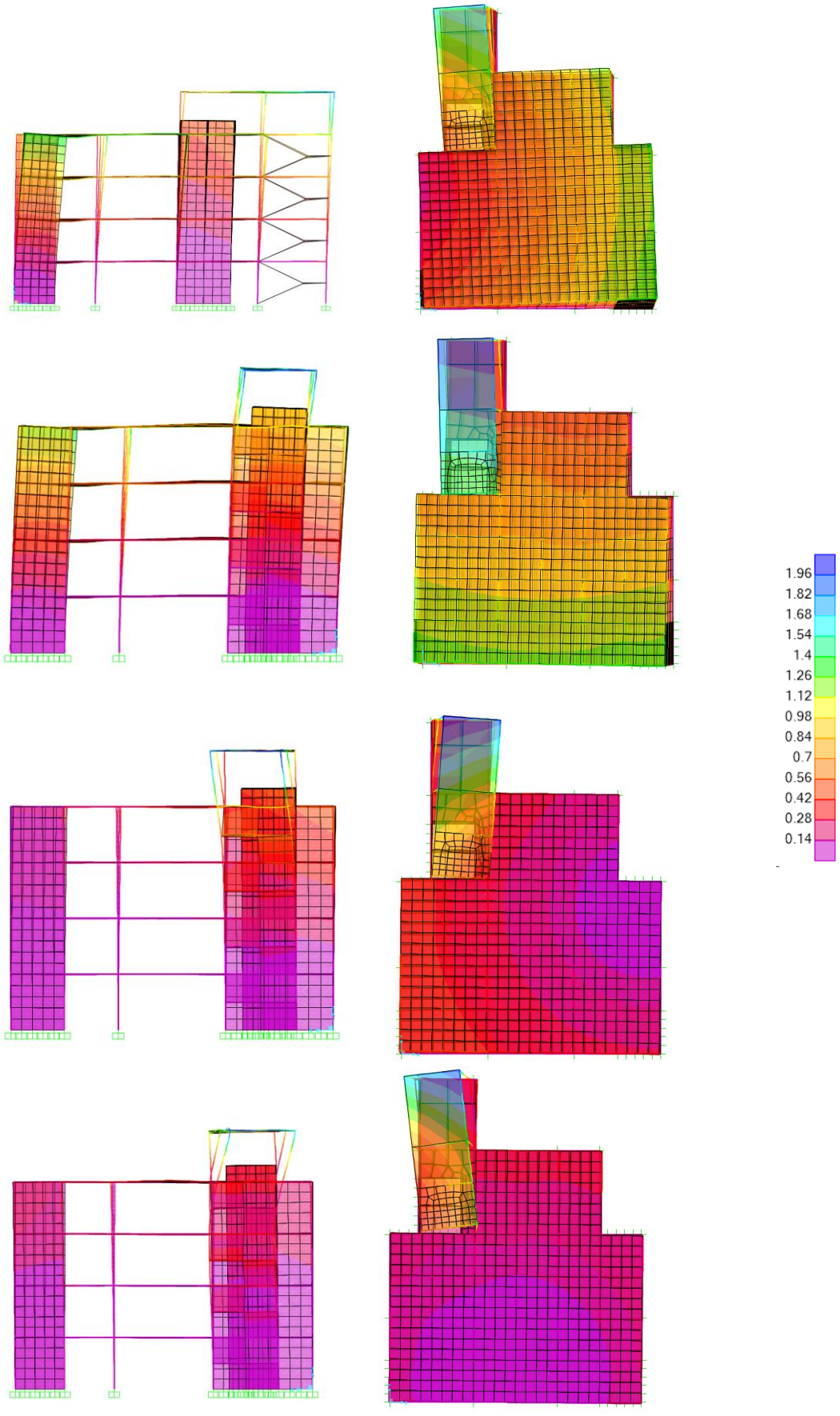

Figure 5-9 - First four mode shapes in ascending order. Color-coding show resultant displacement.

As the behavior of the stairway seems to be of great significance regarding the structural reliability, the inter-story drift calculated in the following chapters are calculated for both the gravity center and corner of the stairway.

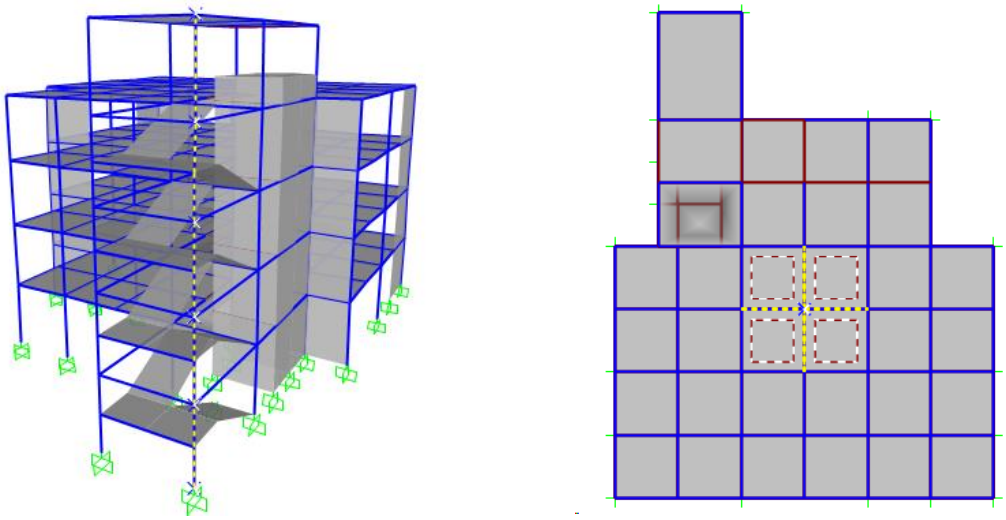

Figure 5-10 - Location of nodes for calculation of inter-story drift. L.S Stairway, R.S. gravity center

For the nonlinear analysis model some changes were made to account for nonlinearity and to improve computational efficiency.

Table 5-8 - Changes to analysis model for nonlinear behavior

	Pushover	**Time History**
Column hinges	Fiber P-M2-M3	Fiber P-M2-M3
Primary beam hinges	M3-Hinges (Auto ASCE 41-13)	Fiber P-M2-M3
Secondary beam hinges	M3-Hinges (Auto ASCE 41-13)	No hinge assigned
Shear wall	No additional meshing	No additional meshing

For the direct integration time-history analysis, the rebar configurations of the columns in the stairway was increased. This is further discussed in Chapter 5.4.3

5.2 EC8

The building is regular in elevation while irregular in plan, so a spatial analytical model is required. The original design considered a high degree of ductility due to a dual frame-, and shear wall system. In a comparative study of code provisions for ductile reinforce concrete structures [23], the highest ductility category for dual frames after IS1893 (SMRF) was seen to approximate the ductility category DCM in Eurocode 8. The structure is therefor set to follow the criteria of DCM.

Values for peak ground acceleration were obtained from the conference paper *"Comparative study of seismic hazard of Kathmandu valley, Nepal with other seismic prone cities"* [9]. The seismic hazard described in this paper is based probabilistic seismic hazard analysis, were the level of seismicity and obtained PGA is comparative to cities such as Sendai, Japan and Los Angeles, USA.

The following design parameters were used in the analysis:

Table 5-9 - Seismic design parameters - EC8

Peak ground acceleration (95-year return)	0,26 [g]
Peak ground acceleration (475-year return)	0,49 [g]
Peak ground acceleration (2475-year return)	0,76 [g]
Design vertical ground motion	$0.9a_g$
Ground type: [24]	C
Soil factor (S)	1,15
Tb(s)	0,2 [s]
Tc(s)	0,6 [s]
Td(s)	2 [s]
Damping	5%
Importance factor IV	1,4

The design ground accelerations are then calculated as:

$$a_{g,No\ Collapse} = 1.4 \cdot a_{g,475} = 0.69g \tag{5.1}$$

$$a_{g,Damage\ Limitation} = 1.4 \cdot a_{g,475} = 0.36g \tag{5.2}$$

Dead loads obtained from the architectural design, and imposed loads according to EC8 are as follows:

Table 5-10 – Characteristic loads - EC8

Dead loads	Floor finishing and partitions	2,5 kN/m^2
	Brick walls (350x3650mm)	19 kN/m
Imposed Loads	Rooms	2 kN/m^2
	Stairways and passages	4 kN/m^2
	Accessible roof	1,5 kN/m^2
	Inaccessible roof	0,75 kN/m^2

For the imposed loads a quasi-permanent load factor is assigned:

$$\psi_{E,floor} = \psi_{2,floor} \cdot \varphi_{floor} = 0.15$$
$$\psi_{E,roof} = \psi_{2,roof} \cdot \varphi_{roof} = 0.28 \quad (5.3)$$

The seismic weight considered in all seismic analysis is then:

$$\sum G_{k,i} + \sum(\psi_{E,i} \cdot Q_{k,i}) \quad (5.4)$$

For the damage limitation demand, the following limits are set:

Table 5-11 - Drift limits, Damage limitation

Nonstructural component	Drift limit
Brittle	0.5%
Ductile	0.75%
Non-interfering	1%

5.2.1 Behavior factor

The process of determination of the behavior factor was done in two parts. First the initial behavior factor was determined by the regulations in the code. After a preliminary response spectrum analysis, with the initial behavior factor, a pushover analysis was performed to modify the behavior factor.

5.2.1.1 Initial behavior factor:

The building is deemed irregular in plan and regular in elevation. The building is set to satisfy DCM. The structure is classified as a dual frame system, as it is a combination of columns for vertical loads, and shear walls to resist the majority of the lateral loads.

First, an elastic lateral force analysis is performed to determine if the dual structural system is classified as *frame-* or *wall-equivalent.* In a preliminary analysis it was determined how much of the base shear that was obtained by the shear walls:

$$\frac{V_{wall,x}}{V_{b,x}} = \frac{8\,821kN}{10\,759kN} = 82\% \tag{5.5}$$

$$\frac{V_{wall,y}}{V_{b,y}} = \frac{8\,336kN}{10\,759kN} = 77\% \tag{5.6}$$

As more than half the total base shear is sustained by the shear walls, the structural system is classified as a *wall-equivalent dual system.* Per clause 4.3.6.1 (4) the interaction of masonry infills can then also be neglected.

Furthermore, it is investigated if the structure is classified as torsional rigid, according to clause 5.2.2.1 (4).

Table 5-12 - Evaluation of torsional effect

	Eccentricity [mm]		**Torsional radius [mm]**				**Radius of gyration [mm]**
	e_{0x}	e_{0y}	$0.3r_x$	$0.3r_y$	r_x	r_y	l_s
Story 2-Roof	798	820	3 512	2 984	11 707	9 946	1 417
Mumty	333	935	1 601	1 850	5 339	6 116	1 461

After the following relations, it is determined that the structural system is torsional rigid:

$$[e_{0x}, e_{0y}] \leq 0.3[r_x, r_y] \tag{5.7}$$

$$l_s \leq [r_x, r_y] \tag{5.8}$$

With this classification set, the factor k_w is set after clause 5.2.2.2 (11), where α_0 is the prevailing aspect ratio of the walls in the structural system.

$$\alpha_{0,x} = \frac{3 \cdot 14.6m}{2 \cdot 3.5 + 4.66} = 3.76 \geq 2 \tag{5.9}$$

$$\alpha_{0,y} = \frac{5 \cdot 14.6m}{4 \cdot 3.5 + 7} = 3.91 \geq 2 \tag{5.10}$$

$$k_{w,x} = 1 \tag{5.11}$$

$$k_{w,y} = 1 \tag{5.12}$$

The initial behavior factor is thereby set to:

$$q = q_0(= 3) \cdot \left(\frac{1 + 1.2}{2}\right) \cdot k_w = 3.3 \tag{5.13}$$

After a pushover analysis is performed, see chapter 5.2.3, the behavior factor is modified.

$$q = q_0(= 3) \cdot 1.5 \cdot k_w = 4.5 \tag{5.14}$$

5.2.2 Linear elastic analysis

For linear-elastic analysis the effective stiffness (cracked concrete) is reduced from the gross stiffness due to the hysteretic loading effect that earthquakes yield, according to clause 4.3.1(7). The torsional stiffness is reduced per recommendations in the book *"Seismic Design of Concrete Buildings to Eurocode 8"* [18].

Table 5-13 - Cracked concrete stiffness

Effective moment of inertia – column	50% of uncracked
Effective moment of inertia – beam	50% of uncracked
Effective torsional stiffness	10% of uncracked

The linear elastic analyses follow the procedure of appendix B-1:.

The lateral force method is applied for the first mode in the x-y- direction. The modes are obtained by modal analysis of the structure, as the model is already prepared for more detailed analysis.

To achieve a modal load participation ratio of 90% for x-, y- and z- direction a total of 450 modes were used in the response history analysis.

For all linear analysis, horizontal directional values are calculated as:

$$E_{Edx} \pm 0.3E_{Edy} \tag{5.15}$$

$$E_{Edy} \pm 0.3E_{Edx} \tag{5.16}$$

Results from initial lateral force- and response spectra analysis with behavior factor $q = 3.3$.

Table 5-14 - Initial response spectrum analysis

	Z [m]	**Seismic weight [kN]**	**Response spectrum - X**		**Response spectrum – Y**	
			F_x	F_y	F_x	F_y
Mumty	18.25	550	748	419	648	563
Roof	14.6	6 045	5 389	2 061	2 085	4 681
4	10.95	7 625	8 679	2 937	3 155	7 337
3	7.3	7 625	10 587	3 606	3 876	9 078
2	3.65	7 625	11 646	4 118	4 579	10 109
Sum/base	0	**29 470**	**11 646**	**4 118**	**4 579**	**10 109**

After the pushover analysis was conducted the behavior factor was increased to $q = 4.5$. As the main mode of vibration for x-, y-direction yields the same spectral acceleration, the results for lateral force method will be equal in both directions.

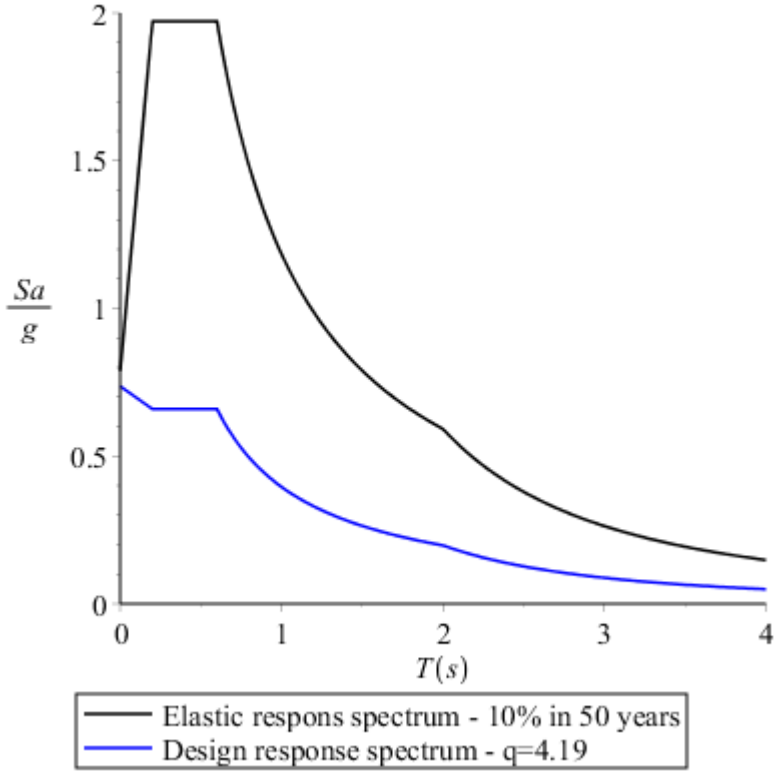

Figure 5-11 - Design response spectrum - Eurocode 8

Table 5-15 - Response spectrum analysis - modified behavior factor

	Z [m]	Seismic weight [kN]	L.F [kN]		R.S.-X [kN]		R.S.-Y [kN]	
			X/Y	Y/X	X	Y	X	Y
Mumty	18.25	1 009	373	118	566	330	167	491
Roof	14.6	5 559	4 341	1 325	4 102	1 617	3 557	1 673
Story 4	10.95	7 636	7 562	2 280	6 473	2 230	5 457	2 424
Story 3	7.3	7 636	9 699	2 919	7 949	2 728	6 747	3 028
Story 2	3.65	7 636	10 965	3 289	8 876	3 212	7 636	3 539
Sum/Base	**0**	**29 476**	**10 965**	**3 289**	**8 876**	**3 212**	**7 636**	**3 539**

With both the peak ground acceleration of 50% and 10% probability of occurrence available, the reduction factor to transform the drifts can be calculated directly.

$$\nu = \frac{a_{g,475}}{a_{g,95}} = 0.53 \tag{5.17}$$

This is higher than the recommended values from the Eurocode, which can be explained by the abnormal seismicity of the region in question.

Table 5-16 - Drift limits - Damage limitation

$\frac{d_I}{H_i} \leq \frac{0.5\%}{0.53} = 0.94\%$	Structures with brittle non-structural elements
$\frac{d_I}{H_i} \leq \frac{0.75\%}{0.53} = 1.41\%$	Structures with ductile non-structural elements
$\frac{d_I}{H_i} \leq \frac{1\%}{0.53} = 1.88\%$	Structures with non-interfering non-structural elements

The inter-story drift was calculated for both the gravity center and the stairway and the corner stairway with locations presented in Figure 5-10 - Location of nodes for calculation of inter-story drift.

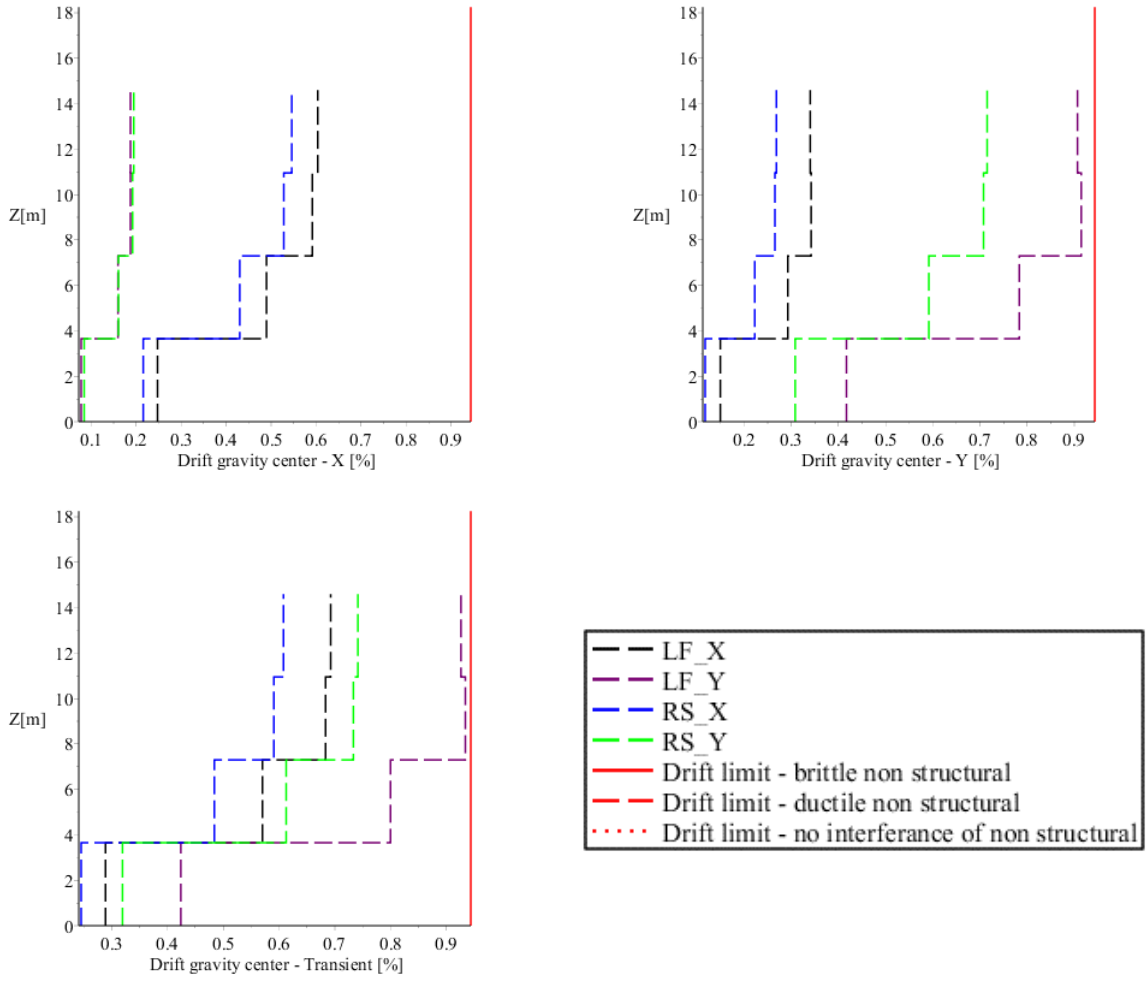

Figure 5-12 - Interstory drifts at gravity center

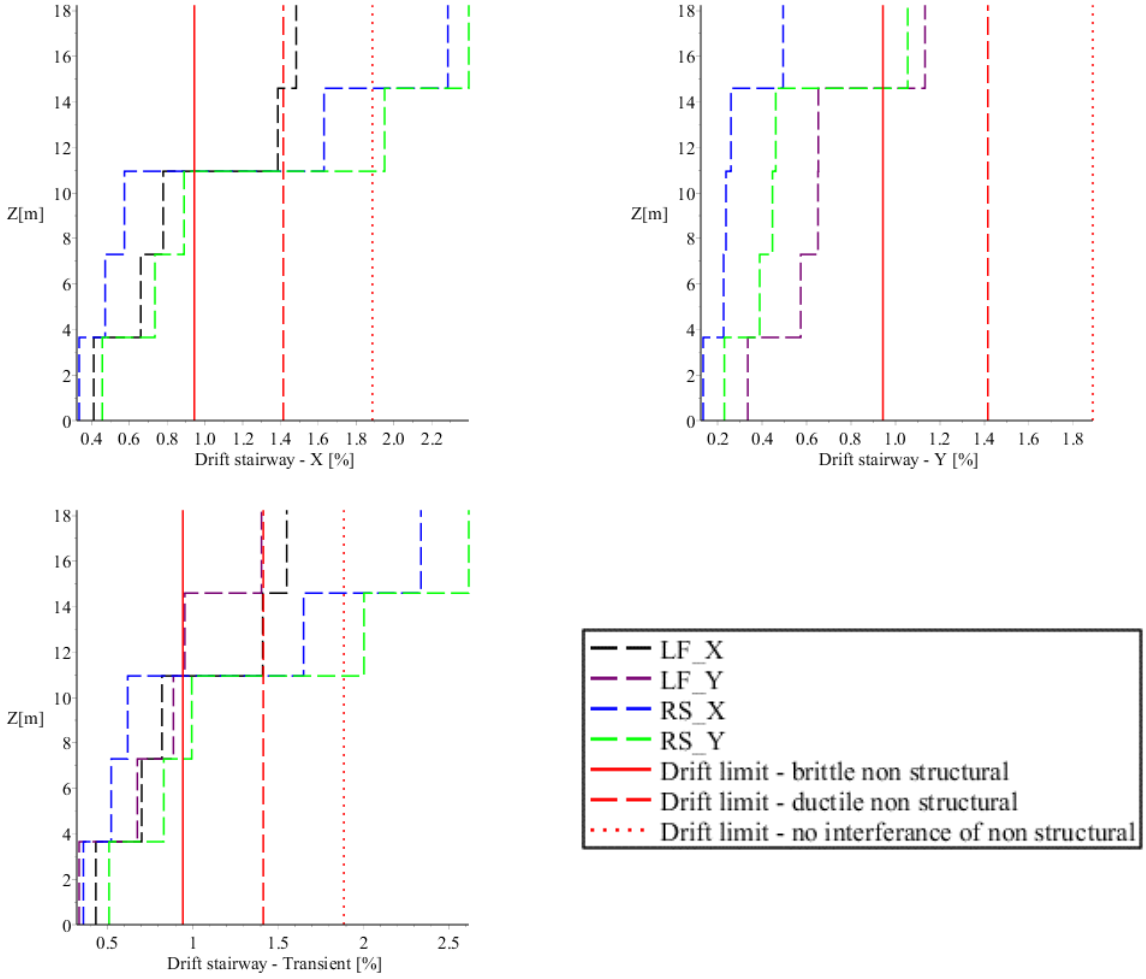

Figure 5-13 - Interstory drifts at stairway

The main building is just within the requirements of *damage limitation* for structures with brittle nonstructural components. The stairway on the other hand does not fulfill these requirements, with the most unfavorable results obtained from the response spectrum analysis.

These analyses also exemplify the difference of the lateral force- and response spectrum analysis methods. Even though the structure fulfills the requirements for use of lateral force method, and said analysis yields a significantly higher base shear, the response spectrum analysis yields a more conservative result with regards to torsional displacements.

Ultimately, the structure does not fulfill the *damage limitation* demand of Eurocode 8.

5.2.3 Non-linear Static Analysis

Plastic hinges were manually assigned to all locations with possibility of plastic hinge formation. For this analysis fiber hinges were assigned to all columns, and M3 hinges to all beams following table 10-7 of ASCE 41-13. In SAP2000 the hinges following ASCE 41-13 has the possibly to display graphically the hinge state, making it very easy to determine the first yield point (as the first yield most likely occur in the beams) for the over-strength factor.

The analysis follows the N2-method (Fajfar 2000) presented Annex B in EC8, and the analysis procedure is presented in appendix B-2:.

As the pushover analysis is mostly suited for regular buildings with regular mode shapes. It is therefore chosen to use the pushover analysis to determine the response of the main structure and including the mumty into the roof-level. The story shear and inter-story drift is though displayed for the target displacements.

To perform the pushover analysis, two load cases were generated in SAP2000. To each load case a lateral acceleration load was introduced. The load was set to increase incrementally until a target displacement in the control node was reached. The control nodes were assigned at the center-edges of the roof-level. P-delta effects were also accounted for.

The target displacement was set way beyond what was expected of the structure to resist, to capture the full behavior of the structure. As the structural model is quite complex, the degradation after peak base force was not captured well by the analysis. The range captured though is sufficient for analysis with the given structural demand.

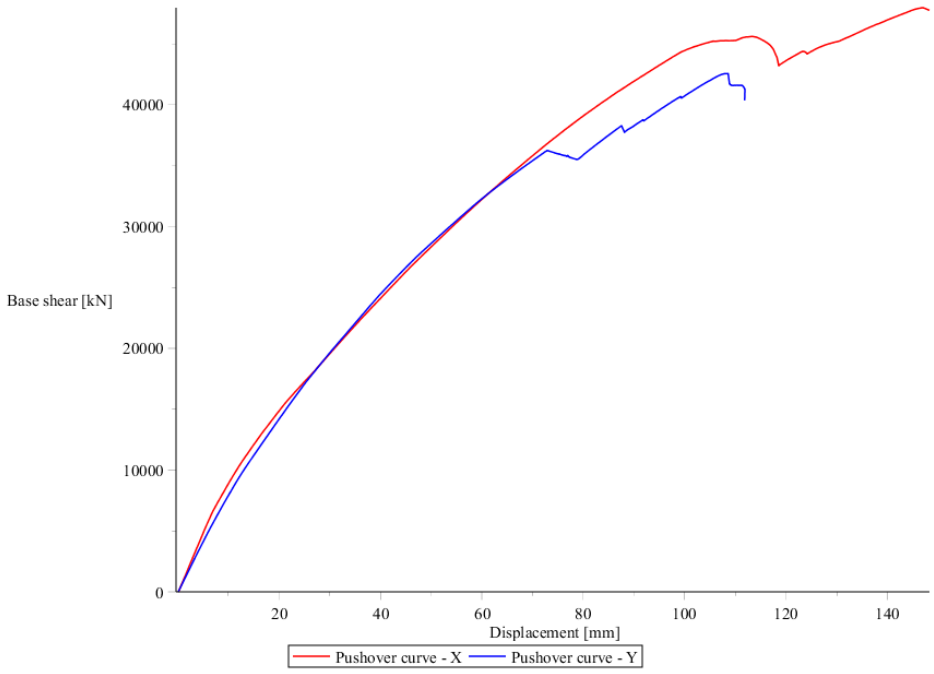

Figure 5-14 -Pushover curve

The displacement shape is derived from the linear part of the pushover analysis:

Table 5-17 - Displacement shape

	Φ_x	Φ_y	Seismic weight [kg]
Roof	1	1	670 521
Level 4	0.70	0.73	778 389
Level 3	0.41	0.45	778 389
Level 2	0.15	0.17	788 389

The transformation factor is established:

$$\Gamma_x = \frac{\sum m_i \Phi_i}{\sum m_i \Phi_i^2} = 1.376 \tag{5.18}$$

$$m_x^* = \sum m_i \Phi_i = 15\,191 kN \tag{5.19}$$

The location of the plastic mechanism "A" is determined graphically from the idealized pushover curve.

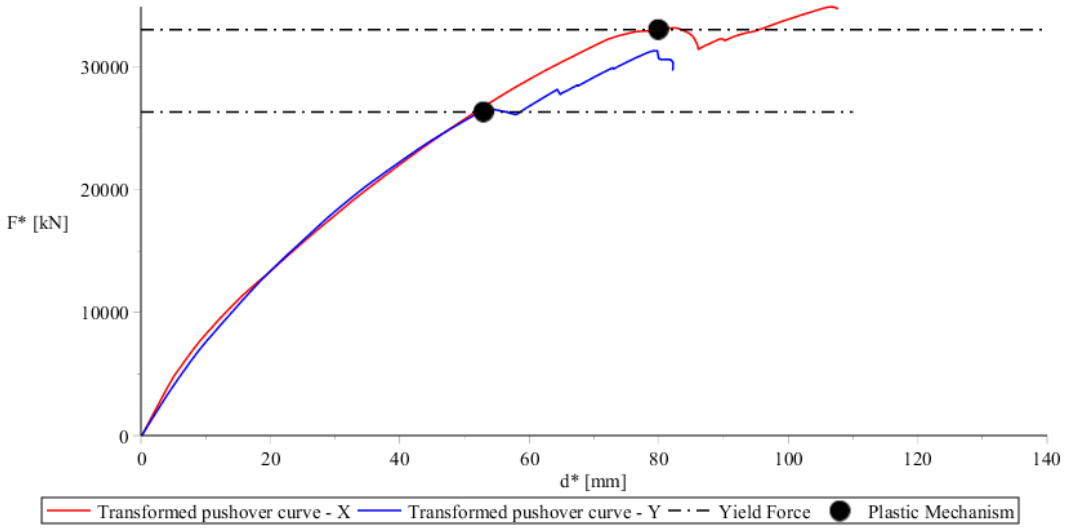

Figure 5-15 - Idealized pushover curves

Further, calculations followed the steps in Chapter 4.1.6.1. The following target displacements and design parameters were obtained:

Table 5-18 - Target displacements – Pushover analysis

	d[mm]	F_{base} *[kN]*
$d_{t,x,no\ collapse}$	80	39 180
$d_{t,x,damage\ limitation}$	42	25 218
$d_{t,y,no\ collapse}$	86	37 842
$d_{t,y,damage\ limitation}$	39	24 179

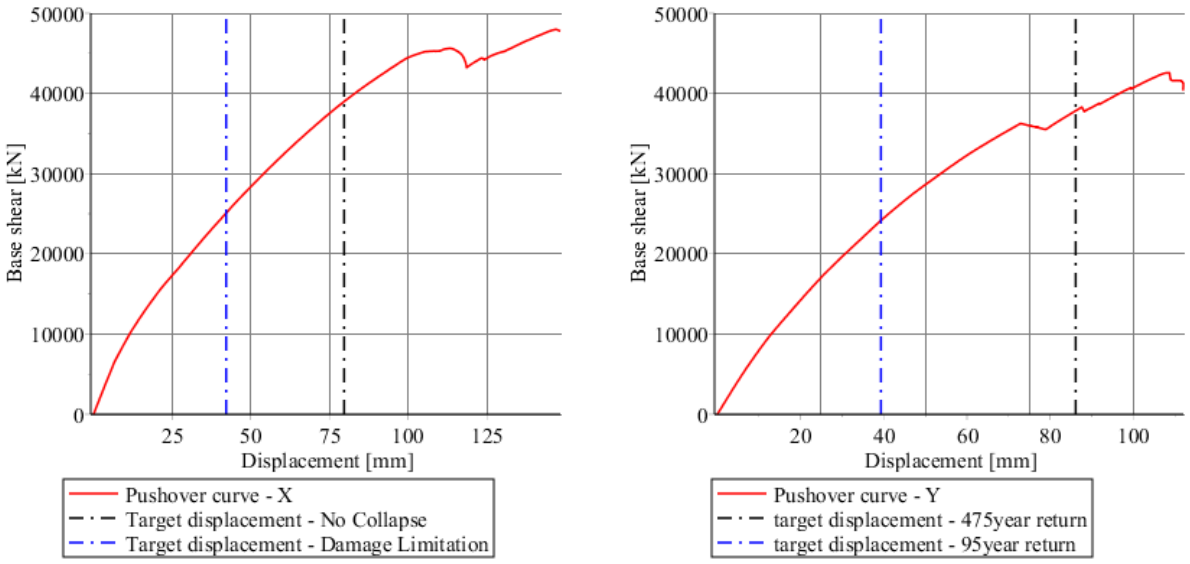

Figure 5-16 - Target displacements in x-, y-direction

At the target displacements, design parameters such as inter-story drifts and story shear forces were obtained:

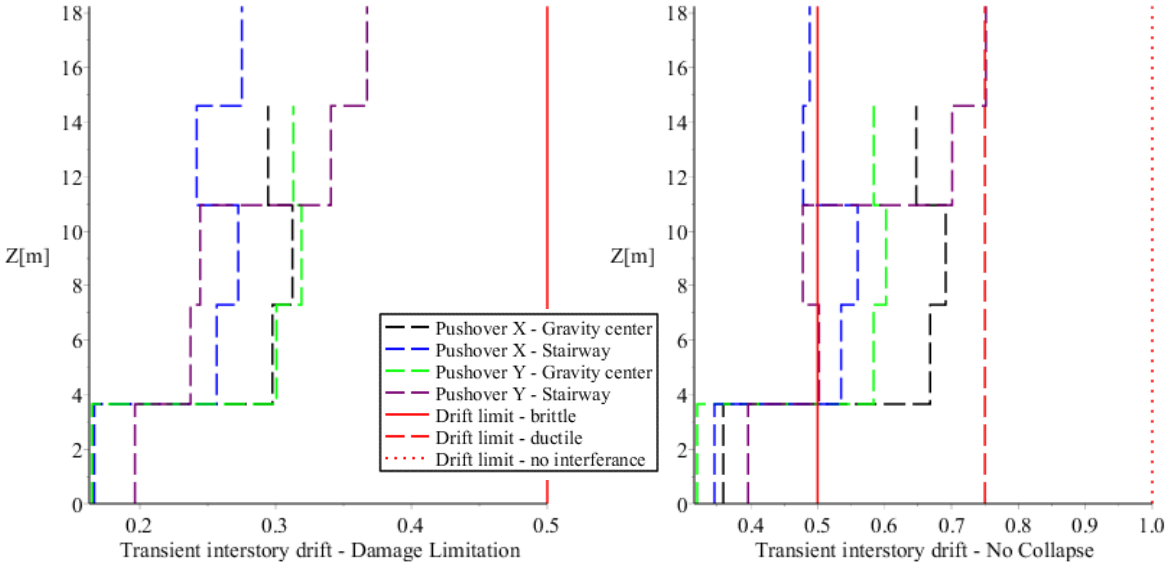

Figure 5-17 - Inter-story drifts at target displacements

Table 5-19 - Design values from pushover analysis

	Damage limitation						Collapse Prevention					
	Pushover X			Pushover Y			Pushover X			Pushover Y		
	Drift [%]		Vx [kN]	Drift [%]		Vy [kN]	Drift [%]		Vx [kN]	Drift [%]		Vy [kN]
	Center	Stair		Center	Stair		Center	Stair		Center	Stair	
Mumty	0.39%	0.37%	388	1.45%	0.27%	355	1.06%	0.70%	649	3.23%	0.47%	892
Roof	0.32%	0.34%	5 812	1.14%	0.22%	5 477	0.58%	0.64%	9 131	2.16%	0.42%	8 276
Level 4	0.32%	0.24%	11 679	0.81%	0.23%	11 237	0.60%	0.43%	18 221	1.55%	0.46%	17 283
Level 3	0.30%	0.24%	17 562	0.48%	0.22%	17 061	0.58%	0.46%	27 309	0.92%	0.45%	26 336
Level 2	0.17%	0.20%	25 218	0.17%	0.14%	24 179	0.32%	0.36%	39 180	0.32%	0.27%	37 842
Base	0%	0%	25 218	0%	0%	24 179	0%	0%	39 180	0%	0%	37 842

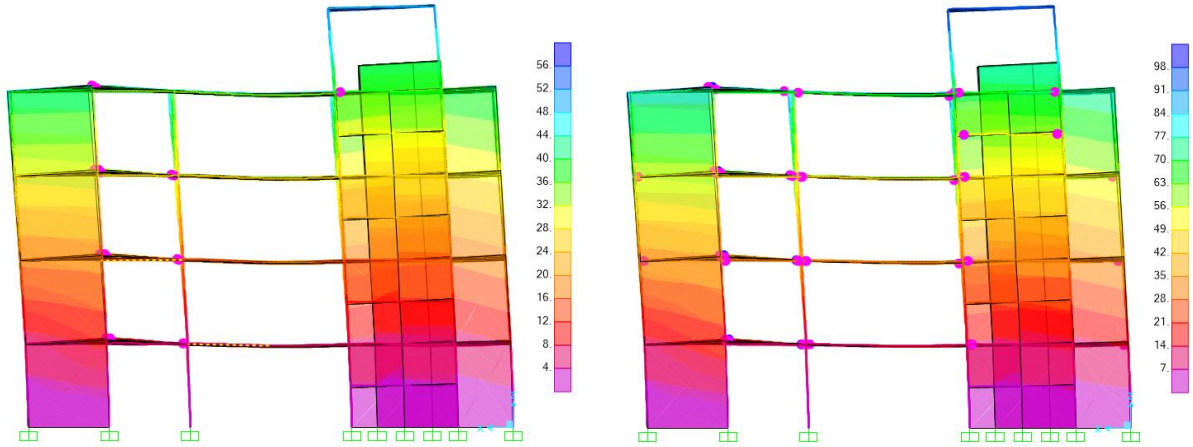

Figure 5-18 - Resultant displacements [mm] – Pushover X. l.s. “Damage limitation”, r.s. “No collapse”

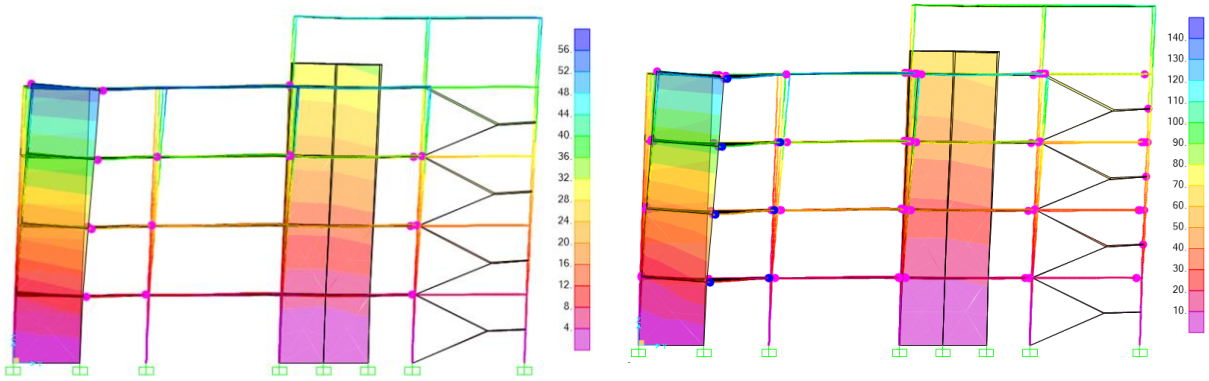

Figure 5-19 - Resultant displacements [mm] – Pushover Y. l.s. “Damage limitation”, r.s. “No collapse”.

Results from the pushover analysis confirms the results from the linear-elastic analysis. The main building complies with the *damage limitation* requirements, while the stairway does not. The interstory of the stairway with *no collapse* seismic hazard is significant. As the pushover analysis has some limitations regarding torsional effects, the results from this analysis should be considered as liberal.

The over-strength value is calculated after clause 5.2.2.2 (3). α_1 is in this case determined by the base shear that first induces a structural member to yield, while $\alpha_1$is determined graphically by the first peak in the pushover curve.

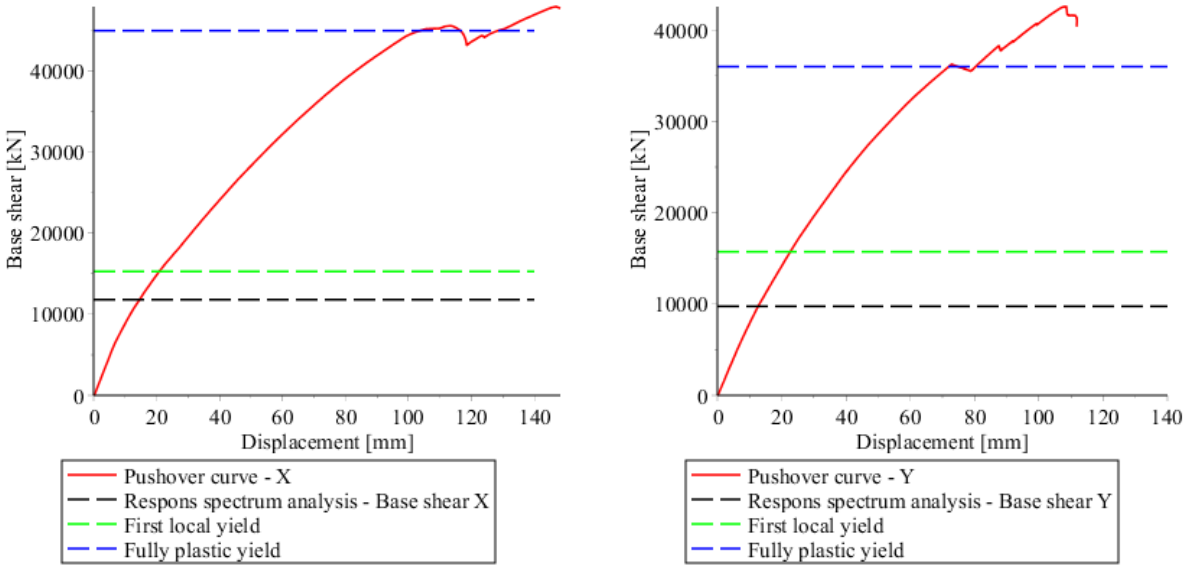

Figure 5-20 - Values for determination of over-strength factor

Table 5-20 - Calculated overstrength factor

	X	**Y**
Shear force – first yield [kN]	15 300	15 725
Shear force – fully plastic [kN]	45 000	36 000
$\frac{\alpha_u}{\alpha_1} \leq 1.5$	2.94	2.29
$\frac{\alpha_u}{\alpha_1}$		1.5

The over-strength factor is further used to modify the behavior factor, which is used in all linear elastic analysis.

Full calculations can be found in appendix C-1:.

5.3 IS1893

For the analysis following IS1893, the following assumptions and requirements are made:

- The lateral load resisting system is classified as *ductile RC structural walls with RC SMRFs.* Structural detailing of the reinforced concrete must comply with IS 456 [25] and IS 13920 [19].
- Seismic zone factor for Nepal, equivalent to Zone V in IS1893. This was used in the proposed structural design and considered "common practice".

The analysis process follows mainly the same steps as the linear-elastic analysis for Eurocode in chapter 5.2.

Table 5-21 - Seismic design parameters - IS1893

Seismic Zone (Z): V	0,36
Ground type: [24]	II
Damping	5%
Importance factor	1,5
Behavior factor	5

For the loading scheme, the same dead loads as defined for Eurocode 8 is used, while imposed loads have been obtained from IS 875 [26].

Table 5-22 - Loading scheme – IS1893

Dead loads	Floor finishing and partitions	2.5 kN/m^2
	Brick walls (270x3650mm)	19 kN/m
Live Loads	Rooms	2 kN/m^2
	Stairways and passages	4 kN/m^2
	Accessible roof	1.5 kN/m^2
	Inaccessible roof	0.75 kN/m^2

The seismic weight of the building is comprised of; characteristic dead loads, 25% of live loads less or equal to $3kN/m^2$, and 50% of imposed loads over $3kN/m^2$.

Table 5-23 - Seismic weight after IS1893

	Weight [kN]
Story 2	7 636
Story 3	7 636
Story 4	7 635
Roof	6 058
Mumty	508
Full seismic weight	**29 930**

Per clause 6.4.31 the moment of inertia for the columns and beams are reduced to the cracked moment of inertia. As with the linear elastic analysis after Eurocode 8, the effective torsional stiffness is also reduced.

Table 5-24 - Cracked concrete stiffness

Effective moment of inertia – column	70% of uncracked
Effective moment of inertia – beam	35% of uncracked
Effective torsional stiffness	10% of uncracked

The building is classified as irregular in plane, and regular in elevation. From the modal analysis, the criteria defined in chapter 4.2.2.3. The three first modes yields a modal mass participation of $[M_x, M_y] = [61\%, 68\%]$, and so does not comply with the criteria. The difference between the two first modes are $0.33s \geq 0.9 \cdot 0.43 = 0.39s$, and so does comply with the criteria.

5.3.1 Lateral force method

The linear elastic analyses follow the procedure of appendix B-1:, with some configurations to comply with IS1893.

The first modes in x-, y-direction are within the range [0.1s, 0.55s], so the seismic design factors are calculated as:

$$A_{h,x}(0.42) = A_{h,y}(0.34) = \frac{\left(\frac{Z}{2}\right)\left(\frac{S_a}{g}\right)}{\left(\frac{R}{I}\right)} = 0.135 \tag{5.20}$$

$$A_v = \frac{\left(\frac{2}{3}\right)\left(\frac{Z}{2}\right)2.5}{\frac{\mathrm{R}}{\mathrm{I}}} = 0.09 \tag{5.21}$$

The total base shear is then calculated by the following:

$$V_B = A_V \cdot W_{seismic} \tag{5.22}$$

Table 5-25 - Base shears - Lateral force method

	Ah	W [kN]	Base shear [kN]
X-direction	0.135	29 963	3 932
Y-direction	0.135		3 932
Z-direction	0.09		2 697

Further, the base shear is distributed to the floors with a linear pattern after the following formula:

$$Q_i = \left(\frac{W_i h_i^2}{\sum(W_i h_i^2)}\right) V_B \tag{5.23}$$

Table 5-26 - Design lateral loads - Lateral force method

	Z [m]	Weight [kN]	V_B [%]	G_i [kN]	V_i [kN]
Mumty	18.25	508	6%	228	228
4	14.6	6 058	44%	1 742	1 970
3	10.95	7 799	32%	1 261	3 231
2	7.3	7 799	14%	561	3 792
1	3.65	7 799	4%	140	3 932
Sum/Base		**29 963**	**100%**	**3 932**	**3 932**

The design shear force is further used to scale the horizontal design spectrum for the response spectrum analysis.

5.3.2 Response Spectrum analysis

With the design parameters from Table 5-21, a preliminary response spectrum analysis was performed. The base results were the used to calculate a scaling factor, to scale the horizontal design spectrum to provide base shears equivalent to the ones obtained by the lateral force method:

Table 5-27 - Scaling of response spectrum

	Base shear – L.F [kN]	**Base shear – R.S [kN]**	$V_{B,L.F} / V_{B,R.S}$
X-direction	3 932	2 538	1.549
Y-direction	3 932	2 206	1.782

Another response spectrum analysis was then performed with increased values. From this point, the seismic response was computed with the following combination:

$$E_{Edx} \pm 0.3E_{Edy} \quad (5.24)$$

$$E_{Edy} \pm 0.3E_{Edx} \quad (5.25)$$

Table 5-28 - Response spectrum analysis results

	Z [m]	**Seismic weight [kN]**	**Response spectrum - X**		**Response spectrum – Y**	
			$F_x[kN]$	$F_y[kN]$	$F_x[kN]$	$F_y[kN]$
Mumty	18.25	508	264	152	224	252
Roof	14.6	6 058	1 833	786	1 894	733
4	10.95	7 799	2 960	1 138	2 968	1 111
3	7.3	7 799	3 609	1 401	3 675	1 364
2	3.65	7 799	3 965	1588	4 093	1 620
Sum/base	0	**29 963**	**3 965**	**1588**	**4 093**	**1 620**

5.3.3 Deformation control

Torsional regularity must be verified, following the procedure of chapter 4.2.2.3. The displacements are obtained from the response spectrum analysis conducted, and the least favorable pair of deflections were selected.

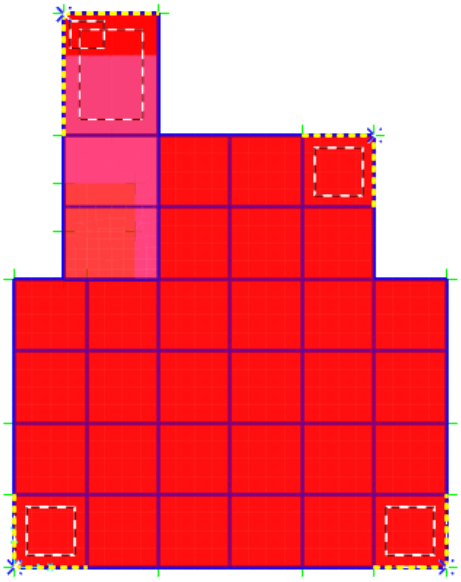

Figure 5-21 - Evaluated nodes

Table 5-29 - Torsional irregularity

	South	West	North	East
Δ_{max}	11.3mm	5.7mm	9.9mm	5.7mm
Δ_{min}	3.8mm	2.9mm	4.4mm	2.9mm
$\frac{\Delta_{max}}{\Delta_{min}}$	3.0	1.9	2.3	1.9

These results are critical. Values of $\frac{\Delta_{max}}{\Delta_{min}} > 2$ deems the building torsionally flexible and is thereby not compliant, as IS1893 does not allow for torsional irregular structures.

The inter-story drift limit is set by clause 7.11.1.1, and is to be obtained by the unscaled response spectrum analysis results:

$$\frac{d_r}{h} \leq 0.4\% \tag{5.26}$$

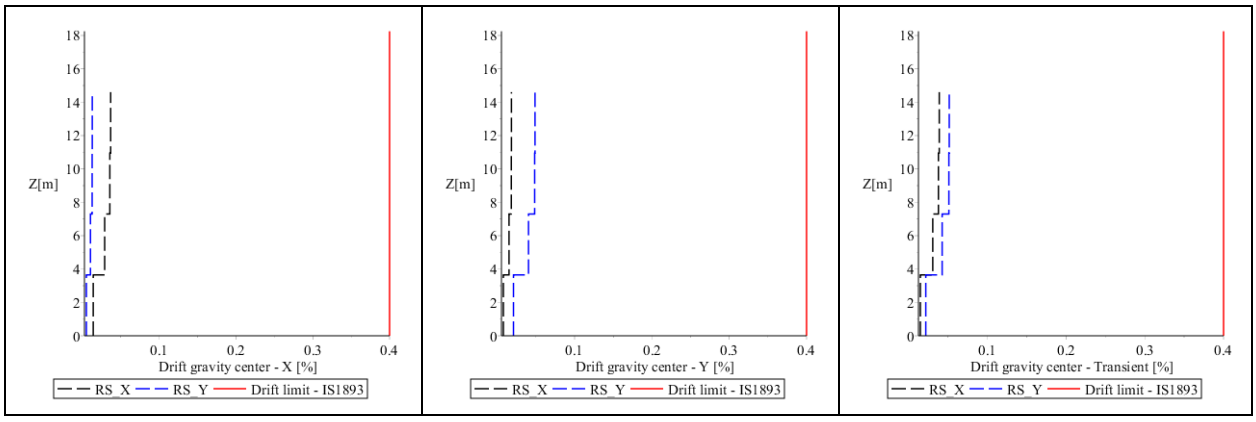

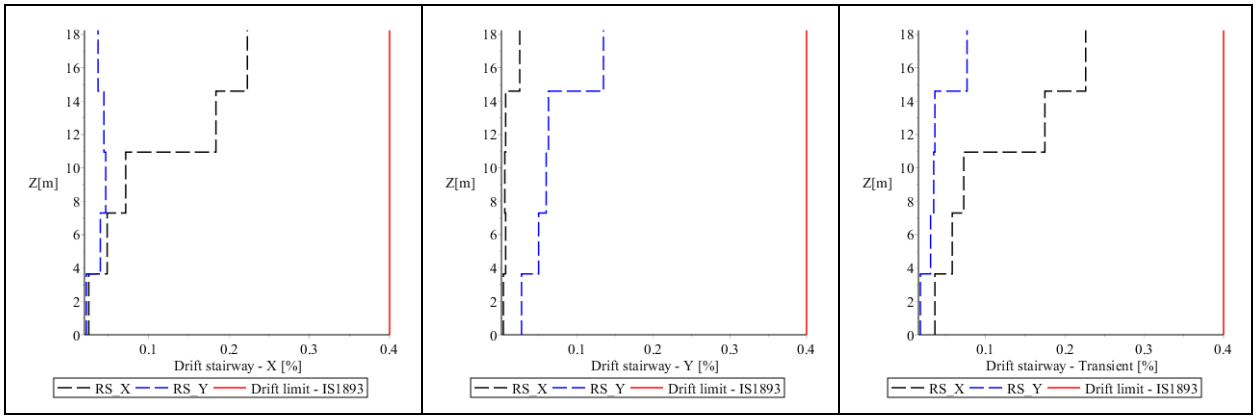

Figure 5-22 - Inter-story drifts, response spectrum analysis, IS1893

The structures behavior is well within the drift-limits established in IS1893.

5.4 Time History Analysis - PBSD

For the time-history analysis seven earthquake ground motions are selected and scaled according to the elastic horizontal spectrum after clause 3.2.2.2 in Eurocode 8. For these spectrums the importance factor is not included in the design ground motion, and the values for 50%-, 10%- and 2% probability of occurrence in 50 years were used.

The ground motions are selected based on earthquake characteristics similar to the specific site, and the records are matched by the first mode and response spectra. It is chosen only one ground motion per earthquake, and in the selection process it was focused on getting variation in response in the records

Table 5-30 - Ground motion selection criteria

Fault type	Reverse + Oblique [7]
Magnitue min,max	6.5-8
Rupture distance	20-60 (far field)
Shear velocity	160-320 (soil classification)
Scaled for period of vibration	[0.36s, 0.3s, 0.28s]

Seven ground motions, which fulfilled the criteria of Table 5-30, were selected from the PEER NGA West database [16]. They were then scaled to match the period of vibrations using minimized square error.

Table 5-31 - Selected time histories

EQ-Name	Mag.	Fault type	Year	Distance [km]	Shear Vel. [m/sec]	S.F. 95year	S.F. 475year	S.F. 2475year
Loma Prieta	6.93	Reverse oblique	1989	25	215	0.82	1.55	2.28
Cape Mendocino	7.01	Reverse	1992	42	337	1.44	2.71	3.98
Northridge	6.69	Reverse	1994	59	338	1.26	2.38	3.50
Chi-Chi, Taiwan	6.62	Reverse oblique	1999	38	318	1.09	2.07	3.05
Taiwan, SMART1	7.3	Reverse	1986	56	275	1.58	2.98	4.38
Chuetsu	6.8	Reverse	2007	23	278	0.69	1.31	1.92
Iwate	6.9	Reverse	2008	32	344	1.50	2.84	4.17
Gorkha Nepal	*8.1*	*Reverse*	*2015*	*60*	-		-	-

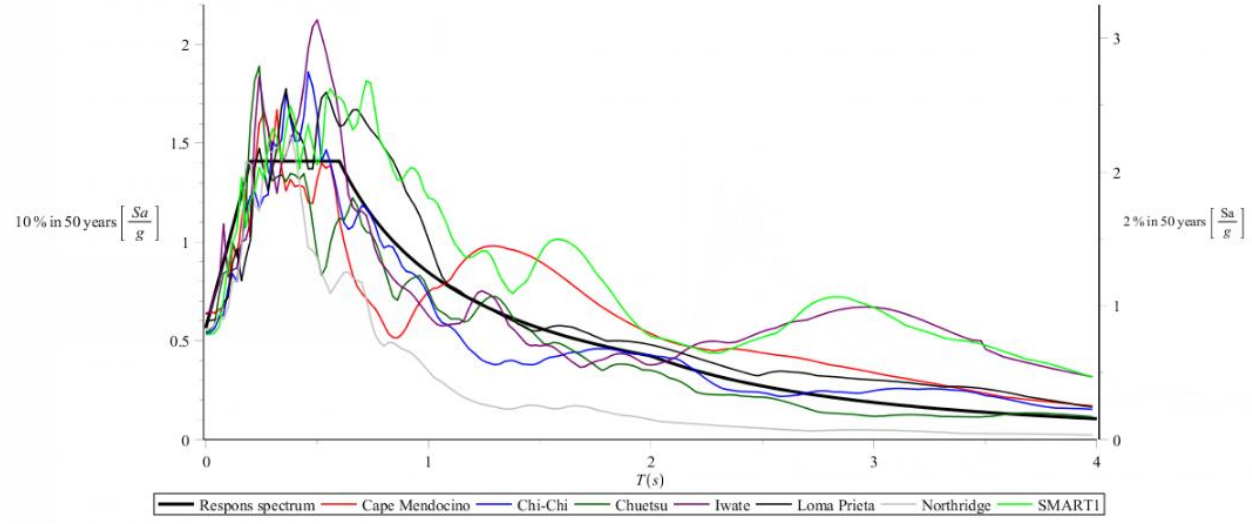

Figure 5-23 - Spectral acceleration of selected ground motions for 475- and 2475year return period

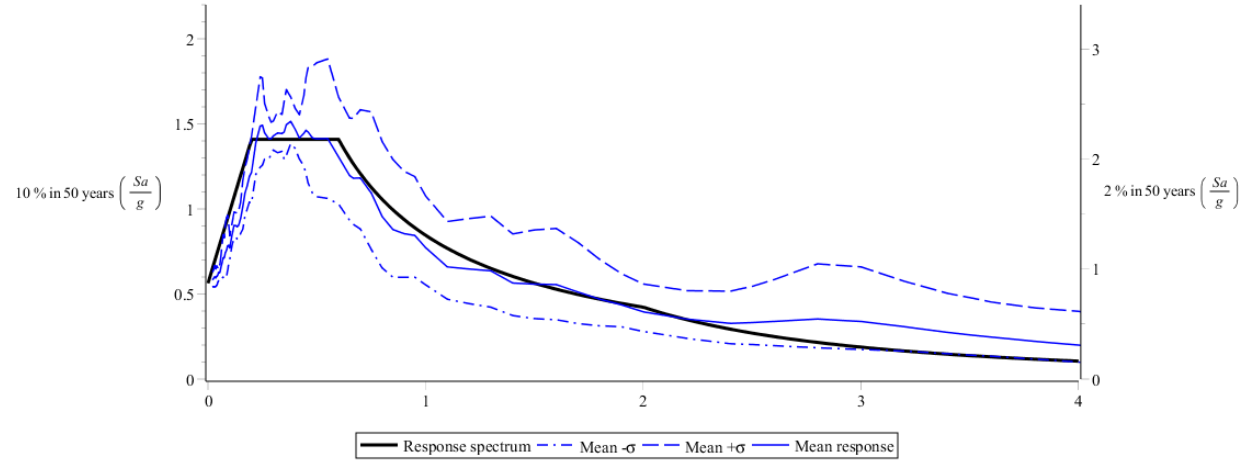

Figure 5-24 - Mean response +- SD for suite of ground motions

As direct integration time-history analysis is very computationally expensive, a further selection was made for a suite of 3 ground motions. This included the ground motions for Cape Mendocino, Northridge and Iwate:

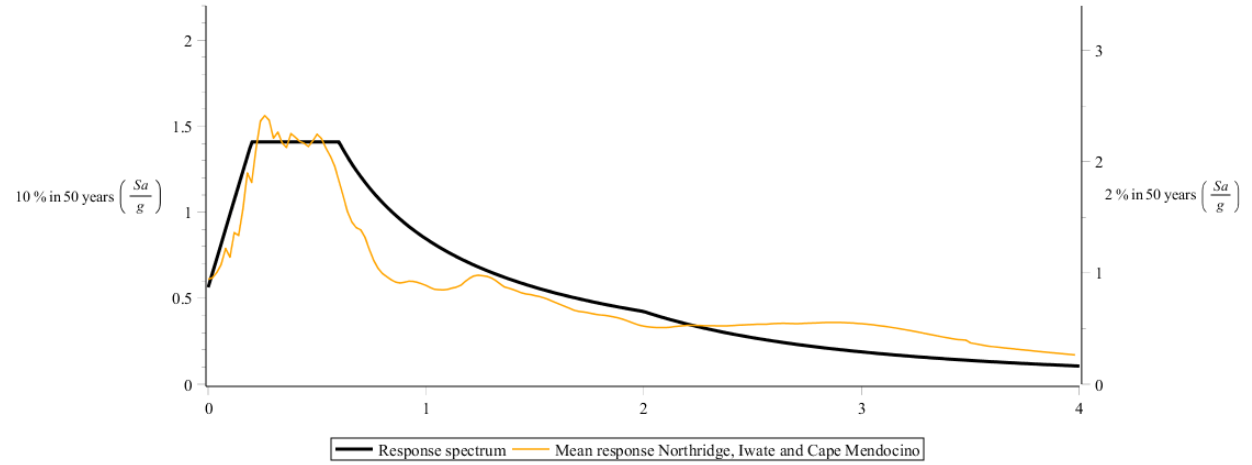

Figure 5-25 - Mean response of three selected ground-motions for direct integration time-history analysis

The three selected ground motions for direct integration time-history analysis were selected based on the mean value in the range 0.1s to 0.4s, as this is the ranges of the modes of vibration of the structure.

The ground motions for the Gorkha earthquake is included as a curiosity to determine the performance of the structure in those circumstances.

Time history analysis were conducted using both *FNA* and *direct integration*. This was done as it was first assumed that the FNA procedure available in SAP2000 would sufficiently represent the non-linear behavior of the structure. Upon further investigation and analysis, this assumption was considered to be incorrect. In the FNA analysis, hinge rotation is greatly underestimated, thereby reducing inter-story drifts and increasing base forces. From investigating hinge results, it seems that when fiber element hinges are transformed to links, the hysteretic degradation is not accounted for. With these limitations in mind, the results are represented in thesis, as the forces and displacements of the analysis model give insight to the behavior of the structure and as a verification of the treatment of the suite of ground motions.

All analyses follow the procedure of the flowchart in appendix B-3:.

5.4.1 Modal linear time-history analysis

Modal linear time-history was conducted for all seven ground motions for earthquakes with 50% probability of occurrence in 50 years. Each ground motion was analyzed in both directions, [N,E,V] and [E,N,V]. A total of 450 modes were considered, resulting in a modal mass participation of 95% in all directions and rotations. It was chosen to perform a linear analysis as the structure is expected to behave solely linearly at these seismic demands. This analysis will therefore only be eligible for evaluating the inter-story drift acceptance criteria.

Results from this analysis can also be used for the linear elastic analysis in Eurocode 8, as the mean spectral acceleration of the suite approximates the design response spectrum of the linear elastic analysis. It will produce slightly conservative results for the main modes of vibration, while the high frequency modes will not properly be represented.

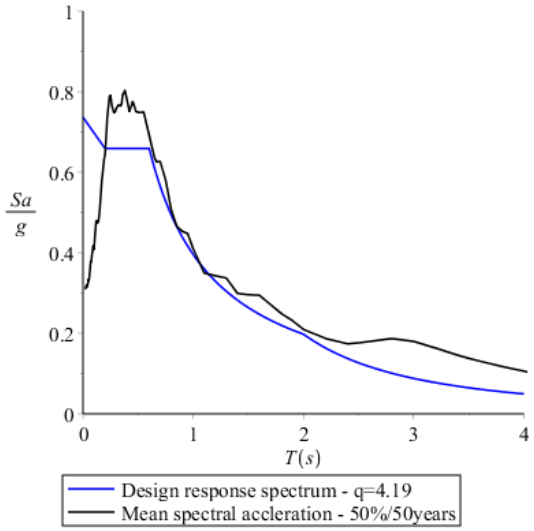

Figure 5-26 - Applicability of ground motions for linear elastic analysis after Eurocode 8

The base reactions from the time-history load cases are combined with a static P-Delta analysis for axial seismic weight. Full base-results and interstory drifts are found in annex D-1:

Table 5-32 - Base reactions for linear modal analysis

	Cape Mendocino	Iwate	Chuetsu	SMART1	Chichi	Northridge	Loma Prieta	**Mean**
Base shear X [kN]	13870	10041	9732	13761	12061	12671	11991	**12018**
Base shear Y [kN]	9867	13214	9143	10625	9834	9697	13553	**10848**
Base force Z [kN]	31519	32845	31949	35062	31376	32319	34804	**32839**
Mx [MNm]	440	498	417	474	455	459	495	**463**
My [MNm]	448	396	415	423	414	419	419	**419**
Mz [MNm]	135	196	122	217	170	129	188	**165**

The small variance in the base forces verifies that the scaling of ground motions is properly performed.

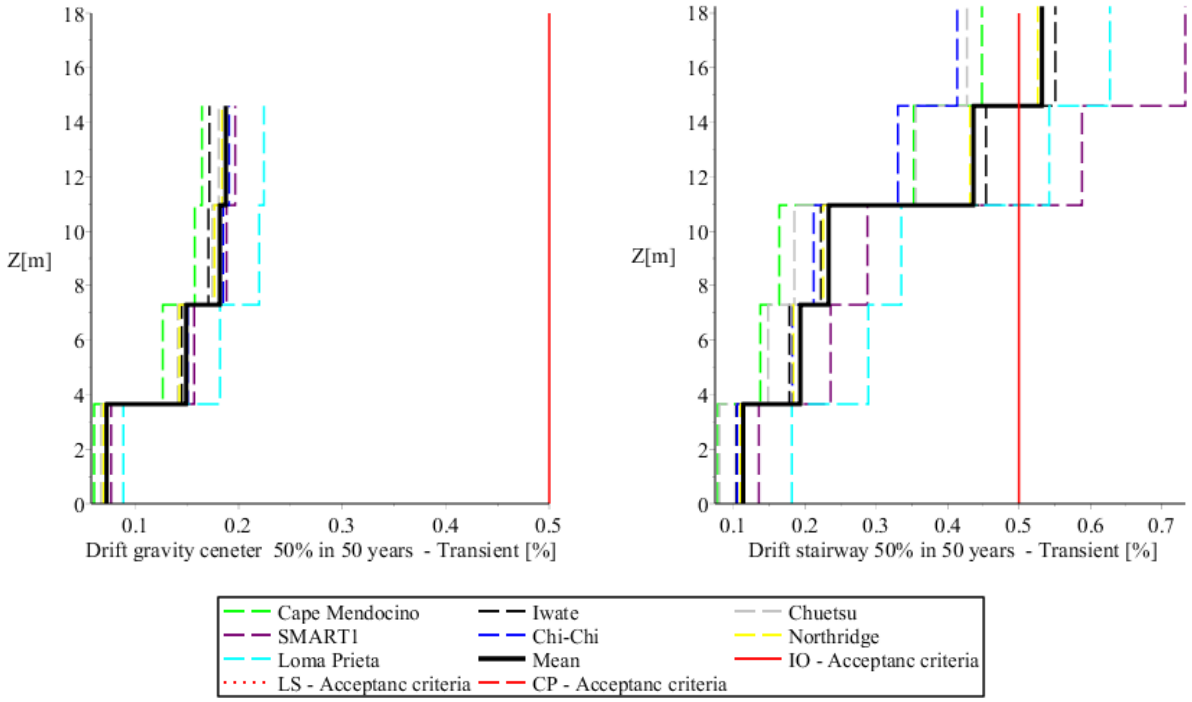

Figure 5-27 - Interstory drifts with 50% probability of occurrence in 50 years

From the interstory drifts it can be interpreted that the core building should be fully operational while the stairway may endure some damage.

5.4.2 Modal nonlinear time-history analysis

FNA analysis was conducted for all seven ground motions for earthquakes of 10%- and 2% probability of occurrence in 50 years. Each ground motion was analyses in both directions, [N,E,V] and [E,N,V]). A total of 450 modes were considered, resulting in a modal mass participation of 95% in all directions and rotations. All non-linear hinges were converted to non-linear links with damping proportional to the tangent stiffness of the hinge. Each FNA analysis conduction took about 1.5 hours to complete, making it a computational efficient analysis procedure in comparison to the direct integration approach.

The base reactions from the time-history load cases are combined with a static P-Delta analysis for axial seismic weight. Full base-results and interstory drifts are found in annex D-2: and D-3:.

Table 5-33 - Base forces for the suite of ground motions

	Cape Mendecino	Iwate	Chuetsu	SMART1	Chichi	Northridge	Loma Prieta	Mean
10% in 50 years								
Base shear X [kN]	23082	23246	20234	21554	20353	21468	17745	**21097**
Base shear Y [kN]	17867	18980	16877	20134	22178	21107	22999	**20020**
Base force Z [kN]	33746	35934	33733	39644	32489	34690	38761	**35571**
Mx [MNm]	505	558	542	548	566	587	515	**546**
My [MNm]	475	490	517	517	499	517	467	**497**
Mz [MNm]	281	285	253	260	291	292	358	**289**
2% in 50 years								
Base shear X [kN]	34532	32321	29478	30890	33808	31892	26851	**31396**
Base shear Y [kN]	27505	26353	24430	29609	32527	31170	33586	**29311**
Base force Z [kN]	32550	38839	35787	44053	33807	37104	43281	**37917**
Mx [MNm]	599	646	635	646	671	706	516	**631**
My [MNm]	557	683	623	617	598	632	554	**609**
Mz [MNm]	407	351	366	381	425	415	529	**411**

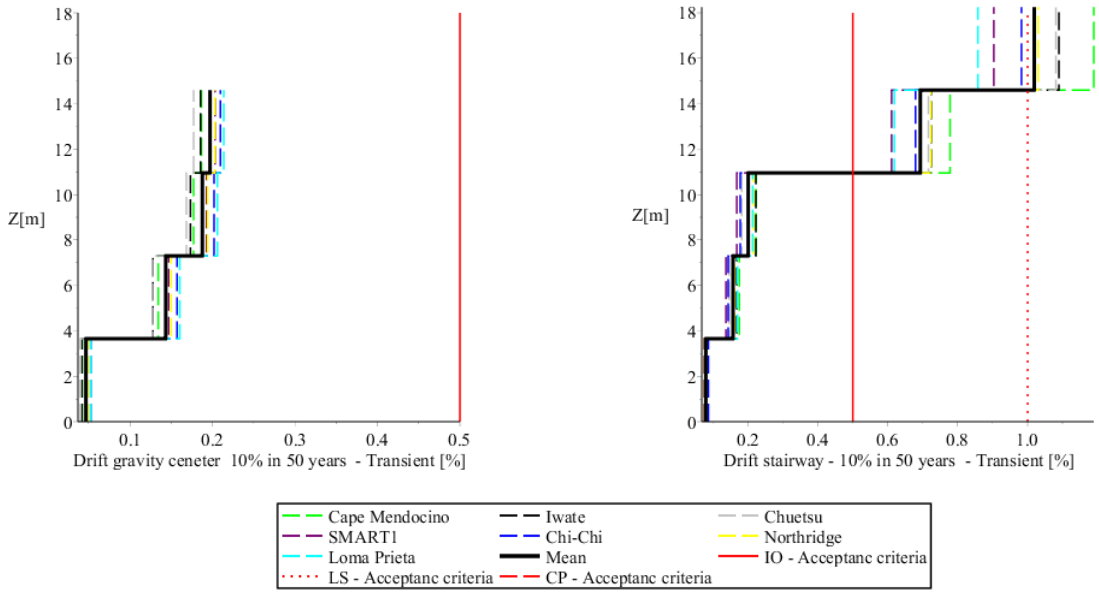

Figure 5-28 – Interstory drifts for FNA analysis with 10% probability of occurrence in 50 years

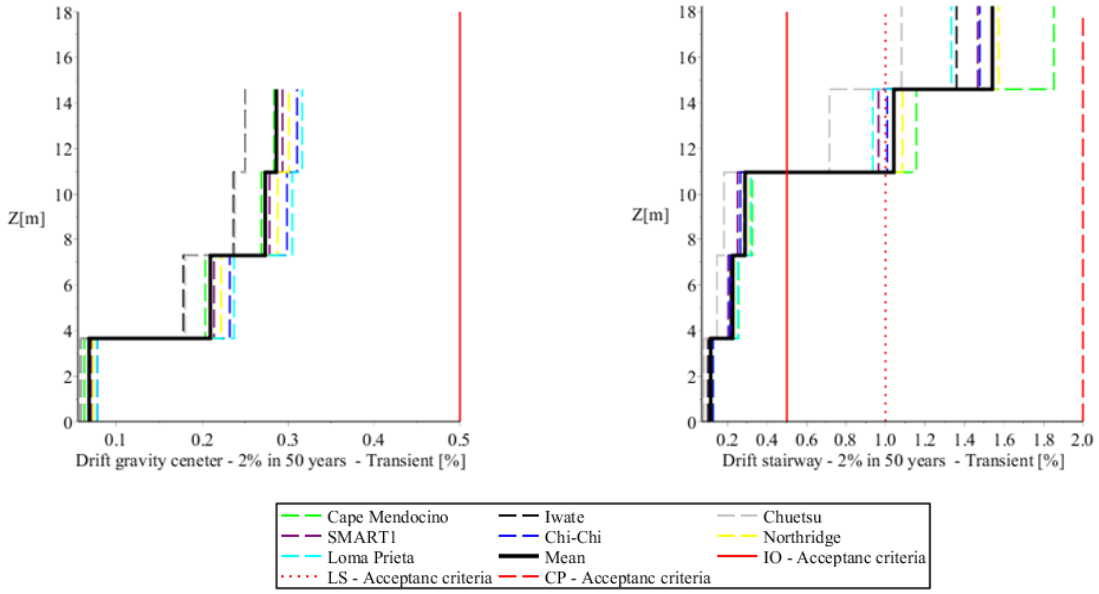

Figure 5-29 – Interstory drifts for FNA analysis with 2% probability of occurrence in 50 years

5.4.3 Direct integration nonlinear time-history analysis

For the structural model for non-linear dynamic analysis, fiber-hinges were assigned to all columns, and primary beams. Secondary beams were not expected to behave nonlinearly, according to results of the pushover analysis (Table 5-39).

For the time integration algorithm, the Hilber-Hughes Alpha-Taylor algorithm was used with alpha value of -0.05. This was done to filter out extensively high frequencies in the time-histories.

Rayleigh damping was calculated with 5% damping of the two first modes after equation (3.4).

During preliminary analysis, there were some convergence errors with origin in the short columns in the stairway tower. This could indicate structural failure in column. As these columns are arguably the most unstable part of the structural design and with a comparatively low rebar ratio, this would seem plausible. The rebar for these columns were therefore increased to the maximum used in the project (6xø25 + 6xø20). This eliminated all convergence errors in the further analysis.

For the all cases the following results were obtained:

- Peak interstory drift
- Base reactions
- Plastic rotation of critical sections

5.4.3.1 10% probability of occurrence in 50 years

For the time history analysis for 10% probability of occurrence in 50 years three ground motions were used. With only three ground motions used in the analyses, the least favorable results were used to perform the assessment. Full results in Appendix D-4: and D-7:.D-7:

Table 5-34 - Base reactions with 10% probability of occurrence in 50 years

	Cape Mendocino	Iwate	Northridge	Least favorable
Base shear X [kN]	13579	21571	16725	**21571**
Base shear Y [kN]	15987	23285	13845	**23285**
Base force Z [kN]	36167	30822	35983	**36167**
Mx [MNm]	555	574	515	**574**
My [MNm]	466	497	474	**497**
Mz [MNm]	200	304	188	**304**

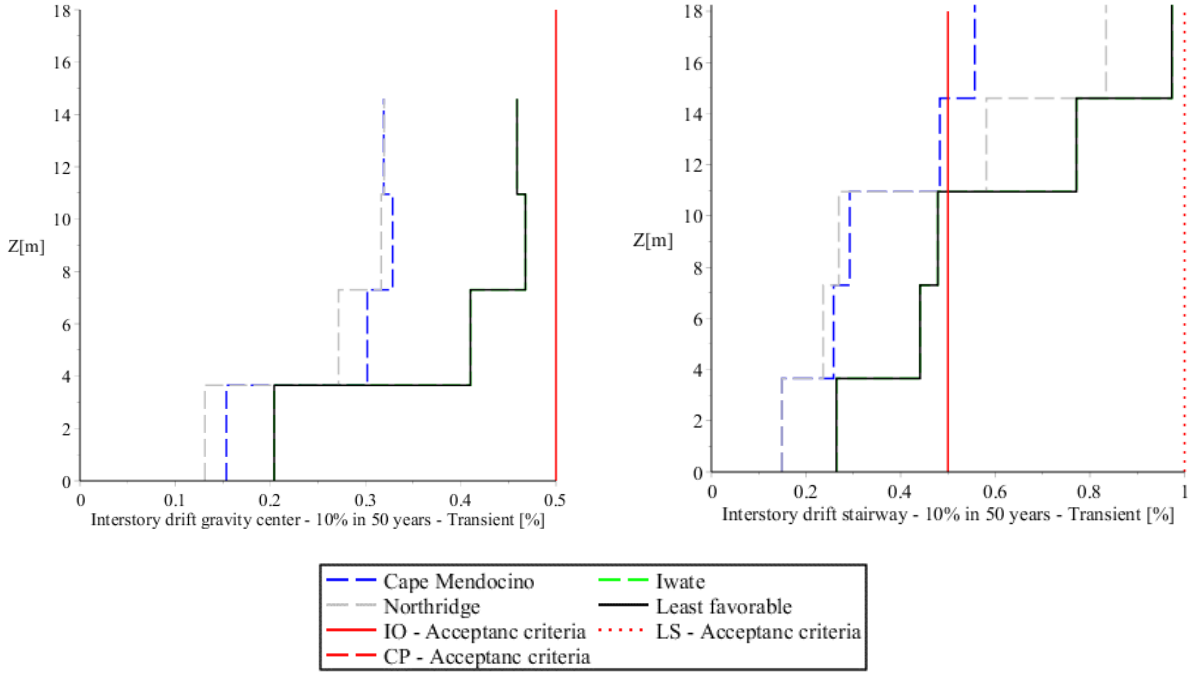

Figure 5-30 - Interstory drifts with 10% probability of occurrence in 50 years

Table 5-35 - Hinge performance with 10% probability of occurrence in 50 years

	Least favorable			
	O	**IO**	**LS**	**NC**
Column	193	5	0	0
Prim. Beam	404	6	0	0

5.4.3.2 2% probability of occurrence in 50 years

For the time history analysis for 2% probability of occurrence in 50 years three ground motions were used. With all seven ground motions were used in the analysis, the mean results were used in the performance assessment. Full results in Appendix D-5: below and D-8: below. The results from this analysis can also be used for the *No collapse* requirements in the Eurocode. This is possible because the Eurocode includes the importance factor in the seismic demand.

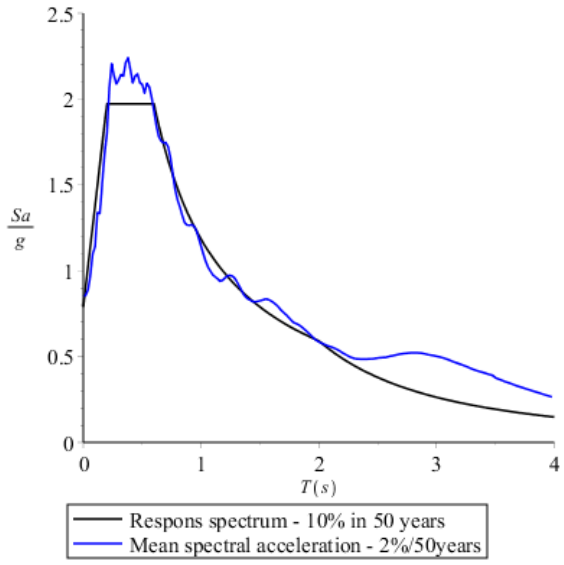

Figure 5-31 - Applicability of ground motions for *No collapse* requirement after Eurocode 8

Table 5-36 - Base reactions with 2% probability of occurrence in 50 years

	Cape Mendocino	Iwate	Chuetsu	SMART1	Chichi	Northridge	Loma Prieta	Mean
Base shear X [kN]	21875	29404	19289	28831	19288	19258	31369	**24188**
Base shear Y [kN]	22681	25279	22570	21484	22570	19145	29222	**23279**
Base force Z [kN]	39504	54942	40831	61336	40831	39209	47957	**46373**
Mx [MNm]	644	958	675	1142	675	623	845	**795**
My [MNm]	529	584	465	645	464	518	602	**544**
Mz [MNm]	271	361	300	518	304	247	400	**343**

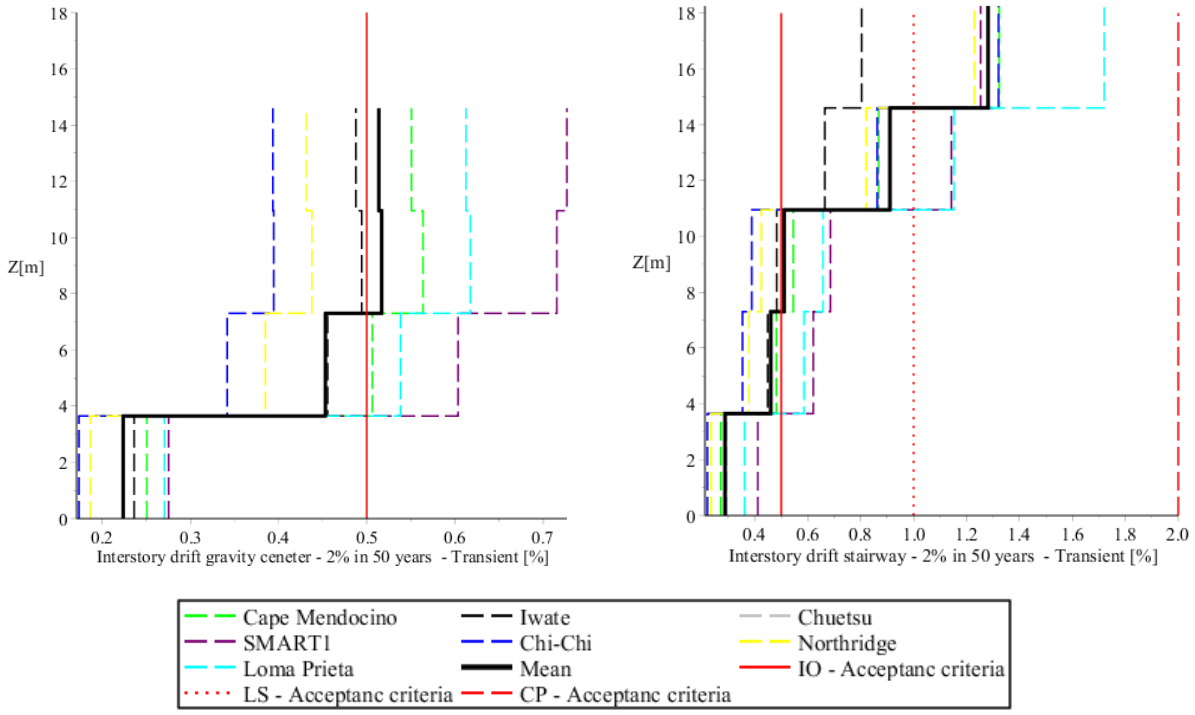

Figure 5-32 - Interstory drifts with 2% probability of occurrence in 50 years

Table 5-37 - Hinge performance with 2% probability of occurrence in 50 years

	Least favorable			
	O	**IO**	**LS**	**CP**
Column	157	38	0	3
Prim. Beam	396	10	4	0

The instances of *CP* column hinge performance occurred in the stairway columns in the Smart1 and Loma Prieta earthquake analyses. For all three cases this was due to the

5.4.3.3 Gorkha Earthquake

As a curiosity, the seismic performance was assessed for the Gorkha earthquake in Nepal. The earthquake occurred in April 2015 and had a magnitude of 7.8M_w and a Mercalli Intensity of VIII.

Ground motions were obtained from Kanti Path station [27], which is located 3.5km from Kanti Children's Hospital, with an epicentral distance of 60km.

Figure 5-33 - Red dot: Kanti Path ground motion location. Blue dot: Kanti Childrens Hospital

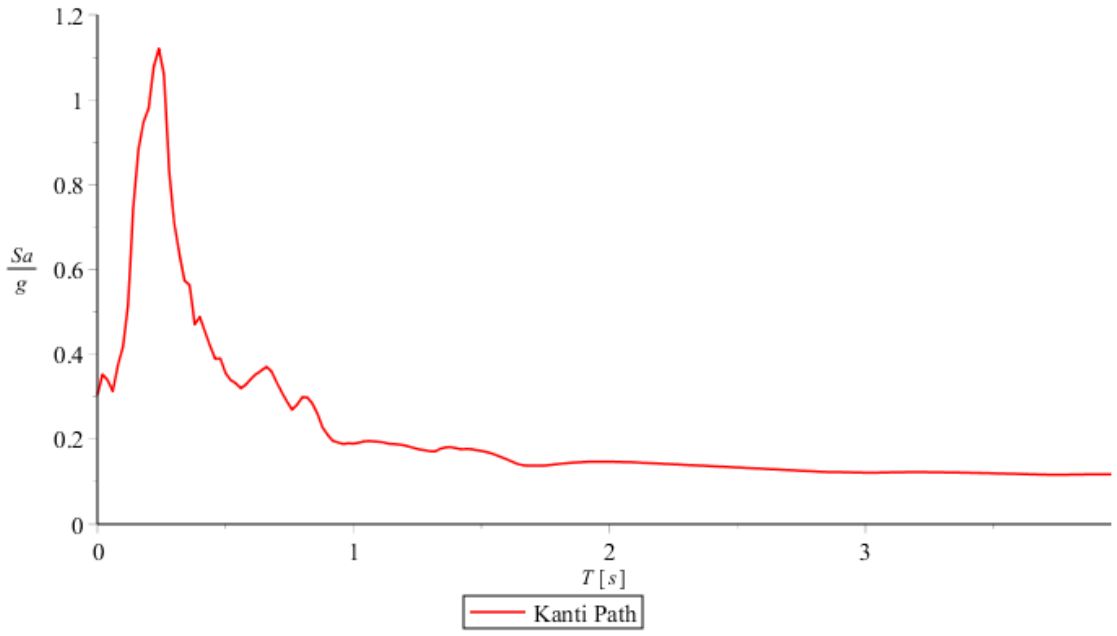

Figure 5-34 - Spectral acceleration for Kanti Path ground motion

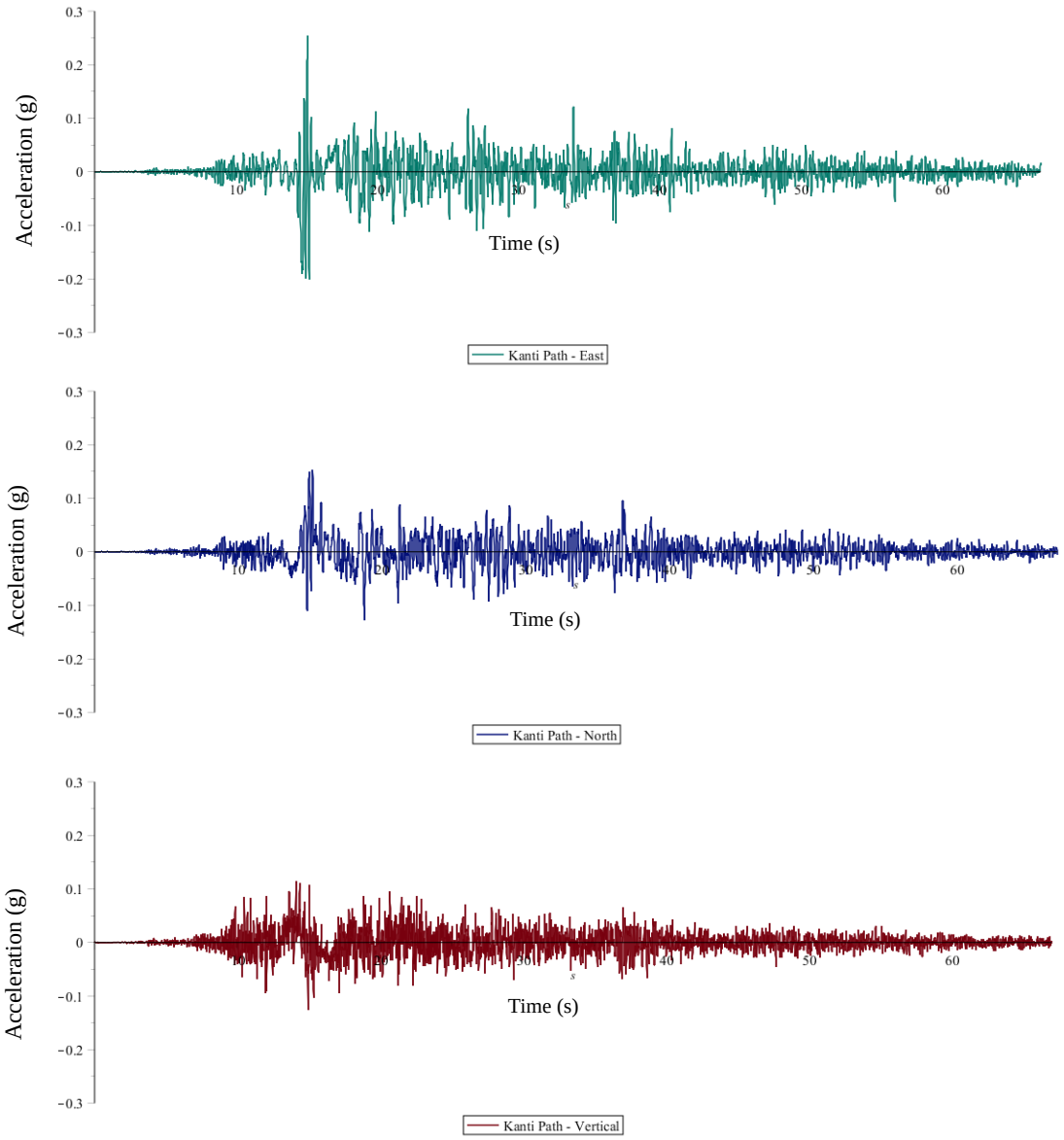

Figure 5-35 - Kanti Path ground motions

The time history was analyzed using direct integration with HHT-value of -0.05. Rayleigh damping was assigned, based on 5% viscous damping of the first two modes of vibration. Two load cases were created with ground motions in N-E and E-N directions. The least favorable results of the two were used.

The following results were obtained:

Table 5-38 - Base reactions from Gorkha earthquake analysis

Base shear X [kN]	9 863
Base shear Y [kN]	8 360
Base force Z [kN]	34 095
Mx [MNm]	410
My [MNm]	393
Mz [MNm]	140

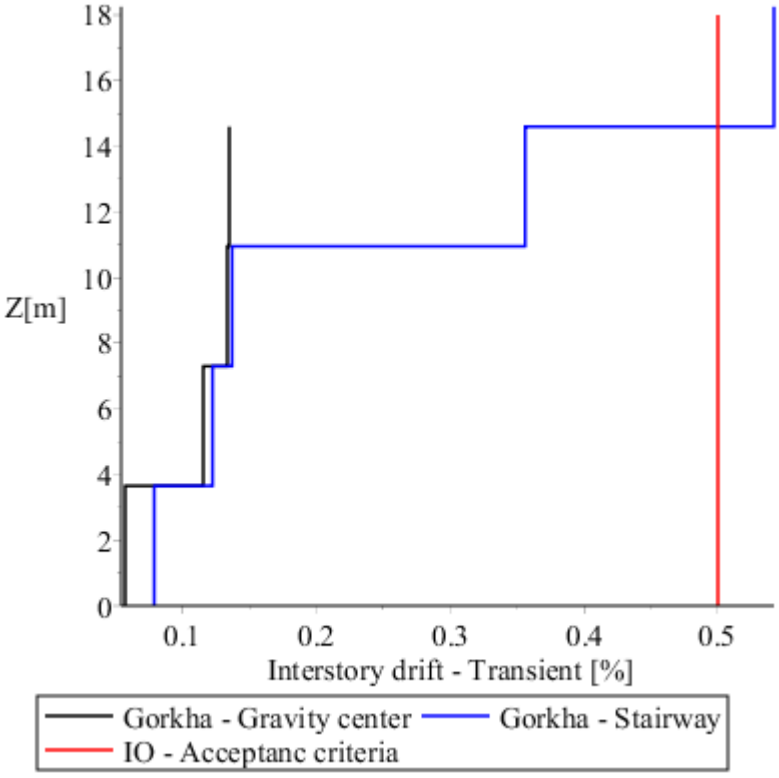

Figure 5-36 - Interstory drifts - Gorkha earthquake

The results are comparable to the linear time-history analysis with 50% probability of occurrence in 50 years, see Figure 5-27 - Interstory drifts with 50% probability of occurrence in 50 years. This would put the performance level for the stairway to *Immediate Occupancy* and *Operational* for the core building.

5.5 Pushover Analysis - PBSD

This chapter is based on the analysis performed in chapter 5.2.3. The script for the N2-pushover analysis, with elastic response spectrum after Eurocode 8, was reused to obtain design values at all three of the performance level. Detailed procedure is found in Appendix C-2:

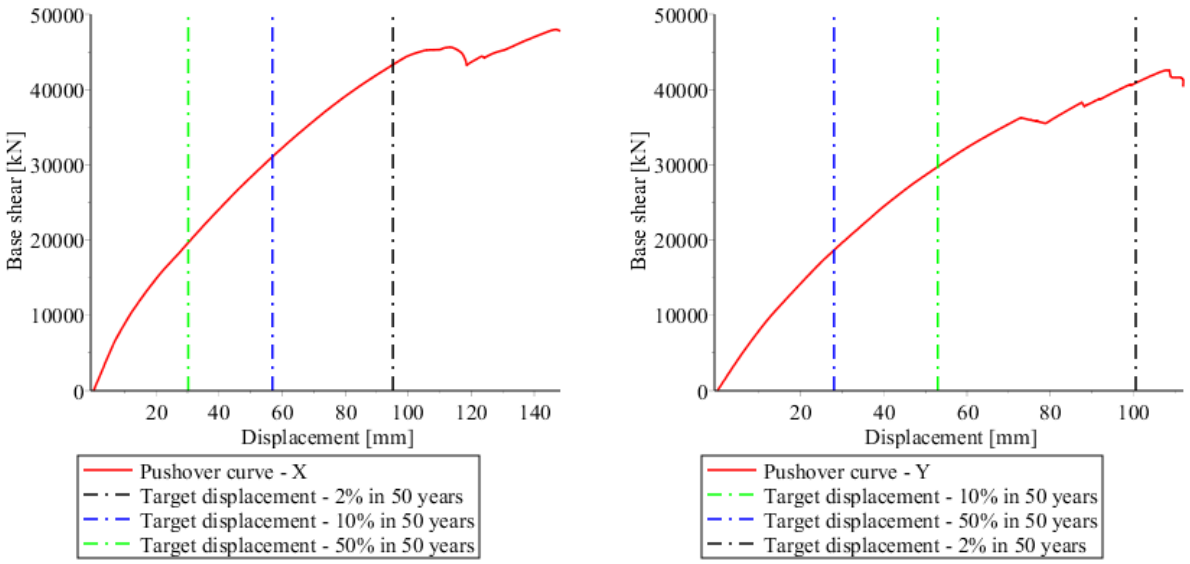

Figure 5-37 - Target displacements for seismic hazard levels

	Pushover X		Pushover Y	
	Target disp. [mm]	**Base shear [kN]**	**Target disp. [mm]**	**Base shear [kN]**
50% in 50 years	30mm	19 663	28mm	18 634
10% in 50 years	57mm	31 254	53mm	29 773
2% in 50 years	95mm	43438	100mm	40 757

From the pushover curves in Figure 5-37 it can be interpreted that the building will not collapse under the seismic demands set for his assessment. The pushover analysis was run until major convergence errors halted the analysis, and its therefore unclear what the structural behavior will be beyond the displacement of the pushover curve. For the pushover analysis in Y-direction, the factor of safety for collapse for the largest seismic demand may be considered as being very low.

5.5.1 Interstory drifts:

Interstory drifts are calculated as transient drifts for each load case. The pushover cases are not combined.

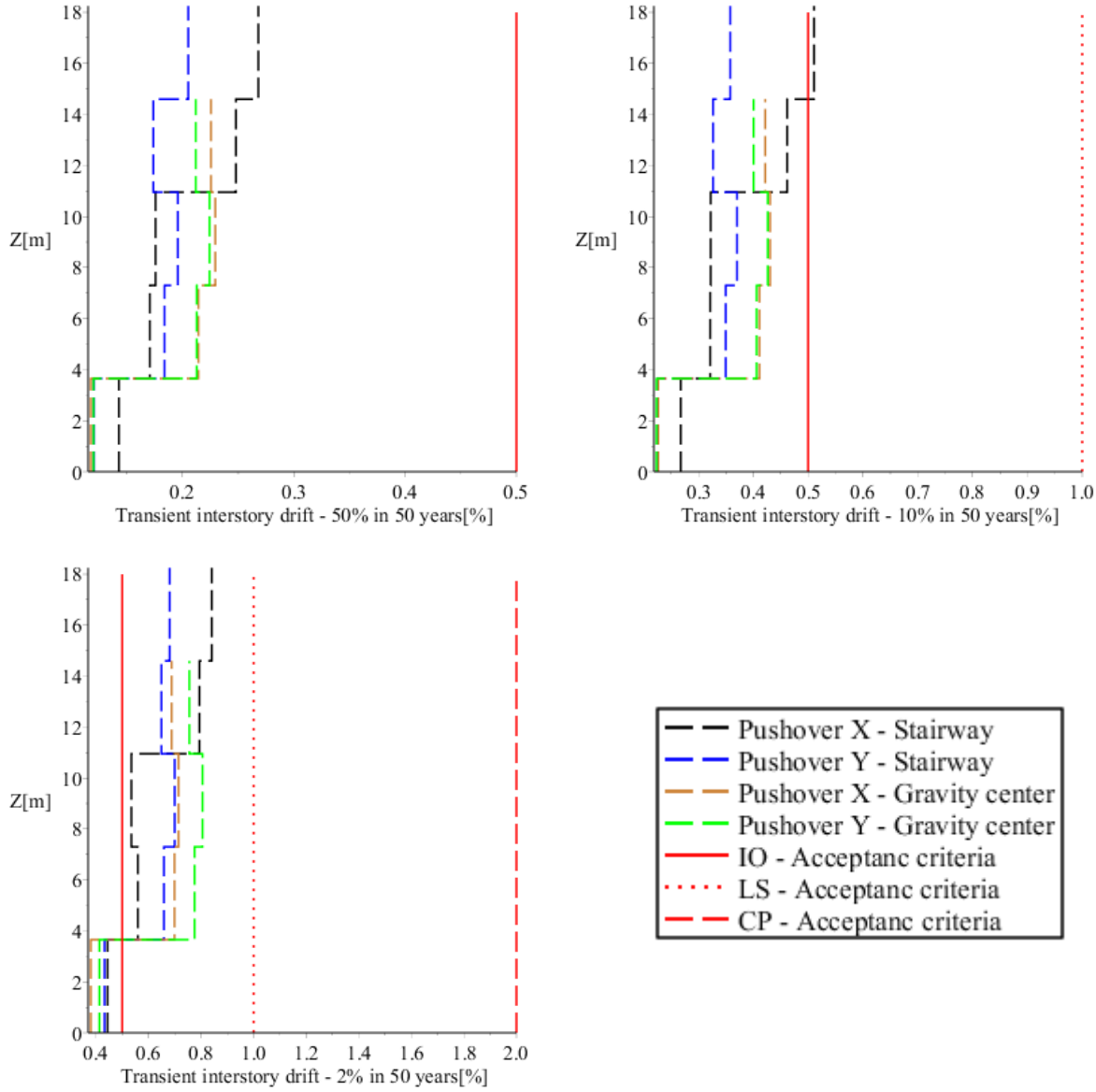

Figure 5-38 - Interstory drift pushover analysis, with acceptance criteria

When comparing the interstory drifts to the ones obtained from time history analysis, the shape of the interstory drift plots (Figure 5-27, Figure 5-30 and Figure 5-32) differ quite significantly. This is especially the case for the stairway, which is indicated to be greatly affected by torsional modes. As torsional effects are greatly underestimated in the N2-pushover procedure, the results should be considered as liberal, with a special concern for the results of the stairway tower.

5.5.2 Hinge results:

As noted in chapter 5.2.3, all beams were modelled using M3 hinges after ASCE 41-13. All columns were modelled using P-M2-M3 fiber hinges. All sections were assigned hinges in both ends. Hinge performance level was set by the acceptance criteria presented in Table 5-41.

Table 5-39 - Hinge performance levels

		Pushover X				**Pushover Y**			
		O	**IO**	**LS**	**CP**	**O**	**IO**	**LS**	**CP**
50% in 50 years	Column	198	0	0	0	198	0	0	0
	Prim. Beam	410	0	0	0	410	0	0	0
	Sec. Beam	240	0	0	0	240	0	0	0
10% in 50 years	Column	196	2	0	0	198	0	0	0
	Prim. Beam	409	1	0	0	407	3	0	0
	Sec. Beam	240	0	0	0	240	0	0	0
2% in 50 years	Column	170	21	7	0	182	3	13	0
	Prim. Beam	400	10	0	0	399	11	0	0
	Sec. Beam	240	0	0	0	240	0	0	0

5.6 Seismic performance assessment

As hospital can be considered safety critical in the event of natural disasters, it is of utmost importance that the facilities are safe and functional under such circumstances. The proposed performance objective is thereby set as:

Table 5-40 - Performance objective for Kanti Childrens Hospital

	Operational (O)	Immediate Occupancy (IO)	Life Safety (LS)	Near Collapse (NC)
50% in 50 years				
10% in 50 years				
2% in 50 years				

With the high number of shear walls, and as the structural system was classified as a *wall-equivalent dual frame system* per chapter 5.2.1, the acceptance criteria for interstory drift for concrete wall systems is adopted. The following acceptance criteria is then established with basis in ASCE 41-13 [21] and FEMA 356 [22]:

Table 5-41 - Acceptance criteria

	Operational O	**Immediate Occupancy IO**	**Life Safety LS**	**Collapse Prevention CP**
Plastic hinge – Beams*	≤0.005 rad	0.005 – 0.015 rad	0.015 – 0.02 rad	≥0.02 rad
Plastic hinge – Columns Max**	≤0.005rad	0.005 – 0.045 rad	0.045 – 0.06 rad	≥0.06 rad
Plastic hinge – Columns Min**	≤0.003rad	0.003 – 0.009 rad	0.009 – 0.06 rad	≥0.06 rad
Max interstory drift	≤ 0.5%	0.5 - 1%	1% - 2%	≥ 2%
Residual drift	≈0	0−0.5%	0.5% - 2%	≥ 2%

* The acceptance criteria based on a high shear-utilization of the beam section

** The acceptance criteria are interpolated between the min- and max-values depending on the axial utilization of the concrete-section for each hinge.

5.6.1 Base reactions

The base reactions of the different seismic hazard level and analysis method is compared. Pushover analyses yields the highest base reactions, which can be explained by the absence of the implementation of torsional modes in the pushover analysis. For the modal nonlinear analyses, the structure was assumed to be stiffer, mainly due to the definition of plastic hinges, which results in slightly higher base reactions.

Table 5-42 - Comparison of base reaction for the different analysis methods

	Linear Modal Mean	Nonlinear Modal Mean	Direct Integration Mean	Direct Integration Least favorable	Pushover
50% probability in 50 years					
Base shear X [kN]	12018	-	-	-	19663
Base shear Y [kN]	10848	-	-	-	18634
Base force Z [kN]	32839	-	-	-	-
Mx [MNm]	463	-	-	-	-
My [MNm]	419	-	-	-	-
Mz [MNm]	165	-	-	-	-
10% probability in 50 years					
Base shear X [kN]	-	21097	-	21571	31254
Base shear Y [kN]	-	20020	-	23285	29773
Base force Z [kN]	-	35571	-	36167	-
Mx [MNm]	-	546	-	574	-
My [MNm]	-	497	-	497	-
Mz [MNm]	-	289	-	304	-
2% probability in 50 years					
Base shear X [kN]	-	31396	24188	-	43438
Base shear Y [kN]	-	29311	23279	-	40757
Base force Z [kN]	-	37917	46373	-	-
Mx [MNm]	-	631	795	-	-
My [MNm]	-	609	544	-	-
Mz [MNm]	-	411	343	-	-

5.6.2 Interstory drifts

When comparing the interstory drifts there are significant differences, while the fulfillment of acceptance criteria is very similar. As the direct integration time-history analyses are considered as being the most accurate, these results are weighted the highest.

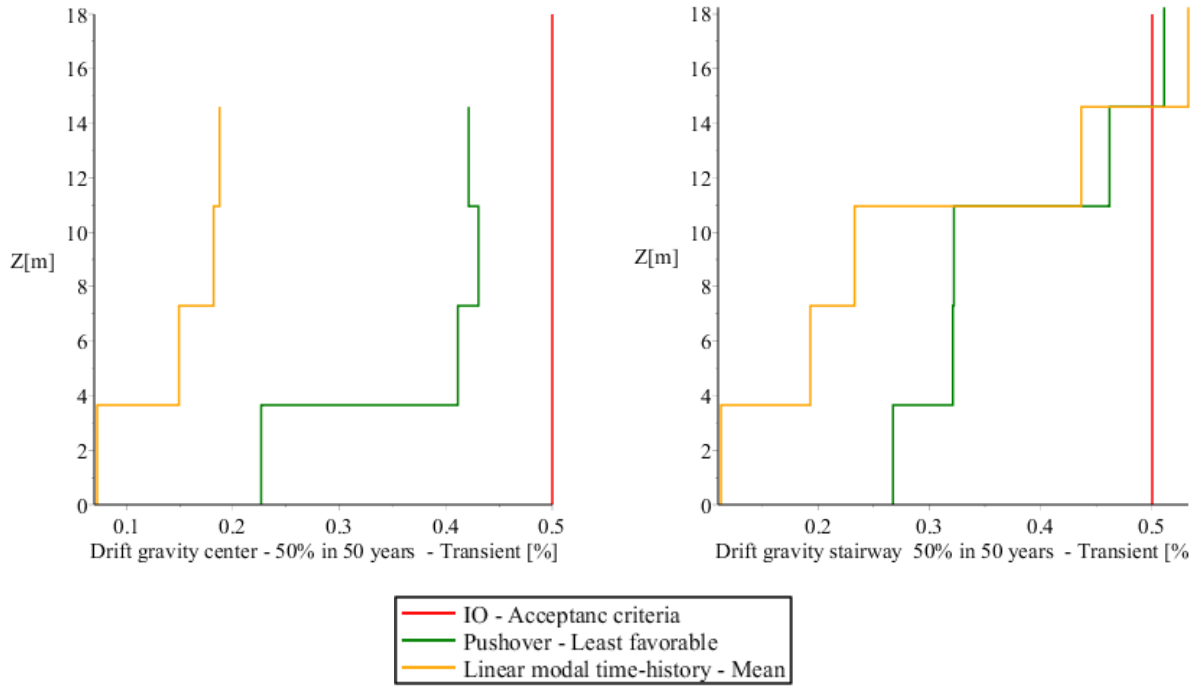

Figure 5-39 - Comparison of performance level for 50% of occurrence 50 years - hazard level

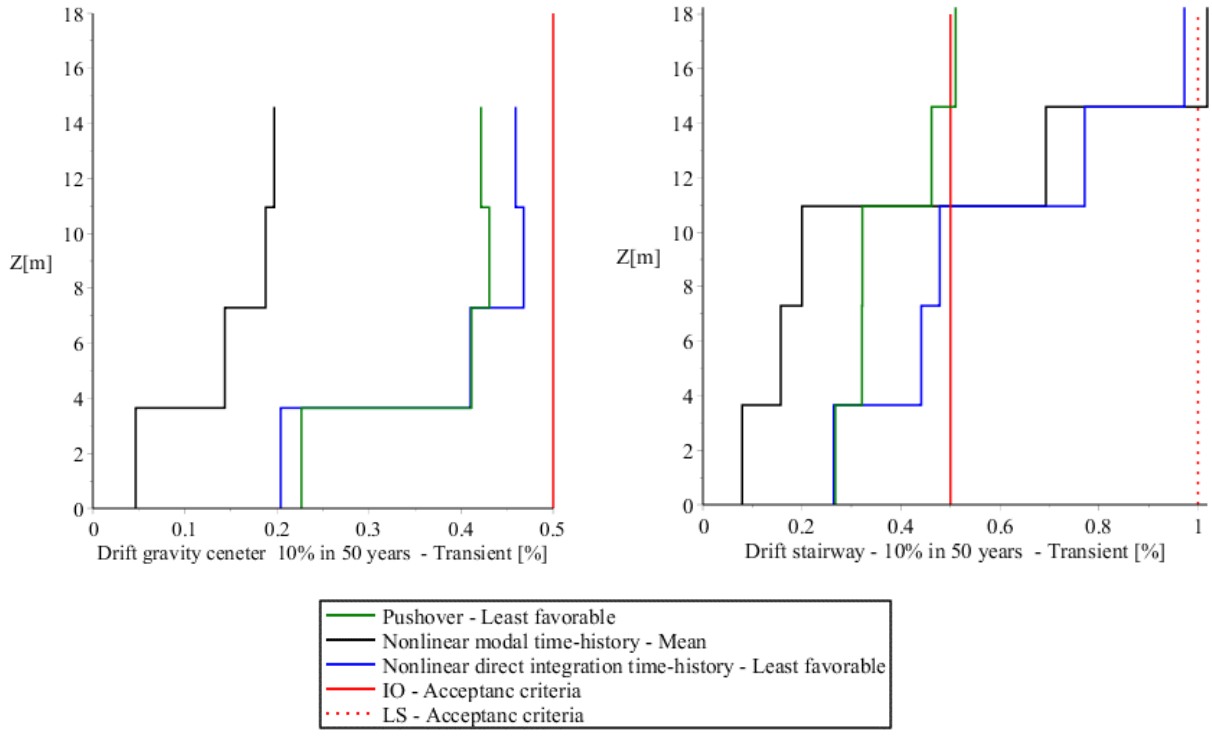

Figure 5-40 - Comparison of performance level for 50% of occurrence 50 years - hazard level

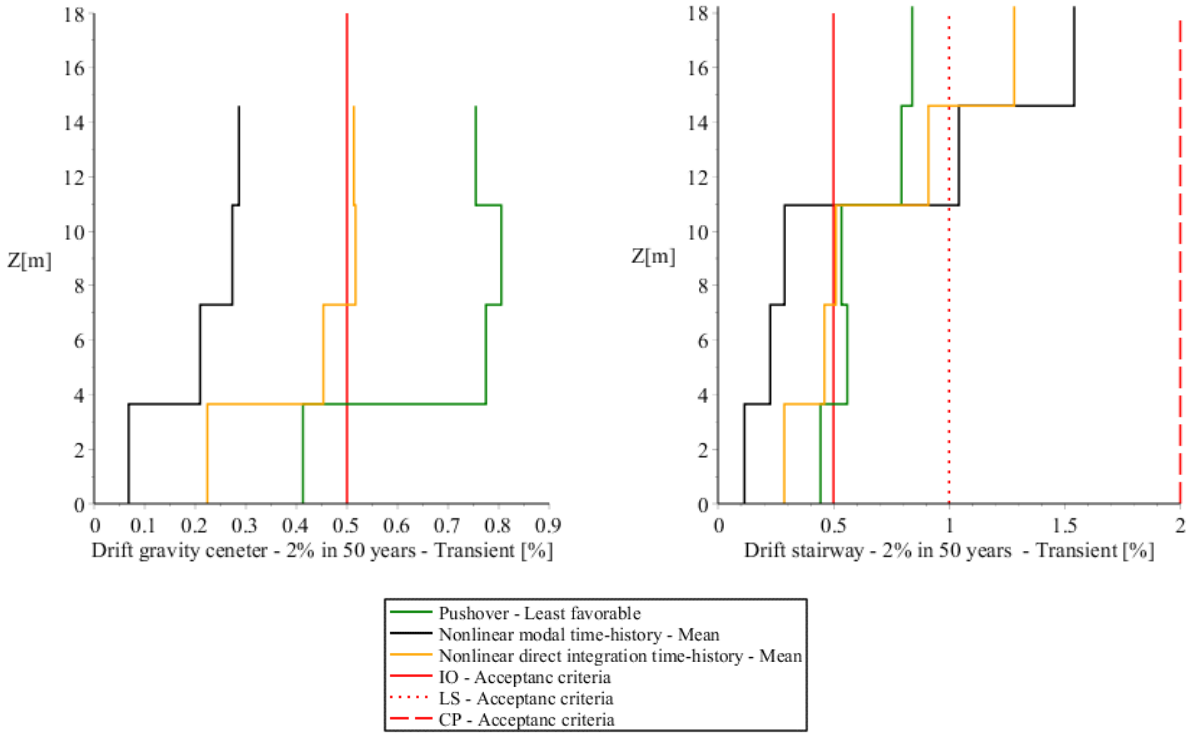

Figure 5-41 - Comparison of performance level for 50% of occurrence 50 years - hazard level

5.6.3 Hinge performance

Hinge performance is evaluated for both pushover- and direct integration time-history analyses.

		Pushover				**Direct Integration Time-history**			
		O	**IO**	**LS**	**CP**	**O**	**IO**	**LS**	**CP**
10% in 50 years	Column	196	2	0	0	198	0	0	0
	Prim. Beam	409	1	0	0	407	3	0	0
	Sec. Beam	240	0	0	0	240	0	0	0
2% in 50 years	Column	170	21	7	0	181	5	13	0
	Prim. Beam	400	10	0	0	399	11	0	0
	Sec. Beam	240	0	0	0	240	0	0	0

5.6.4 Performance level

The classification of performance level is performed based on a combination of the time-history- and pushover analyses, with the governing factor being the interstory drift acceptance criteria. As the structure is classified as a *wall equivalent system*, the performance of the beam- and column hinges performs very well in all load cases. This means that the shear walls are expected to take the most damage. As SAP2000 does not have the ability to directly determine the plastic hinge rotation of the shear walls is not thoroughly determined.

Table 5-43 - Performance assessment according to time-history analysis

	Operational (O)	Immediate Occupancy (IO)	Life Safety (LS)	Near Collapse (NC)
50% / 50 years				
10% / 50 years				
2% / 50 years				

6 DISCUSSION

6.1 Uncertainties in modelling and analysis

"*Engineering is the art of modelling materials we do not wholly understand, into shapes we cannot precisely analyze so as to withstand forces we cannot properly assess, in such a way that the public has no reason to suspect the extent of our ignorance*" – Dr. A.R. Dykes.

In the structural analysis process a number of assumptions and simplifications are performed to get to the end results. It is therefore important to know where these were made, and what impact this might have on the end results. This chapter will highlight the main assumptions and simplifications made in the case study.

6.1.1 Structural analysis model

6.1.1.1 Meshing of shear walls:

The refinement of the mesh of the shear wall elements turned out to be a sensitive point of the analysis model. A more refined mesh yielded a more torsional rigid analysis model and would more realistically model the interaction between the shear wall and the beams. This in-part decreased the computational efficiency drastically. It was therefore chosen to use the refined mesh for linear-elastic analysis, while using the default meshing for nonlinear analysis. This should yield more conservative results for the nonlinear analyses.

6.1.1.2 Constraints and SSI:

Soil-structure interaction is not required for the soil condition on this building site and is thereby not included in this analytical model. The constraints are then considered as rigid, as all columns are connected through should result in more conservative results, as when SSI is considered for relatively stiff soils the soil is expected to sustain some of the energy from the earthquake.

6.1.1.3 Linear analysis model

For the linear analysis model all section was applied modification to account for the stiffness of cracked concrete.

6.1.1.4 Modification for nonlinear analysis

For the shear walls, the software used did not have the capabilities of modelling plastic hinges in shell elements. This means that plastic hinge formation in the shear walls is not properly captured by the software used.

In the pushover analysis model automatic M3-hinges following ASCE 41-13 were used for modelling nonlinear behavior in beams. For all other analysis, P-M2-M3 fiber hinges were used. These are considered to provide the best representation of lumped nonlinear behavior, but there lies some uncertainty on the assigned location of these hinges. All elements were assumed to have a flexural failure mode, and the influence of shear forces is therefore not directly accounted for.

6.1.2 Analysis

6.1.2.1 Response Spectrum

All response spectrum analyses were performed using CQC modal combination. Although this was not required by either code, it is widely considered as a more accurate approach as it considers damping and the interaction of closely spaced modes.

6.1.2.2 Pushover

For the results of the pushover analysis it is important to note that the building is irregular in plan and has big torsional contribution in its first modes. The real seismic behavior of the structure might therefore not follow the same evolution as the pushover analysis indicates. This is a known limitation to the N2 pushover procedure recommended by the Eurocode.

Other procedures have been proposed which include torsional effects, but these are much more complicated. With the main advantages of the N2-pushover procedure being its efficiency and relatively low complexity, the step in complexity towards the more accurate nonlinear time analysis might not be much greater than the added complexity of a modal pushover analysis.

In the determination of the target displacements there is performed a bi-linearization of the pushover curve, based on the displacement of plastic mechanism. In the Eurocode there are no guidelines for determining this plastic mechanism. Although it might not have a significant impact, it is an added uncertainty.

The design parameters obtained from the target displacements of the pushover analysis should therefore not be used as a single source of structural design parameters. They do though make a reasonable prediction of the overall performance level of the core building, and with a much more efficient analysis process, compared to time-history analysis approaches.

The analysis was used to obtain the over-strength factor to modify the behavior factor, as the margin from the calculated value to the maximum value allowed by the code was so significant.

6.1.2.3 Time-history

Non-linear time history is complex tool for seismic analysis. When performed right, it is considered the most accurate analysis method, but there are many pitfalls along the way. In the Eurocode, very few criteria are presented, so the output of the procedure is very much dependent on the structural engineer. The uncertainties in such analysis are:

- Criteria for selection of ground motions
- Scaling and processing of ground motions
- Hinge- type and properties
- Assumed locations of plastic hinges
- Acceptance criteria for hinge rotation
- Choice of analysis form; direct integration- or modal time history
- Time integration algorithm
- Damping ratio

Both the benefits and limitations of the FNA- modal time history analysis, available in SAP200, are exemplified in the case study of this thesis. The pros of the FNA method is its computational efficiency and the consistency in evaluating of ground motions.

The direct integration analysis performed in this case study were very computational expensive, with computing times between 10-24 hours per analysis for the case study. Direct integration interpretation of ground motions is more sensitive to noise and errors in the ground motion signals. In the case study, the results from direct integration time history analysis had a much greater variability than that of modal time-history analysis. This could indicate that the ground motion was not sufficiently processed.

The main difference of the procedures is the way the non-linear hinges are idealized. When direct integration, and hinges are modeled within the structural elements, it can be seen that the full expected behavior of a non-linear hinge is captured. As the earthquake progresses, the cyclic degradation effect results in substantial increase in hinge rotation with similar bending moments. For the FNA-model, the fiber hinge does show some non-linear behavior with the loading and unloading of the hinge. The cyclic degradation seems though not be present, resulting in a substantial underestimation of hinge rotation, which in-part affects the deflections of the building.

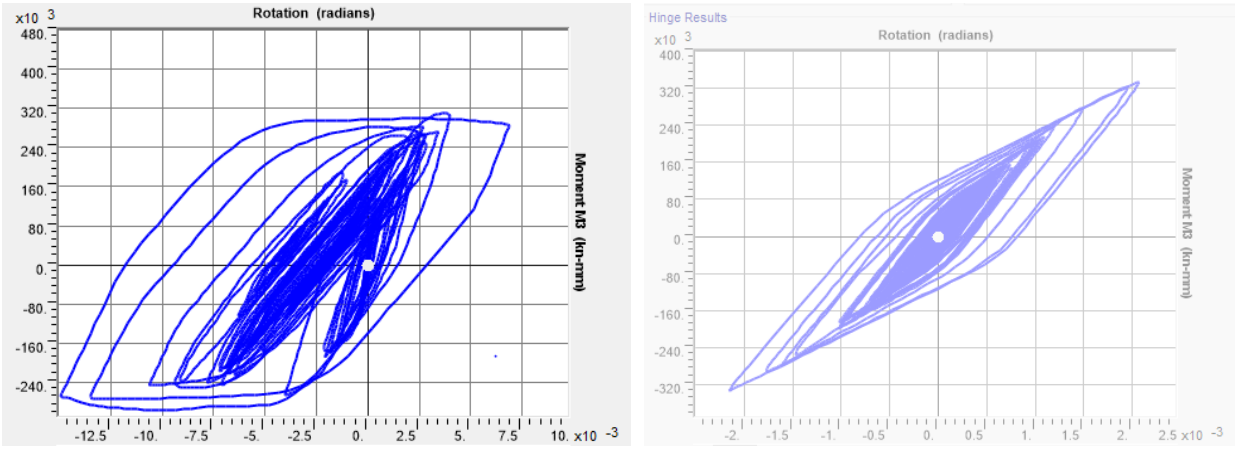

Figure 6-1 - Comparison of fiber-hinge result. L.S Direct integration, R.S. FNA

6.1.3 Results

6.1.3.1 Inter-story drifts

The inter-story drifts were evaluated at gravity center and corner of the stairway. These were chosen to represent the overall behavior of the main structure and the stairway. There is through a possibility that other parts of the structure do experience drifts. A vertical line of special interest could be the elevator shaft. This could be further used to assess the performance and operationality of the elevator.

6.1.3.2 Hinge rotations

Plastic hinges are modelled using M3 hinges following ASCE 41-13 and P-M2-M3 fiber hinges. Both hinge models used does not account the effect of shear, as the failure mode is assumed to be contributed by flexure. For beams the effect of shear, and for columns the axial force, is incorporated into the acceptance criteria.

In the pushover analyses hinges were assigned to all beams and columns. For all the performance levels there was no nonlinear behavior in the secondary beams. In the time-history analyses it was therefore chosen to not include hinges in secondary beams to improve computational efficiency. As

M3 hinges:
M3 hinges were for modelling nonlinear behavior in beams in the pushover analyses. Hinge properties were set automatically after ASCE 41-13. These hinges allow the possibility of assigning hinge rotation acceptance criteria in the program, allowing for graphically interpretation of performance level. This simplifies the performance process substantially.

Fiber hinges:
Fiber hinges are the easiest to set up in SAP2000, as the hinge properties are set automatically depending on the section properties.

In the pushover analyses, fiber hinges were used to model the nonlinear behavior of the columns. The main reason behind this choice was the automatic P-M2-M3 hinges after ASCE 41-13 led to convergence errors and the full behavior of the structure was not captured. When using P-M2-M3 fiber hinges, the analysis.

In the time-history analysis, the processing of the hinge results was very computationally expensive. Retrieving all hinge results for one analysis took between 3-12 hours, depending on the output steps.

6.1.3.3 Shear wall performance

The performance of the shear walls was determined solely by inter-story drifts. This was in-part due to the fact that the analysis software did not have the capability to model nonlinear hinges in shell elements.

6.2 Code comparison

This subchapter will highlight the main differences of Eurocode 8 and IS1893.

6.2.1 Seismic Hazard

The peak ground motions used in the case study was based on a probabilistic seismic hazard analysis [7] for the Kathmandu valley. This report indicates a PGA much higher than what is presented in IS1893. This then raises the question of the applicability of the seismic zoning factors prescribed in IS1893 and NBC105.

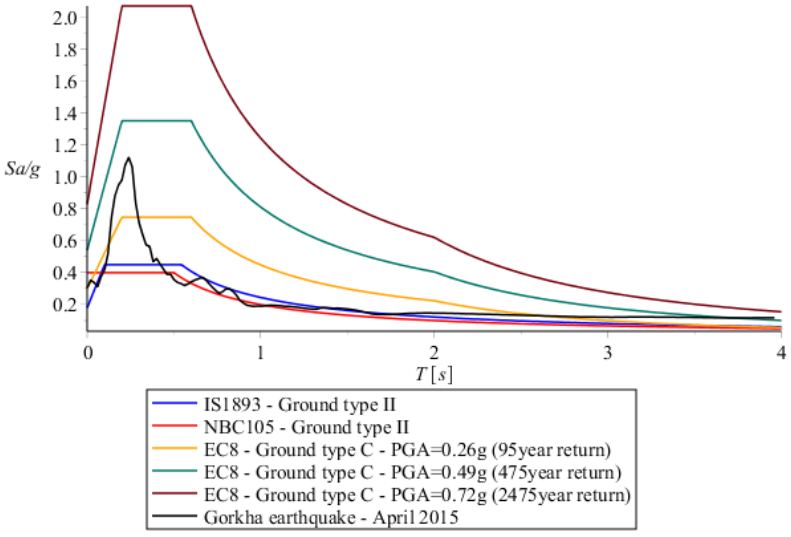

Figure 6-2 - Comparison of design seismic hazard for Kathmandu, Nepal

When comparing these design seismic hazards with the spectral response of the 2015 Gorkha earthquake it is shown that the seismic demand of the earthquake is higher than what the code requires for periods of 0.2s to 0.5s. This is problematic as buildings with code sufficient structural design will have a high probability of being subjected to an even larger seismic demand within its life-span, based on the recent history of earthquakes of high magnitudes (see Table 2-3).

The PGA-values used were further verified with the comparability of the responses of the linear analysis with 50% probability of occurrence in 50years with the direct integration analysis of the 2015 Gorkha earthquake. Historically, there have been two earthquakes with this magnitude in the last century (Table 2-3 - Earthquakes (>6.5Mw) in Nepal in the last century (From *NCEI*), which further strengthen this claim

6.2.2 Analysis model

Both codes require the use of effective (cracked concrete) stiffness in the analysis model. There are here only minor differences between the two codes. Neither of the does though require a reduction of torsional stiffness, but it was included in the case study as it was recommended in the book *Seismic Design of Concrete Buildings to Eurocode 8* [18].

Table 6-1 – Effective stiffness to model cracked moment of inertia

	Beam	**Columns**
Eurocode 8	50%	50%
IS1893	35%	70%

While the Eurocode has clear guidelines for the analysis model (planar or spatial), see Table 4-3, IS1893 requires in clause 7.7.2 requires that irregularities are to be represented in the analysis model. IS1893 therefore relies upon the judgement of the engineer for the use of analysis model.

6.2.3 Ground types

With IS1893 as a basis, the comparative ground types for NBC105 and Eurocode 8 is presented. The main difference is for the classification of high-stiffness/bedrock ground types.

Table 6-2 - Comparison of ground types

IS1893	**NBC 105**	**Eurocode 8**	**SPT-Value**
Type 1	Type 1	Type A	-
		Type B	>50
		Type C	30-50
Type 2	Type 2		10-30
Type 3	Type 3	Type D	<10

6.2.4 Behavior factor

Eurocode 8 and IS1893 has a slightly different approach to the behavior factors. The Eurocode sets an initial behavior factor depending on structural- and ductility classification, for then to

modify it depending on a number of factors (presented in Table 6-3 - Comparison of behavior factor for Eurocode 8 and IS1893). After IS1893 the behavior factor is based solely on the structural- and ductility classification, and no further modifications are allowed.

Table 6-3 - Comparison of behavior factor for Eurocode 8 and IS1893

	Eurocode 8	**IS1893**
Ductility class	DCL, DCM, DCH	OMRF, SMRF, ductile shear walls
Torsional irregularity	Reduced value	Not allowed
Plan irregularity	Decreased multiplication factor	No effect
Vertical irregularity	20% reduced value	No effect
Multiplication factor dependent on structural system	Up to 50% increased value	Not allowed
Modification through pushover analysis	Increased/decreased value	Not allowed
Modification through quality assurance	Max 20% increase	Not allowed

While the Eurocode allows for higher behavior factors, the additional criteria set for the structural system makes it harder to obtain a high behavior factor. For IS1893 there are fewer criteria to obtain a medium-high behavior factor, but less room for modification and stricter regulations for torsional irregularity. In-fact, IS1893 does not allow for torsional irregular structures.

6.3 Case Study

Through the analysis, the weakest points of the structural design were discovered. The most prominent weakness is the stairway. This is due to the combined effect of irregularity in plan, discontinuity in floor diaphragms, and short columns due to repose in the stairs.

The stairway can also be considered crucial in the evaluation of operationality of the hospital in the case of larger earthquakes, as it would both hinder the access of floor 2-4 and, in the event of collapse, hinder the main entrance to the building.

6.3.1 Comparison of code-compliant design forces

As discussed in chapter 6.2.1, the seismic demand differs significantly between Eurocode 8 and IS1893. While IS1893 includes the conservative measure of scaling the response spectrum analysis to match the base shears of the lateral force method, the difference in seismic demand is still large:

Table 6-4 - Comparison of code-compliant design forces

	Later force method			**Response spectrum**		
	IS1893	**Eurocode 8**	**Difference**	**IS1893**	**Eurocode 8**	**Difference**
Base shear X [kN]	3 932	10 965	278%	3 965	8 876	224%
Base shear Y [kN]	3 932	10 965	278%	4 093	7 636	186%

As the approach to determining the interstory drifts differ between the codes, the interstory drifts of IS1893 is multiplied by a factor of 5 (R – Behavior factor) as in Eurocode to compare the results:

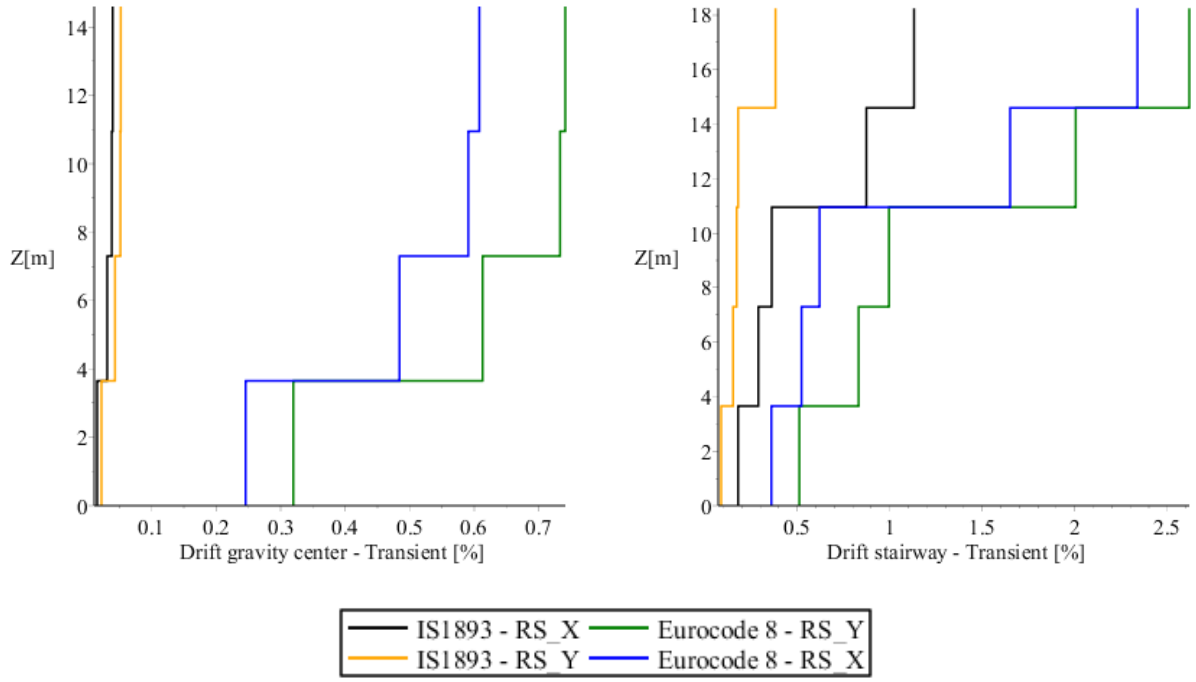

Figure 6-3 - Comparison of inter-story drifts - Response spectrum anlysis

6.3.2 Eurocode 8

With regards to code compliance of Eurocode 8, the main problem is the difference in seismic hazard (as discussed in chapter 6.2.1) consider in the code limit state. The structural design originally is design after IS1839, with a seismic demand approximately half of the seismic demand of the Eurocode (using PGA from source [23]). This resulted in the *Damage limitation* criteria not being met for interstory drifts in the stairway. There is not performed member verification after Eurocode 2, but from the performance assessment for seismic hazard of 2% probability of occurrence in 50 years (2475-year return period, Table 4-1) it is suggested that the stairway will be near the collapse limit.

As there was conduct both linear analysis, including behavior factors, and nonlinear analyses with no reduction in seismic hazard, the results are compared separately:

6.3.2.1 Comparison of analysis results

All linear elastic load cases have the seismic weight included:

Table 6-5 - Comparison of base reactions for linear elastic analyses - EC8

	L.F. - X	L.F. - Y	R.S. - X	R.S. - Y	R.S. - Z	Linear Modal TH
Base shear X [kN]	10 965	3 289	8 876	7 636	3 548	**12 018**
Base shear Y [kN]	3 289	**10 965**	3 212	3 539	2 789	10 848
Base force Z [kN]	29 469	29 469	33 163	33 163	**40 403**	32 839
Mx [MNm]	373	459	407	456	**481**	463
My [MNm]	406	320	416	356	**423**	419
Mz [MNm]	100	71	118	138	68	**165**

For the nonlinear procedures, pushover- and time-history analyses were performed. As the seismic hazard for the case study approximates the performance assessment time history with 2% probability of occurrence in 50 years, these results are presented:

Table 6-6 - Comparison of base reactions for nonlinear analyses - EC8

	Pushover X	Pushover Y	Direct integration TH
Base shear X [kN]	39 180	0	24188
Base shear Y [kN]	0	37 842	23279
Base force Z [kN]	29 469	29 469	46373
Mx [MNm]	338	672	795
My [MNm]	646	283	544
Mz [MNm]	446	365	343

6.3.3 IS1893

The initial structural design is designed after IS1893-2002 and is assumed to be sufficiently modelled at member level for IS1893-2016. Through the analysis, two criteria's regarding regularity was found to non-compliant:

Table 6-7 - Non-compliant criteria - IS1893

Clause	Criteria	Comment

7.1 – Table 5 (i)	Torsional irregularity	Structure is considered torsional irregular, which is not permitted for seismic zone V.
7.1 – Table 6 (vii)	Irregular modes of oscillation in two principal plan directions	The first three modes contribute less than 65% mass participation in principle plan directions.

With regards to the seismic demand calculated after IS1893, there are questions to be raised regarding the applicability of the zoning factors and return period of evaluation. This is further discussed in chapter 6.2.1, and recommendation for further projects are given in chapter 7.

	L.F. – X – EC8	L.F. – X – IS1893	Dif. %	R.S. – X – EC8	R.S. – X – IS1893	Dif. %
Base shear X [kN]	10 965	3 932	179%	8 876	3 965	124%
Base shear Y [kN]	3 289	1 192	176%	3 212	1 559	101%
Base force Z [kN]	29 469	29 469	-	33 163	29 996	11%
Mx [MNm]	373	351	6%	407	358	14%
My [MNm]	406	335	21%	416	223	87%
Mz [MNm]	100	36	178%	118	55	115%

6.3.4 Seismic performance assessment

The seismic performance assessment was made on the basis of pushover analysis and time-history analyses. To assess the performance, acceptance criteria was established for interstory drift and for plastic hinge rotations for beams and columns. The interstory drift limits were set to account for the performance of a *wall-equivalent system* and was assumed to be sufficient to assess the performance of the shear walls. This was done as the software did not have the capability of assigning nonlinear hinges to shell elements, and other procedures examined were too complicated with regards to the time available. This is then considered as the greatest weakness of this seismic performance assessment.

The seismic performance related to the different seismic hazard levels, as well as expected damages are further discussed:

6.3.4.1 50% in 50 years

For the performance assessment for earthquakes of 50% probability of occurrence in 50 year, the results from the pushover- and linear modal time history analysis were used. For the time-history analysis the full suite of seven ground motions were used, so the mean results from this analysis is used. From the pushover analysis it was evaluated that the structure would behave solely linearly, with all hinges being classified as *Operational* as well as the interstory drifts being well within the demand. With this in mind, it was assumed that it would be sufficient to perform a linear modal time-history analysis.

As the time-history analyses does a better job of representing the real behavior of the structure, it was the guiding analysis for the performance assessment.

The structure was classified right at the limit of *Immediate Occupancy*. This was due to the interstory drift of the stairway. The following expectations are made for an earthquake of this magnitude:

- The stairway might endure some damage which will most likely be related to the infill walls, and not the structural system (columns and beams).
- The core building will, according to the analysis, not endure any significant damage and will be operational.

6.3.4.2 10% in 50 years

For the performance assessment for earthquakes of 10% probability of occurrence in 50 year, the results from the pushover- and nonlinear direct integration time-history analysis were used. For the time-history analysis a suite of three ground motions were used (Cape Mendocino, Iwate and Northridge), so the least favorable results were used.

Again the, time-history analysis was the governing factor in the performance assessment. The results for the core building was though very similar.

The structure was classified as being right at the limit of *Life Safety*. The following expectations are made for an earthquake of this magnitude:

- The stairway might endure significant damage in the infill walls, and columns and beams will endure some damage and permanent deformations.
- The core building will, according to the analysis, not endure any significant damage and will be operational.

6.3.4.3 2% in 50 years

For the performance assessment for earthquakes of 2% probability of occurrence in 50 year, the results from the pushover- and nonlinear direct integration time-history analysis were used. For the time-history analysis the full suite of seven ground motions were used, so the mean values were used.

The structure was classified as being right at the limit of *Collapse prevention*. The following expectations are made for an earthquake of this magnitude:

- In the stairway infill walls may collapse and significant damage is to be expected for beams and columns.
- The core building is classified as *Immediate Occupancy*. Larger damage is expected for nonstructural components, such as dividing walls and ceiling finishing, while the beams and columns will have minor permanent deformations. This results in the core building being habitable but not necessarily operational.

6.3.5 Measures to improve performance level

As noted throughout the case study, the stairway is considered the weakest point of the structural system and is the governing factor for all performance assessments. This should therefore be the main focus when considering measures to improve the seismic performance. The underlying problem is the torsional irregularity the stairway poses, and so the measures should focus on deceasing the torsional irregularity. This can be measured by checking the modal mass

participation for the selected measures. For the original linear-elastic analysis model has the following modal mass participation are found the horizontal- and torsion rotational direction:

Table 6-8 - Modal mass participation ratio - Linear elastic analysis model

Modal mass participation ratio

Mode	Period [s]	U_x	U_y	R_z
1	0.43	0%	46%	23%
2	0.33	61%	0%	4%
3	0.30	0%	22%	30%
4	0.22	7%	0%	10%

The best measure to improve the seismic performance would be to reconfigure the plan configuration to satisfy the criteria of regularity in plan. As this would have great impact on the progress of the project, some measures with a lower impact is further discussed:

6.3.5.1 Slanted roof in stairway

As the largest interstory drifts occur at the top of the stairway tower, a possible solution is to reduce the height. With the slanted roof extending from the beam of the terrace level to the top of the stairway, the minimum height in the stairway would be 1.8m. This is on the low-side, but might be permissible if the roof is not intended for large activity.

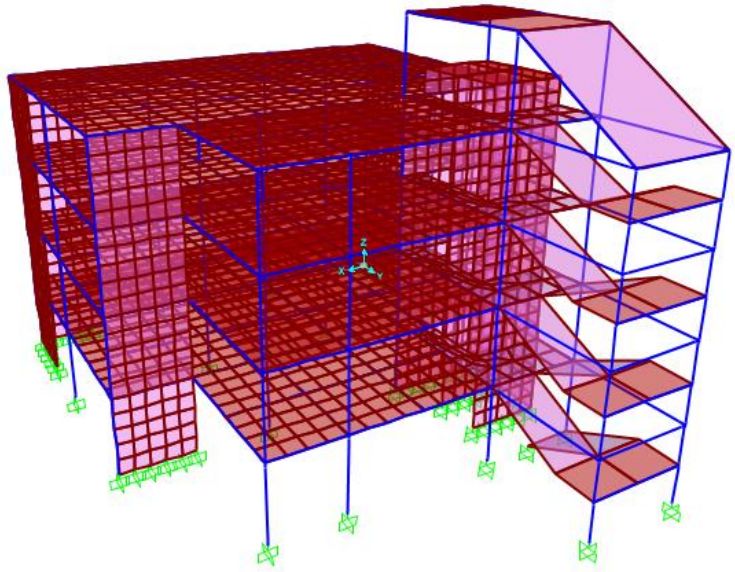

Figure 6-4 - Proposed design change - slanted roof in stairway

The following results are obtained from a modal analysis:

		Modal mass participation ratio			Change in modal mass participation		
Mode	Period [s]	U_x	U_y	R_z	ΔU_x	ΔU_y	ΔR_z
1	0.42	0%	49%	23%	0%	3%	0%
2	0.33	62%	0%	7%	1%	0	3%
3	0.28	7%	22%	39%	7%	0	9%
4	0.19	0%	0%	0%	-7%	0	-10%

This measure increases the modal mass participation slightly in the horizontal directions. The increase is enough to satisfy the demand in IS1893 of 65% modal mass participation in horizontal directions for the first three modes of vibration.

6.3.5.2 Extend elevator shaft to top of building

To improve the torsional stiffness of the stairway roof, the shear walls of the elevator shaft could be extended to the roof.

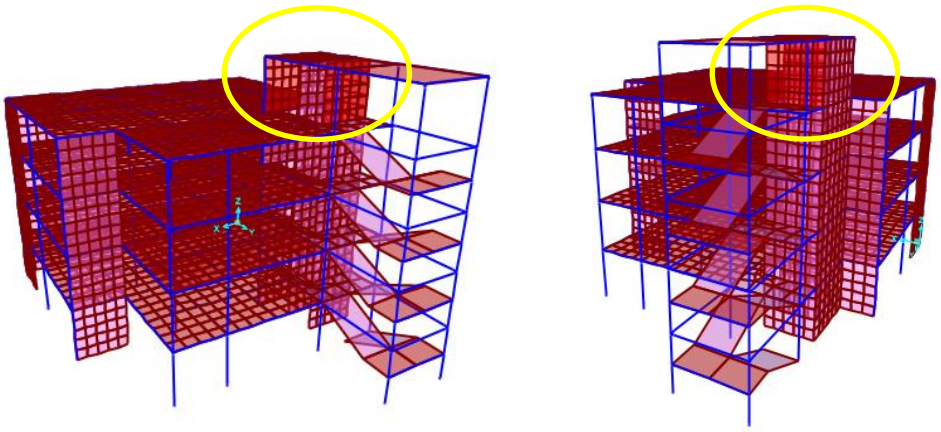

Figure 6-5 - Proposed design change - extend elevator shaft to stairway-roof

		Modal mass participation ratio			Change in modal mass participation		
Mode	Period [s]	U_x	U_y	R_z	ΔU_x	ΔU_y	ΔR_z
1	0.43	0.3%	48%	23%	0.3%	2%	0%
2	0.33	62%	1%	7%	1%	1%	3%
3	0.28	7%	23%	39%	7%	1%	9%
4	0.19	0%	0%	0%	-7%	0%	-10%

This measure increases the modal mass participation slightly in the horizontal directions. The increase is enough to satisfy the demand in IS1893 of 65% modal mass participation in horizontal directions for the first three modes of vibration.

6.3.5.3 Increase rebar in stairway columns

In the nonlinear time history analyses with 2% probability of occurrence in 50 years, the axial impact on the stairway columns was significantly higher than what the other analyses suspected. Increasing the amount of rebar in the columns of the stairway will not greatly affect the torsional rigidity of the overall structure. It will though improve the capacity of the columns, and thereby increasing the performance of the stairway.

7 CONCLUSION

The case study of this thesis had three purposes; to determine if the structure is code compliant after IS1893, to determine how this compares to seismic design after Eurocode 8, and lastly to determine the true structural performance for earthquakes of 50%- 10%- and 2%- probability of occurrence in 50 years. There was also performed analyses using ground motions from the 2015 Gorkha earthquake, which was found to have a seismic hazard equivalent of the 50%/50years hazard level.

The following conclusion are made:

- The structure is considered to partly code compliant to IS1893, with one limitation. The structure is considered to be torsional irregular, which is not allowed by the code. To comply with this demand there needs to be a change to increase the torsional stiffness or reduce the torsional radius of the building.
- The structure is not compliant to Eurocode 8. This is mostly due to the difference in seismic demands, which for the Eurocode analysis is based on PGA's from a PSHA [9]. Though the structure is not expected to collapse, it is expected to sustain more damage than what is considered acceptable by the code.
- The structural performance was evaluated after FEMA 356 and ASCE 41-13 to be the following:

Table 7-1 - Performance level of Kanti Children's hospital

	Operational (O)	Immediate Occupancy (IO)	Life Safety (LS)	Near Collapse (NC)
50% / 50 years*				
10% / 50 years				
2% / 50 years				

* equivalent to the 2015 Gorkha earthquake.

The stairway is identified as the weakest spot of the building and is governing the performance assessment. The following proposals are med to improve the structural performance of the building, and are arranged from least- to most-impacting:

- Increase amount of rebar in column B-5 and C-5 (Stairway)
- Recalculate the whole structural system with a higher zone factor. From the PSHA for Kathmandu it is suggested to use a zone factor of Z=0.49g.
- Relocate, add, and/or extend shear walls to reduce torsional irregularity.
- Reduce the height of the stairway tower.
- Architectural redesign to incorporate the stairway into the main building and reducing the irregularity in plan.

For further projects in Nepal, seismic prone regions, the following recommendations are made for the contractors or subsidiaries involved in the project, to ensure good seismic performance:

- Ensure that the seismic demand set for the building is reasonable with regards to PSHA for the project site.
- Specify, and value, structural regularity in preliminary design phase.
- Specify the wanted performance level for the structure for different earthquake scenarios.

REFERENCES

[1] H. Sucuoglu and S. Akkar, Basic Earthquake Engineering - From Seismology to Analysis to Design, Springer, 2014.

[2] United States Geological Survey, "Figur, tektoniske plater," [Online]. Available: https://pubs.usgs.gov/gip/dynamic/slabs.html. [Accessed 15 2 2017].

[3] United States Geological Survey (USGS), "Seismographs - Keeping track of eartquakes," USGS, [Online]. Available: https://earthquake.usgs.gov/learn/topics/keeping_track.php. [Accessed 27 May 2018].

[4] V. Kárník, N. D. Kondorskaya, J. V. Riznitchenko, E. F. Savarensky, S. L. Soloviev, N. V. Shebalin, J. Vanek and A. Zátopek, "Standarization of the earthquake magnitude scale," *Studia Geophysica et Geodaetica - Volume 6, Issue 1 p41-48*, Mars 1962.

[5] Buerau of Indian Standards, *IS1893 (Part 1) : 2016 - Criteria for Earthquake Resistand Design of Structrues*, Buerau of Indian Standards, 2016.

[6] United States Geological Survey, "Magnitude / Intensity comparrison," USGS, [Online]. Available: https://earthquake.usgs.gov/learn/topics/mag_vs_int.php. [Accessed 5 May 2018].

[7] H. Chaulagain, H. Rodrigues, V. Silva, E. Spacone and H. Varum, "Seismic risk assessment and hazard mapping in Nepal," *Nat Hazards*, 12 April 2015.

[8] National Centers for Enviornmental Information, "Significant earhtquakes in Nepal between year 1900-2018," NCEI, [Online]. Available: https://www.ngdc.noaa.gov/nndc/struts/results?bt_0=1900&st_0=2018&type_17=EXACT&query_17=None+Selected&op_12=eq&v_12=NEPAL&type_12=Or&query_14=None+Selected&type_3=Like&query_3=&st_1=&bt_2=&st_2=&bt_1=&bt_4=6.5&st_4=9&bt_5=&st_5=&bt_6=&st_6=&bt_7=&st_7=&b. [Accessed 27 05 2018].

[9] L. Sunuwar, M. B. Karkee, G. Pokharel and T. N. Lohani, "Comparative study of seismic hazard of Kathmandu valley, Nepal with other seismic prone cities," in *Proceedings of the 16th International Conference on Soil Mechanics and Geotechnical Engineering*, Osaka, 2005.

[10] CSI - Computers and Strcutrues, INC., "CSI Analysis Reference Manual - For SAP2000, ETABS, SAFE and CSI Bridge," CSI - Computers and Strcutrues, INC., 2017.

[11] G. Li and K. Wong, Theory of Nonlinear Structural Analaysis : The Force Analogy Method for Earthquake Engineering, Wiley, 2014.

[12] Applied Technology Council , "NIST GCR 17-917-46v3 - Guidlines for Nonlinear Structural Analysis for Design of Buildings - Part 2b - Reinforced Concrete Moment Frames," National Institute of Standards and Technology, Redwood City, 2017.

[13] Applied Techonolgy Council, "NIST GCR 17-917-46v1 - Guidlines for Nonlinear Structural Analysis for Design of Buildings - Part 1 - General," National Institute of Standards and Technology, 2017.

[14] A. K. Chopra, Dynamics of Structures - Theory and Application to Earthquake Engineering - Fourth Edition, Prentice Hall, 20112.

[15] Y. M. Fahjan, I. F. Kara and A. Mert, "Chapter 1 - Selection and Scaling Time History Records for Performance-Based Design," in *Performance-Based Seismic Design of Concrete Structure and Infrastructure*, IGI Global, 2017.

[16] PEER Research Center, "PEER Ground Motion Database," PEER Research Center, [Online]. Available: https://ngawest2.berkeley.edu/. [Accessed 28 May 2018].

[17] European Comittee for Standardization, *Eurocode 8: Design of structures for earthquake resistance - Part 1: Genral rules, seismic actions and rules for buildings*, European Comittee for Standardization, 2004.

[18] M. N. Fardis, E. C. Carvalho, P. Faajfar and A. Pecker, Seismic Design of Concrete Buildings to Eurocode 8, CRC Press - Taylor & Francis Group, 2015.

[19] Buerau of Indian Standards, *IS 13920-1993 - Ductile detailing of reinforced concrete structures subjected to seismic forces - Code of practice*, Buerau of Indian Standards, 1993.

[20] Department of Urban Development and Building Construction, *NBC 105 - Seismic Design of Buildings in Nepal*, Government of Nepal, 1994.

[21] American Society of Civil Engineers, *ASCE 41-13 - Seismic Evaluation and Retrofit of Excisting Buildings*, American Society of Civil Engineers, 2013.

[22] Federal Emergency Managment Agency, American Society of Civil Engineers, *FEMA 356 - Prestandard and Commentary for the Seismic Rehabilitation of Buildings*, Federal Emergency Managment Agency, 2000.

[23] Y. N. Khose, Y. Singh and D. Lang, "Comparative Study of Design Base shear for RC Buildings in Selected Seismic Design Codes," *Earthquak Spectra 28(3),* August 2012.

[24] NGC Pvt LTD, "Final report on soil investigation, geotechnical analysis of proposed building site at Kanti Hospital, Maharajgunj, kathmandu," NGC Pvt LTD, Kathmandu, 2017.

[25] Buerau of Indian Standards, *IS 456-2000 Plain and Reinforced Concrete - Code of Practice,* Buerau of Indian Standards, 2000.

[26] Buerau of Indian Standards, *IS 875 (Part 2) - Code of practice for deisgn loads*, Buerau of Indian Standards, 1987.

[27] N. Takai, S. Rajaure, M. Shigefuji, S. Bijukchhen, M. Ichiyanagi, M. R. Dhital and T. Sasatani, "Strong Ground Motion in the Kathmandu Valley during the 2015 Gorkha, Nepal, Earthquake," *Earth Planets and Space 68:10,* 2016.

[28] Britannica Academic, "Encyclopedia Britannica," 9 February 2018. [Online]. Available: http://academic.eb.com/levels/collegiate/article/earthquake/106195.

Appendix A – Architectural drawings of Kanti Children's hospital

Architectural drawings by Monika Shrestha at TEAM Consultants.

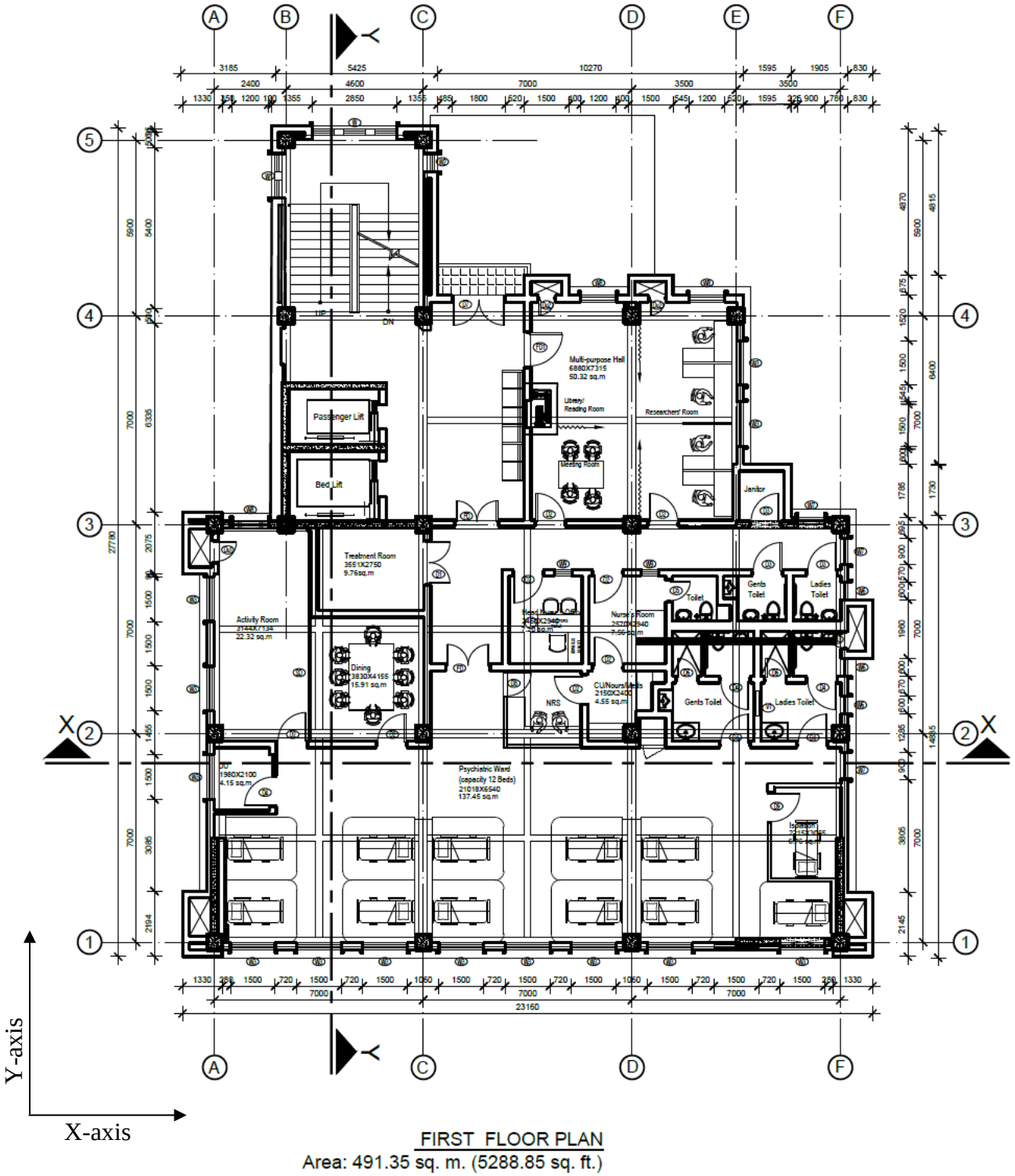

FIRST FLOOR PLAN
Area: 491.35 sq. m. (5288.85 sq. ft.)

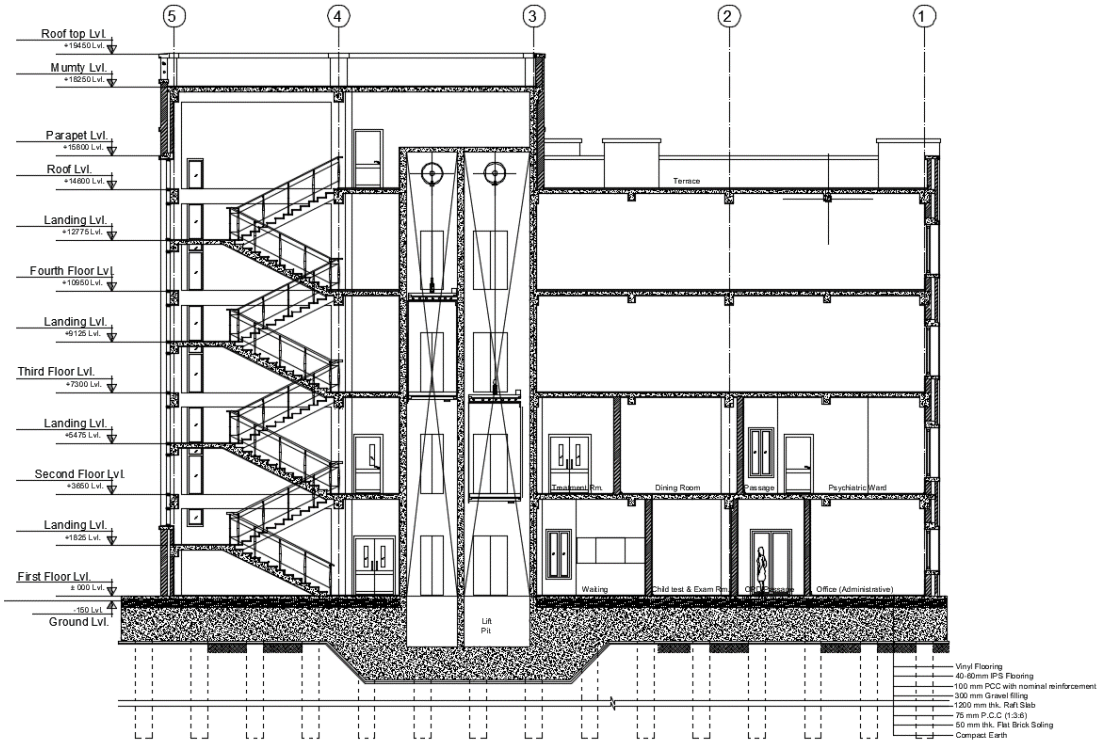

SECTION AT Y-Y

EAST ELEVATION

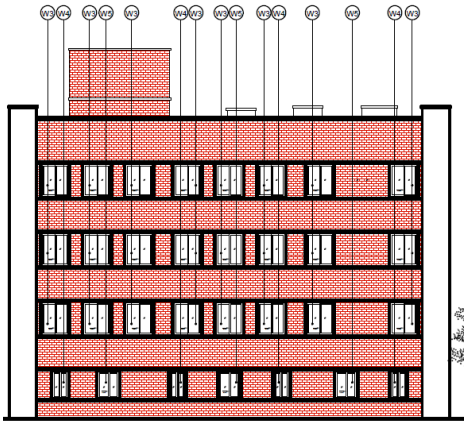

SOUTH ELEVATION

WEST ELEVATION

NORTH ELEVATION

Appendix B – Flowcharts
B-1: Linear elastic analysis flowchart

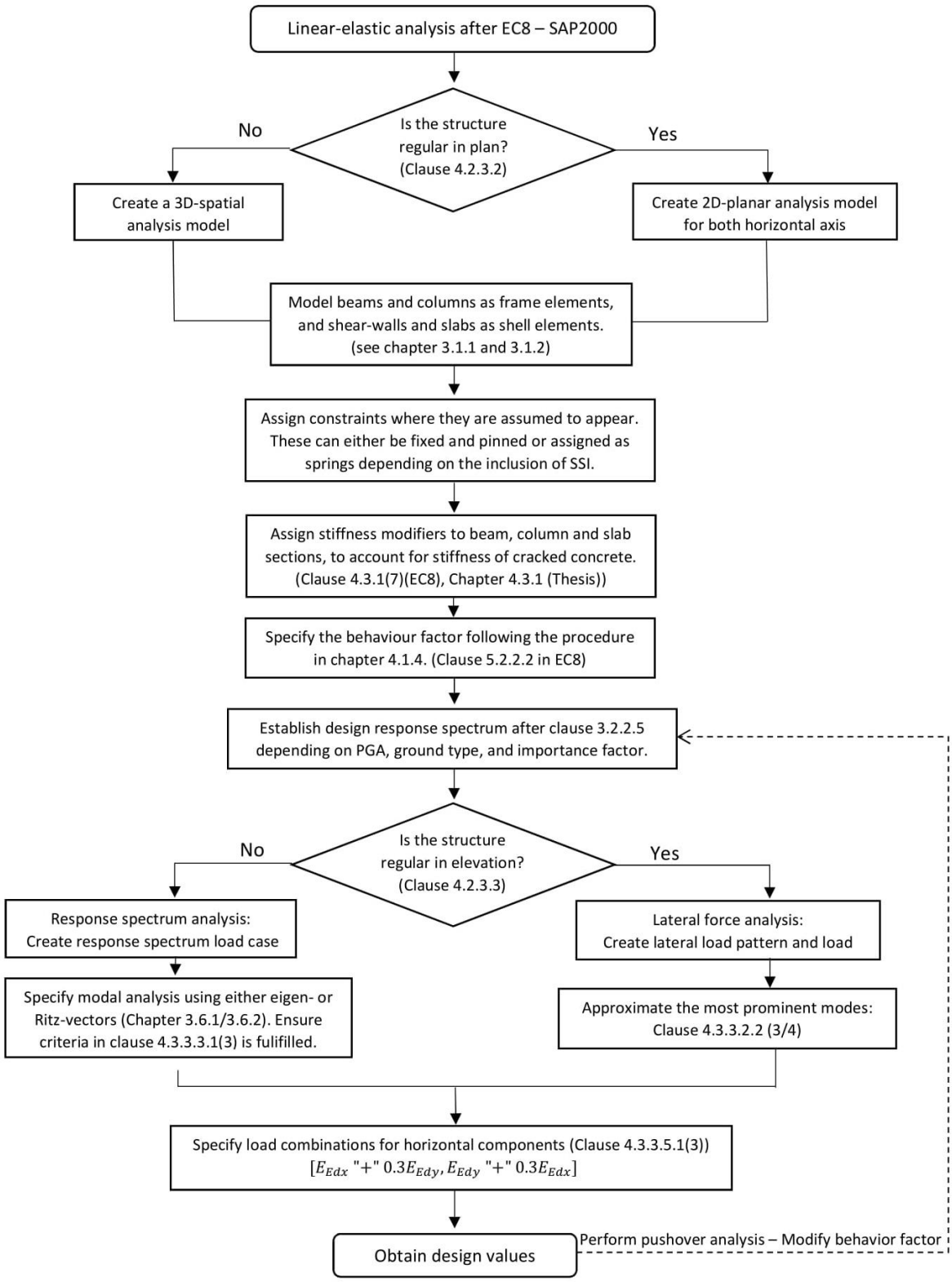

B-2: Pushover analysis flowchart

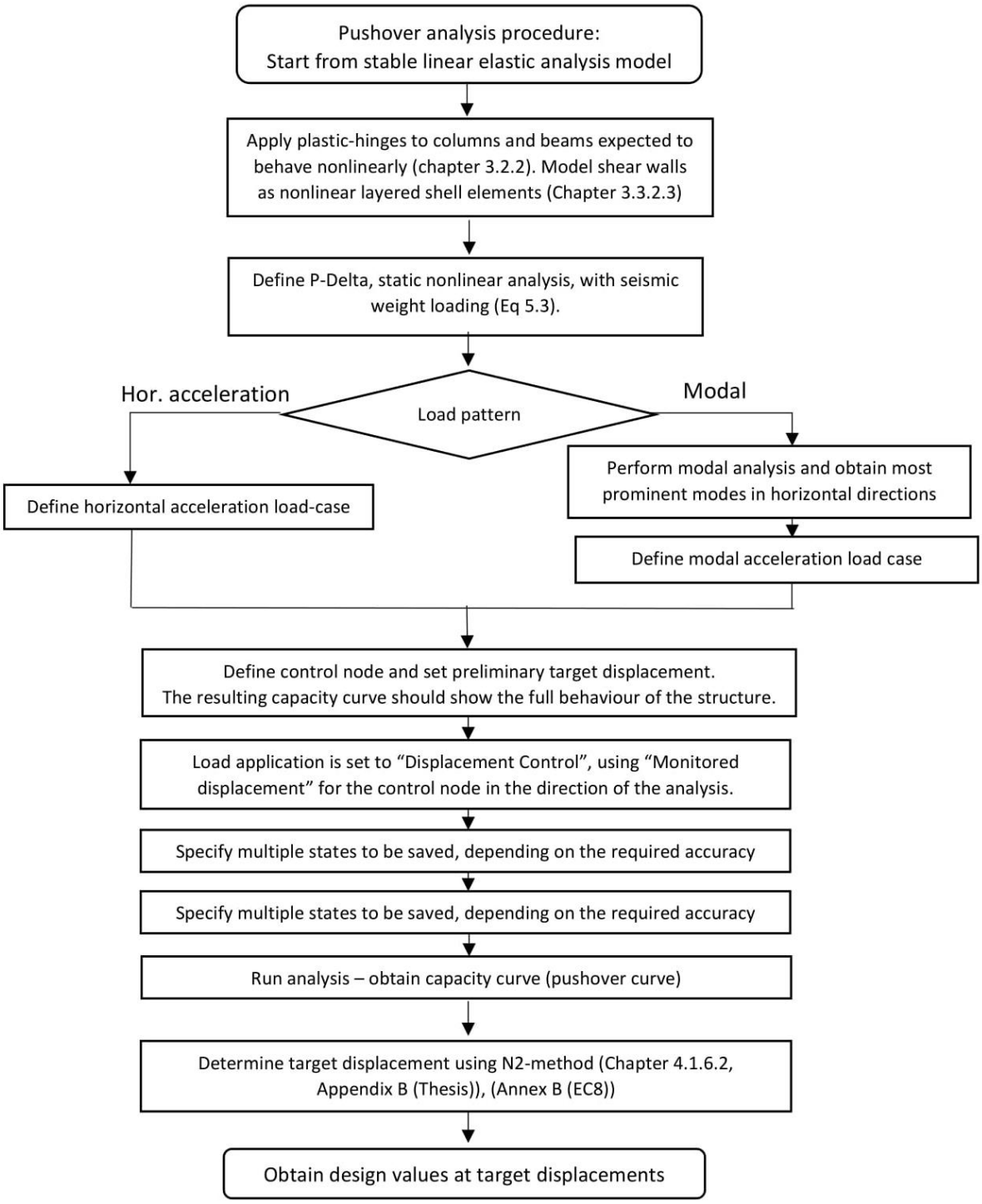

B-3: Time-history analysis flowchart

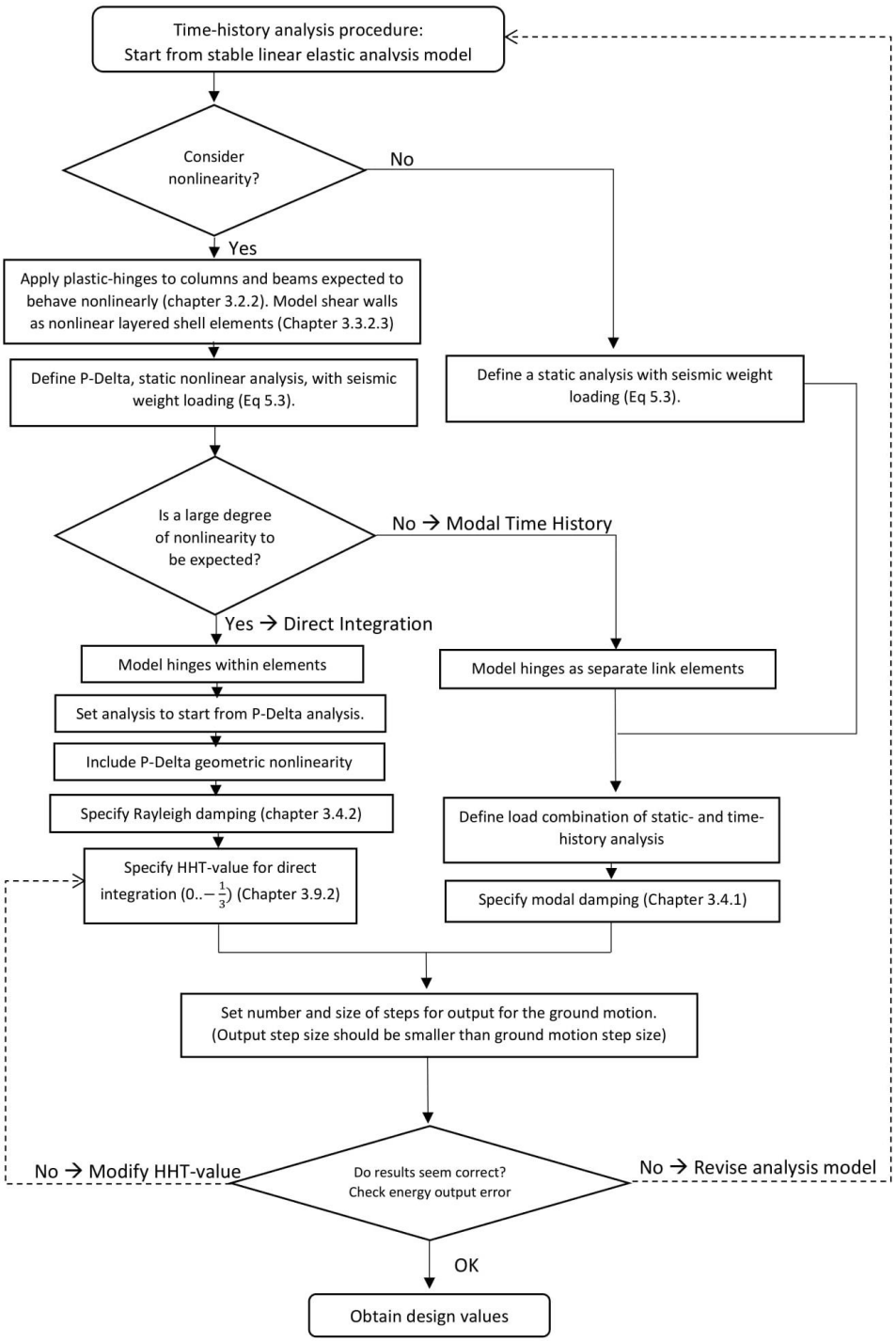

Appendix C – N2-Pushover Procedure
C-1: Eurocode 8:

Initializing data

```
> restart;
  with(plots):
  with(LinearAlgebra):
> PX:=ExcelTools:-Import("C:\\Users\\thoma\\OneDrive - Universitetet i Stavanger\\Masteroppgave-Thomass
  MacBook Pro\\2 - Case Study - Kanti Hospital\\Analysis\\Pushover\\Mai\\Pushover X.xls", "Pushover Capacity
  Curve");
  PY:=ExcelTools:-Import("C:\\Users\\thoma\\OneDrive - Universitetet i Stavanger\\Masteroppgave-Thomass
  MacBook Pro\\2 - Case Study - Kanti Hospital\\Analysis\\Pushover\\Mai\\Pushover Y.xls", "Pushover Capacity
  Curve");
```

$$PX := \begin{bmatrix} 1..653 \text{ x } 1..19 \text{ Array} \\ \text{Data Type: anything} \\ \text{Storage: rectangular} \\ \text{Order: Fortran\_order} \end{bmatrix}$$

$$PY := \begin{bmatrix} 1..614 \text{ x } 1..19 \text{ Array} \\ \text{Data Type: anything} \\ \text{Storage: rectangular} \\ \text{Order: Fortran\_order} \end{bmatrix} \quad (1.1)$$

Displacement shape is taken from the linear part of the pushover analysis in each direction.

```
> Phi_x:=Matrix(4,1,[1,0.7,0.41,0.15]);          #Displacement shape x-direction
  Phi_y:=Matrix(4,1,[1,0.73,0.45,0.17]);         #Displacement shape y-direction
  mass:=Matrix(4,1,1/9.81*[6568,7636,7636,7636]);     #Seismic mass of stories
```

$$Phi\_x := \begin{bmatrix} 1 \\ 0.7 \\ 0.41 \\ 0.15 \end{bmatrix}$$

$$Phi\_y := \begin{bmatrix} 1 \\ 0.73 \\ 0.45 \\ 0.17 \end{bmatrix}$$

$$mass := \begin{bmatrix} 669.5208971 \\ 778.3893987 \\ 778.3893987 \\ 778.3893987 \end{bmatrix} \quad (1.2)$$

Transformation from MDOF to SDOF:

```
> Gamma_x:=(add(mass[i,1]*Phi_x[i,1],i=1..4))/(add(mass[i,1]*Phi_x[i,1]^2,i=1..4));    #Transformation
  factor
  Gamma_y:=(add(mass[i,1]*Phi_y[i,1],i=1..4))/(add(mass[i,1]*Phi_y[i,1]^2,i=1..4));    #Transformation
  factor
```

$$Gamma\_x := 1.376053995$$
$$Gamma\_y := 1.360555865 \quad (1.3)$$

```
> mx:=(add(mass[i,1]*Phi_x[i,1],i=1..4));          #Eqiuvalent mass
  my:=(add(mass[i,1]*Phi_y[i,1],i=1..4));          #Eqiuvalent mass
```

$$mx := 1650.291540$$
$$my := 1720.346585 \quad (1.4)$$

```
> P1:=plot([['PX[i,3],PX[i,4]']$i=4..653],legend="Pushover curve - X",color=red,labels=["Displacement [mm]",
  "Base shear [kN]"],labeldirections=[horizontal,vertical]):
  P2:=plot([['PY[i,3],PY[i,4]']$i=4..614],legend="Pushover curve - Y",color=red,labels=["Displacement [mm]",
  "Base shear [kN]"],labeldirections=[horizontal,vertical]):
  P3:=plot([['PX[i,3]/Gamma_x,PX[i,4]/Gamma_x']$i=4..653],legend="Transformed pushover curve - X",color=
  blue):
  P4:=plot([['PY[i,3]/Gamma_y,PY[i,4]/Gamma_y']$i=4..614],legend="Transformed pushover curve - Y",color=
  blue):
```

Elastic response spectra (for period and displacement), without the behavior factor.

```
> RS:=(T,ag)->piecewise(T<=Tb,ag*S*(1+T/Tb*(eta*2.5-1)),T<=Tc,ag*S*eta*2.5,T<=Td,ag*S*eta*2.5*(Tc/T),T<=4,
  ag*S*eta*2.5*(Tc*Td/T^2));
  RS_D:=(T,ag)->piecewise(0.001*T<=RS(Tb,ag)*(Tb/(2*3.14))^2,ag*S*(1+(eta*2.5-1)*0.001*T/((RS(Tb,ag)*(Tb/(2*
  3.14))^2))),0.001*T<=RS(Tc,ag)*(Tc/(2*3.14))^2,ag*S*eta*2.5,0.001*T<=RS(Td,ag)*(Td/(2*3.14))^2,ag*S*eta*
  2.5*((RS(Tc,ag)*(Tc/(2*3.14))^2))/(0.001*T),0.001*T>=RS(4,ag)*(4/(2*3.14))^2,ag*S*eta*2.5*(((RS(Tc,ag)*
  (Tc/(2*3.14))^2)*(RS(Td,ag))*(Td/(2*3.14))^2))/((0.001*T)^2));
```

$$RS := (T, ag) \rightarrow piecewise\left(T \le Tb, ag\,S\left(1 + \frac{T\,(\eta \cdot 2.5 - 1)}{Tb}\right), T \le Tc, ag\,S\,\eta \cdot 2.5, T \le Td, ag\,S\,\eta \cdot 2.5\,\frac{Tc}{T}, T \le 4, ag\,S\,\eta \cdot 2.5\,\frac{Tc\,Td}{T^2}\right)$$

$$RS\_D := (T, ag) \rightarrow piecewise\left(0.001\ T \le \frac{RS(Tb, ag)\ Tb^2\ \frac{1}{4}}{3.14^2}, ag\ S\left(1 + \frac{(\eta \cdot 2.5 - 1) \cdot 0.001\ T}{\frac{RS(Tb, ag)\ Tb^2\ \frac{1}{4}}{3.14^2}}\right), 0.001\ T \le \frac{RS(Tc, ag)\ Tc^2\ \frac{1}{4}}{3.14^2}, ag\ S\ \eta \cdot 2.5, 0.001\ T \le \frac{RS(Td, ag)\ Td^2\ \frac{1}{4}}{3.14^2}, \frac{ag\ S\ \eta \cdot 2.5\ \frac{RS(Tc, ag)\ Tc^2\ \frac{1}{4}}{3.14^2}}{0.001\ T}, \frac{RS(4, ag) \cdot 4}{3.14^2} \le 0.001\ T, \frac{ag\ S\ \eta \cdot 2.5\ \frac{RS(Tc, ag)\ Tc^2\ \frac{1}{4}\ RS(Td, ag)\ Td^2\ \frac{1}{4}}{3.14^2\ 3.14^2}}{0.001^2\ T^2}\right) \quad (1.5)$$

```
> S:=1.15;
  Tb:=0.2;
  Tc:=0.6;
  Td:=2;
  eta:=1;
  ag_475:=0.49*1.4*9.81;
  ag_95:=0.26*1.4*9.81;
```

$$S := 1.15$$
$$Tb := 0.2$$
$$Tc := 0.6$$
$$Td := 2$$
$$\eta := 1$$
$$ag\_475 := 6.72966$$
$$ag\_95 := 3.57084 \quad (1.6)$$

```
> P5:=plot(RS(T,ag_475),T=0..4,legend="elastic response spectra - No Collapse",labels=[T,Sa/g]):
  P6:=plot(RS_D(T,ag_475),T=0..500,legend="elastic respons spectra - No Collapse",labels=["d* [mm]",Sa],
  color=purple,grid=on):
  P7:=plot(RS(T,ag_95),T=0..4,legend="elastic response spectra - Damage Limitation",labels=[T,Sa/g]):
  P8:=plot(RS_D(T,ag_95),T=0..500,legend="elastic respons spectra - Damage Limitation",labels=["d* [mm]",
  Sa],color=black):
```

Design base shear forces from preliminary response spectrum analysis:

```
> Fb_X:=11820;
  Fb_Y:=9748;
```

$$Fb\_X := 11820$$
$$Fb\_Y := 9748 \quad (1.7)$$

Code to determine target displacement:

```
> target_disp:=proc(F,m,T,ag,d)     #F=yield force, m=mass, T=period, ag=PGA, d=assignment value
      local q,d_et:

      d_et:=evalf(RS(T,ag)*((T/(2*Pi))^2)):     #Target displacement for unlimited elastic behavior

      if
      T<Tc                                      #Checking for short or longe structural period
      then
      if
      F/m>RS(T,ag)                              #Checking if response is linear or nonlinear
      then
      q:=1
      else
      q:=RS(T,ag)*my/Fy
      end if;

      d:=1000*d_et/q*(1+(q-1)*Tc/T);
      else
      d:=d_et;
      end if;

  end proc:
```

X-Direction

```
>   PX1:=plot(33000,x=0..140,linestyle=dashdot,color=black,legend="Yield Force"):
  PX2:=plot([[80,33000]],style=point,symbolsize=20,symbol=solidcircle,color=black,legend="Plastic
  Mechanism"):
  display(P1,P3,PX1,PX2);
```

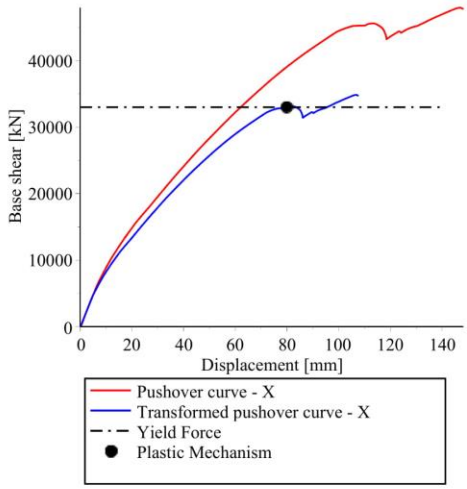

Yield strength read from graph:

```
> step:=494:
  Fy:=PX[step,4]/Gamma_x;
  dm:=PX[step,3]/Gamma_x;
```

$$Fy := 33030.19370$$

$$dm := 80.65048421 \quad (2.1)$$

Integration using trapezoidal method to find deformation energy up to formation of plastic mechanism:

```
> A:=0:
  C[1]:=0:
  i:='i':
  for i from 4 to (step-1) do
  A[i-3]:=((((PX[i,4]+PX[i+1,4])/2)/Gamma_x)*((PX[i+1,3]-PX[i,3])/Gamma_x)):
  C[i-2]:=C[i-3]+A[i-3]:
  end do:
  Em:=C[step-3];
```

$$Em := 1.674630229\ 10^{6} \quad (2.2)$$

Yield displacement

```
> dy:=2*(dm-Em/Fy);
```

$$dy := 59.9010042 \quad (2.3)$$

```
> f:=(x,y,t)->piecewise(x<=t,y*x,x>=t,y*t):
  PX3:=plot(f(x,Fy/dy,dy),x=0..100,legend="Idealized elasto-perfect plastic",color=red,labels=["Displacement
  [mm]","Base shear [kN]"]):
  PX4:=plot([dy,y,y=0..40000],linestyle=dashdot,color=black,legend="d_y*"):
  PX5:=plot([dm,y,y=0..40000],linestyle=dashdot,color=grey,legend="d_m*"):
  PX6:=plot(Fy,x=0..100,linestyle=dashdot,color=red,legend="F_y*"):
  display(P3,PX3,PX4,PX5,PX6);
```

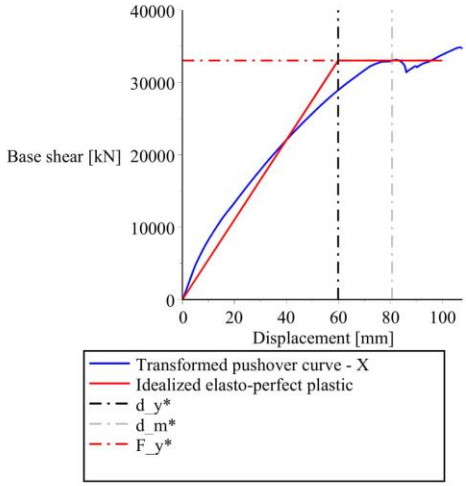

Period of idealized equivalent SDOF:

```
> T:=evalf(2*Pi*sqrt(mx*(dy/1000)/Fy));
```

$$T := 0.3437333704 \quad (2.4)$$

The target displacement (SDOF) for 95- and 475-year return period is found by the function:

```
> target_disp(Fy,mx,T,ag_475,d_t_x_NC);
  target_disp(Fy,mx,T,ag_95,d_t_x_DL);
```

57.90480829
30.72500032 (2.5)

```
> T:='T':
  RESP_X:=T->piecewise(T<=1000*(Fy/mx)/(RS(0.34,ag_475)/(RS(0.34,ag_475)*(0.34/(2*3.14))^2)),0.001*RS(0.34,
  ag)/(RS(0.34,ag)*(0.34/(2*3.14))^2)*T,T>=(Fy/mx)/(RS(0.34,ag)/(RS(0.34,ag)*(0.34/(2*3.14))^2)),Fy/mx):
  PX7:=plot([[d_t_x_NC,RS(0.34,ag_475)]],style=point,color=red,legend="Performance point - No Collapse",
  labels=["d*","Sa"],symbol=solidcircle,symbolsize=15):
  PX8:=plot([[d_t_x_DL,RS(0.34,ag_95)]],style=point,color=red,legend="Performance point - Damage
  Limitation",labels=["d*","Sa"],symbol=solidcircle,symbolsize=15):
  PX9:=plot([d_t_x_NC,y,y=0..25],color=black,linestyle=dashdot,legend="d_t_NC*"):
  PX10:=plot([d_t_x_DL,y,y=0..25],color=green,linestyle=dashdot,legend="d_t_DL*"):
  PX11:=plot([1000*(Fy/mx)/(RS(0.34,ag)/(RS(0.34,ag)*(0.34/(2*3.14))^2)),y,y=0..25],color=blue,linestyle=
  dashdot,legend="d_y*"):
  PX12:=plot(RESP_X(T),T=0..300,color=red,legend="idealized response"):
  PX13:=plot(Fy/mx,x=0..300,color=red,linestyle=dashdot,legend="F_y*/m*"):
  display(P6,P8,PX7,PX8,PX9,PX10,PX11,PX12,PX13);
```

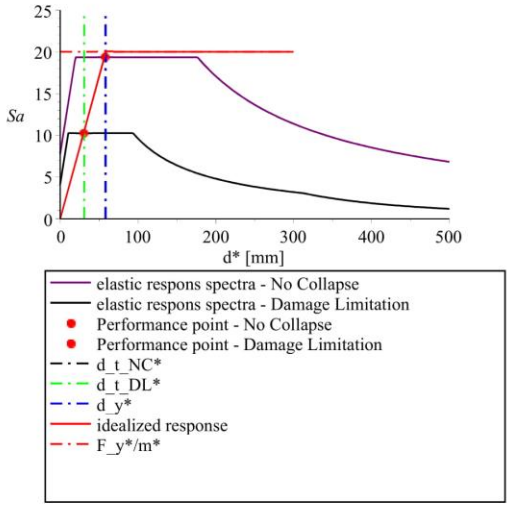

Transfer back to real pushover curve

```
> d_target_x_NC:=d_t_x_NC*Gamma_x;
  d_target_x_DL:=d_t_x_DL*Gamma_x;
  PX14:=plot([d_target_x_NC,y,y=0..50000],linestyle=dashdot,color=black,legend="Target displacement - No
  Collapse"):
  PX15:=plot([d_target_x_DL,y,y=0..50000],linestyle=dashdot,color=blue,legend="Target displacement - Damage
  Limitation"):

  display(P1,PX14,PX15);
```

$$d\_target\_x\_NC := 79.68014278$$
$$d\_target\_x\_DL := 42.27925944$$

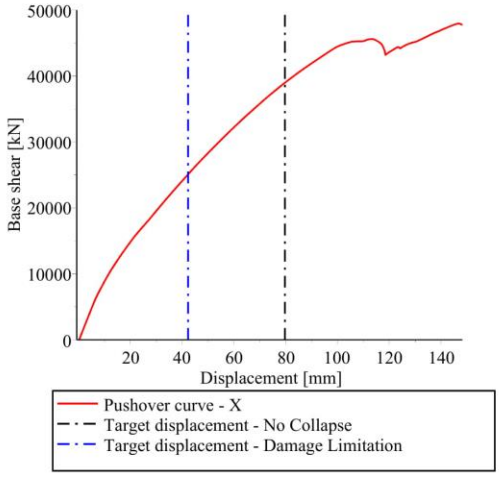

Checking the overstrength factor:
Base shear obtained from a preliminary response spectrum analysis, with behavior factor q=3.1.
First yield is determined by first instance of plastic hinge "IO".
Plastic yield in a significant amount of members is determined by the yield point of the pushover curve

```
> Yield_X:=15300:
  Plastic_X:=45000:
  PX13:=plot(Fb_X,x=0..140,legend="Respons spectrum analysis - Base shear X",color=black,linestyle=dash):
  PX14:=plot(Yield_X,x=0..140,legend="First local yield",color=green,linestyle=dash):
  PX15:=plot(Plastic_X,x=0..140,legend="Fully plastic yield",color=blue,linestyle=dash):
  display(P1,PX13,PX14,PX15);
```

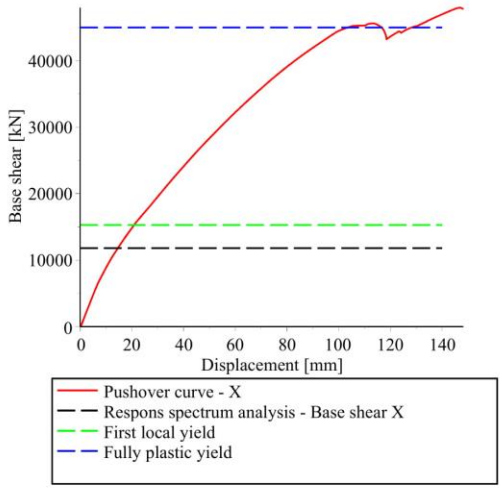


```
> 'alpha_u/alpha_1'='Plastic_X/Yield_X';
  'alpha_u/alpha_1'=evalf(Plastic_X/Yield_X);
```

$$\frac{alpha\_u}{alpha\_1} = \frac{Plastic\_X}{Yield\_X}$$

$$\frac{alpha\_u}{alpha\_1} = 2.941176471 \qquad (2.6)$$

Y-Direction

```
> PY1:=plot(26300,x=0..110,linestyle=dashdot,color=black,legend="Yield Force"):
  PY2:=plot([[53,26300]],style=point,symbolsize=20,symbol=solidcircle,color=black,legend="Plastic
  Mechanism"):
  display(P2,P4,PY1,PY2);
```

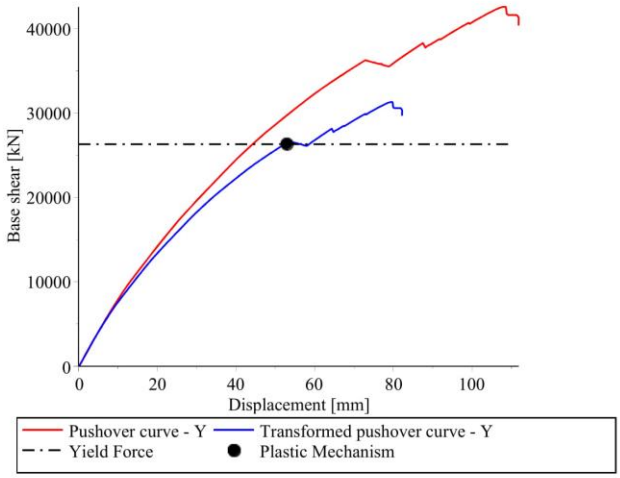

Yield strength read from graph:

```
> step:=410:
  Fy:=PY[step,4]/Gamma_y;
  dm:=PY[step,3]/Gamma_y;
```

$$Fy := 26611.03445$$

$$dm := 53.82990429 \qquad (3.1)$$

Integration using trapezoidal method to find deformation energy up to formation of plastic mechanism:

```
> A:=0:
  C[1]:=0:
  i:='i':
  for i from 4 to (step-1) do
  A[i-3]:=((((PY[i,4]+PY[i+1,4])/2)/Gamma_x)*((PY[i+1,3]-PY[i,3])/Gamma_x)):
  C[i-2]:=C[i-3]+A[i-3]:
  end do:
  Em:=C[step-3];
```

$$Em := 8.278379471\ 10^{5} \quad (3.2)$$

Yield displacement

```
> dy:=2*(dm-Em/Fy);
```

$$dy := 45.44216362 \quad (3.3)$$

```
> f:=(x,y,t)->piecewise(x<=t,y*x,x>=t,y*t):
  PY3:=plot(f(x,Fy/dy,dy),x=0..100,legend="Idealized elasto-perfect plastic",color=red,labels=["Displacement
  [mm]","Base shear [kN]"]):
  PY4:=plot([dy,y,y=0..40000],linestyle=dashdot,color=black,legend="d_y*"):
  PY5:=plot([dm,y,y=0..40000],linestyle=dashdot,color=grey,legend="d_m*"):
  PY6:=plot(Fy,x=0..100,linestyle=dashdot,color=red,legend="F_y*"):
  display(P4,PY3,PY4,PY5,PY6);
```

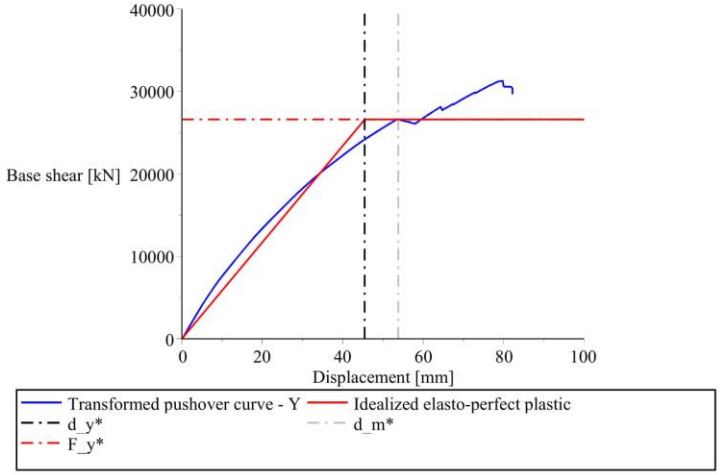

Period of idealized equivalent SDOF:

```
> T:=evalf(2*Pi*sqrt(mx*(dy/1000)/Fy));
```

$$T := 0.3335483732 \quad (3.4)$$

The target displacement (SDOF) for 95- and 475-year return period is found by the function:

```
> target_disp(Fy,my,T,ag_475,d_t_y_NC);
  target_disp(Fy,my,T,ag_95,d_t_y_DL);
```

63.25742644
28.93118065 (3.5)

```
> T:='T':
  RESP_Y:=T->piecewise(T<=1000*(Fy/my)/(RS(0.33,ag)/(RS(0.33,ag)*(0.33/(2*3.14))^2)),0.001*RS(0.33,ag)/(RS
  (0.33,ag)*(0.33/(2*3.14))^2)*T,T>=(Fy/my)/(RS(0.33,ag)/(RS(0.33,ag)*(0.33/(2*3.14))^2)),Fy/my):
  PER_Y:=T->0.001*RS(0.33,ag)/(RS(0.33,ag)*(0.33/(2*3.14))^2)*T:
  PY7:=plot([[d_t_y_NC,RESP_Y(d_t_y_NC)]],style=point,color=red,legend="Performance point",labels=["d*",Sa],
  symbol=solidcircle,symbolsize=15):
  PY8:=plot([[d_t_y_DL,RESP_Y(d_t_y_DL)]],style=point,color=red,legend="Performance point",labels=["d*",Sa],
  symbol=solidcircle,symbolsize=15):
  PY9:=plot([d_t_y_NC,y,y=0..25],color=black,linestyle=dashdot,legend="d_t_y_NC*"):
  PY10:=plot([d_t_y_DL,y,y=0..25],color=green,linestyle=dashdot,legend="d_t_y_DL*"):
  PY11:=plot([1000*(Fy/my)/(RS(0.33,ag)/(RS(0.33,ag)*(0.33/(2*3.14))^2)),y,y=0..25],color=grey,linestyle=
  dashdot,legend="d_y*"):
  PY12:=plot(RESP_Y(T),T=0..300,color=red,legend="idealized response"):
  PY13:=plot(Fy/my,x=0..300,color=red,linestyle=dashdot,legend="Fy*/m*"):
  PY14:=plot(PER_Y(T),T=0..70,color=red,linestyle=dot,legend="T=0.33s"):

  display(P6,P8,PY7,PY8,PY9,PY10,PY11,PY12,PY13,PY14);
```

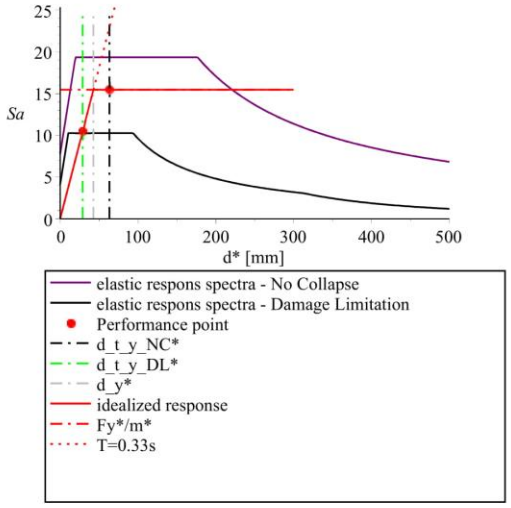

Transfer back to real pushover curve.

```
> d_target_y_NC:=d_t_y_NC*Gamma_y;
  d_target_y_DL:=d_t_y_DL*Gamma_y;
  PY15:=plot([d_target_y_NC,y,y=0..50000],color=black,linestyle=dashdot,legend="Target displacement - No
  Collapse"):
  PY16:=plot([d_target_y_DL,y,y=0..50000],color=blue,linestyle=dashdot,legend="Target displacement - Damage
  Limitation"):
  display(P2,PY15,PY16);
```

$$d\_target\_y\_NC := 86.06526255$$
$$d\_target\_y\_DL := 39.36248751$$

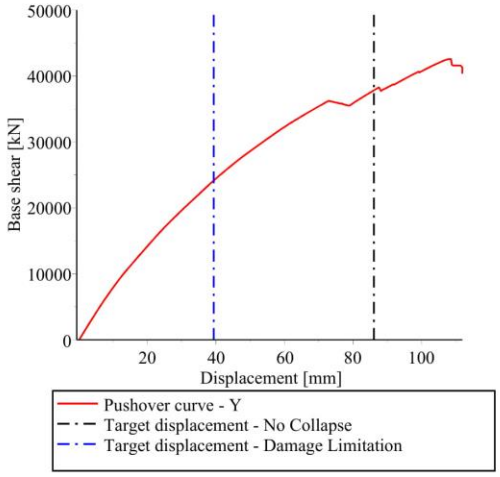

Checking the overstrength factor:
Base shear obtained from a preliminary response spectrum analysis, with behavior factor q=3.1.
First yield is determined by first instance of plastic hinge "IO".
Plastic yield in a significant amount of members is determined by the yield point of the pushover curve

```
> Yield_Y:=15725:
  Plastic_Y:=36000:
  PY14:=plot(Fb_Y,x=0..140,legend="Respons spectrum analysis - Base shear Y",color=black,linestyle=dash):
  PY15:=plot(Yield_Y,x=0..140,legend="First local yield",color=green,linestyle=dash):
  PY16:=plot(Plastic_Y,x=0..140,legend="Fully plastic yield",color=blue,linestyle=dash,labels=["Displacement
  [mm]","Base shear [kN]"],labeldirections=[horizontal,vertical]):
```

```
display(P2,PY14,PY15,PY16);
```

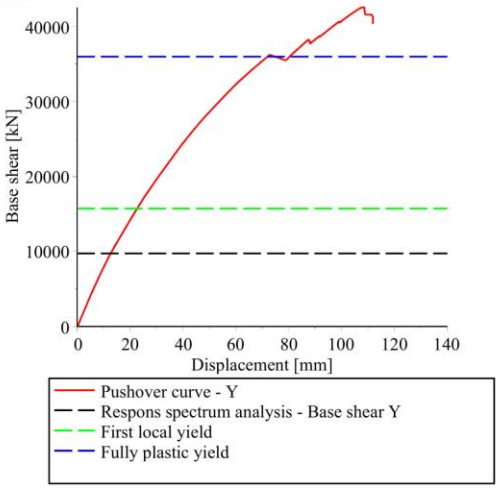


```
> 'alpha_u/alpha_1'='Plastic_Y/Yield_Y';
  'alpha_u/alpha_1'=evalf(Plastic_Y/Yield_Y);
```

$$\frac{alpha\_u}{alpha\_1} = \frac{Plastic\_Y}{Yield\_Y}$$

$$\frac{alpha\_u}{alpha\_1} = 2.289348172 \qquad (3.6)$$

C-2: Performance assessment using N2-Pushover procedure

Initializing data

```
> restart;
  with(plots):
  with(LinearAlgebra):
> PX:=ExcelTools:-Import("C:\\Users\\thoma\\OneDrive - Universitetet i Stavanger\\Masteroppgave-Thomass
  MacBook Pro\\2 - Case Study - Kanti Hospital\\Analysis\\Pushover\\Mai\\Pushover X.xls", "Pushover Capacity
  Curve");
  PY:=ExcelTools:-Import("C:\\Users\\thoma\\OneDrive - Universitetet i Stavanger\\Masteroppgave-Thomass
  MacBook Pro\\2 - Case Study - Kanti Hospital\\Analysis\\Pushover\\Mai\\Pushover Y.xls", "Pushover Capacity
  Curve");
```

$$PX := \begin{bmatrix} 1..653 \text{ x } 1..19 \text{ Array} \\ \text{Data Type: anything} \\ \text{Storage: rectangular} \\ \text{Order: Fortran\_order} \end{bmatrix}$$

$$PY := \begin{bmatrix} 1..614 \text{ x } 1..19 \text{ Array} \\ \text{Data Type: anything} \\ \text{Storage: rectangular} \\ \text{Order: Fortran\_order} \end{bmatrix} \quad (1.1)$$

Displacement shape is taken from the linear part of the pushover analysis in each direction.

```
> Phi_x:=Matrix(4,1,[1,0.7,0.41,0.15]);        #Displacement shape x-direction
  Phi_y:=Matrix(4,1,[1,0.73,0.45,0.17]);       #Displacement shape y-direction
  mass:=Matrix(4,1,1/9.81*[6568,7636,7636,7636]);      #Seismic mass of stories
```

$$Phi\_x := \begin{bmatrix} 1 \\ 0.7 \\ 0.41 \\ 0.15 \end{bmatrix}$$

$$Phi\_y := \begin{bmatrix} 1 \\ 0.73 \\ 0.45 \\ 0.17 \end{bmatrix}$$

$$mass := \begin{bmatrix} 669.5208971 \\ 778.3893987 \\ 778.3893987 \\ 778.3893987 \end{bmatrix} \quad (1.2)$$

Transformation from MDOF to SDOF:

```
> Gamma_x:=(add(mass[i,1]*Phi_x[i,1],i=1..4))/(add(mass[i,1]*Phi_x[i,1]^2,i=1..4));    #Transformation
  factor
  Gamma_y:=(add(mass[i,1]*Phi_y[i,1],i=1..4))/(add(mass[i,1]*Phi_y[i,1]^2,i=1..4));    #Transformation
  factor
```

$$Gamma\_x := 1.376053995$$
$$Gamma\_y := 1.360555865 \quad (1.3)$$

```
> mx:=(add(mass[i,1]*Phi_x[i,1],i=1..4));          #Eqiuvalent mass
  my:=(add(mass[i,1]*Phi_y[i,1],i=1..4));          #Eqiuvalent mass
```

$$mx := 1650.291540$$
$$my := 1720.346585 \quad (1.4)$$

```
> P1:=plot([['PX[i,3],PX[i,4]']$i=4..653],legend="Pushover curve - X",color=red,labels=["Displacement [mm]",
  "Base shear [kN]"],labeldirections=[horizontal,vertical]):
  P2:=plot([['PY[i,3],PY[i,4]']$i=4..614],legend="Pushover curve - Y",color=red,labels=["Displacement [mm]",
  "Base shear [kN]"],labeldirections=[horizontal,vertical]):
  P3:=plot([['PX[i,3]/Gamma_x,PX[i,4]/Gamma_x']$i=4..653],legend="Transformed pushover curve - X",color=
  blue):
  P4:=plot([['PY[i,3]/Gamma_y,PY[i,4]/Gamma_y']$i=4..614],legend="Transformed pushover curve - Y",color=
  blue):
```

Elastic response spectra (for period and displacement), without the behavior factor.

```
> RS:=(T,ag)->piecewise(T<=Tb,ag*S*(1+T/Tb*(eta*2.5-1)),T<=Tc,ag*S*eta*2.5,T<=Td,ag*S*eta*2.5*(Tc/T),T<=4,
  ag*S*eta*2.5*(Tc*Td/T^2));
  RS_D:=(T,ag)->piecewise(0.001*T<=RS(Tb,ag)*(Tb/(2*3.14))^2,ag*S*(1+(eta*2.5-1)*0.001*T/((RS(Tb,ag)*(Tb/(2*
  3.14))^2))),0.001*T<=RS(Tc,ag)*(Tc/(2*3.14))^2,ag*S*eta*2.5,0.001*T<=RS(Td,ag)*(Td/(2*3.14))^2,ag*S*eta*
  2.5*((RS(Tc,ag)*(Tc/(2*3.14))^2))/(0.001*T),0.001*T>=RS(4,ag)*(4/(2*3.14))^2,ag*S*eta*2.5*(((RS(Tc,ag)*
  (Tc/(2*3.14))^2)*(RS(Td,ag))*(Td/(2*3.14))^2))/((0.001*T)^2));
```

$$RS := (T, ag) \rightarrow piecewise\left(T \le Tb, ag\,S\left(1 + \frac{T\,(\eta \cdot 2.5 - 1)}{Tb}\right), T \le Tc, ag\,S\,\eta \cdot 2.5, T \le Td, ag\,S\,\eta \cdot 2.5\,\frac{Tc}{T}, T \le 4, ag\,S\,\eta \cdot 2.5\,\frac{Tc\,Td}{T^2}\right)$$

$$RS\_D := (T, ag) \rightarrow piecewise\left(0.001\ T \le \frac{RS(Tb, ag)\ Tb^2\ \frac{1}{4}}{3.14^2}, ag\ S\left(1 + \frac{(\eta \cdot 2.5 - 1) \cdot 0.001\ T}{\frac{RS(Tb, ag)\ Tb^2\ \frac{1}{4}}{3.14^2}}\right), 0.001\ T \le \frac{RS(Tc, ag)\ Tc^2\ \frac{1}{4}}{3.14^2}, ag\ S\ \eta \cdot 2.5, 0.001\ T \le \frac{RS(Td, ag)\ Td^2\ \frac{1}{4}}{3.14^2}, \frac{ag\ S\ \eta \cdot 2.5\ \frac{RS(Tc, ag)\ Tc^2\ \frac{1}{4}}{3.14^2}}{0.001\ T}, \frac{RS(4, ag) \cdot 4}{3.14^2} \le 0.001\ T, \frac{ag\ S\ \eta \cdot 2.5\ \frac{RS(Tc, ag)\ Tc^2\ \frac{1}{4}\ RS(Td, ag)\ Td^2\ \frac{1}{4}}{3.14^2\ 3.14^2}}{0.001^2\ T^2}\right) \quad (1.5)$$

```
> S:=1.15;
  Tb:=0.2;
  Tc:=0.6;
  Td:=2;
  eta:=1;
  ag_2475:=0.76*9.81;
  ag_475:=0.49*9.81;
  ag_95:=0.26*9.81;
```

$$S := 1.15$$
$$Tb := 0.2$$
$$Tc := 0.6$$
$$Td := 2$$
$$\eta := 1$$
$$ag\_2475 := 7.4556$$
$$ag\_475 := 4.8069$$
$$ag\_95 := 2.5506 \quad (1.6)$$

```
> P5:=plot(RS(T,ag_475),T=0..4,legend="elastic response spectra - 10% in 50 years",labels=[T,Sa/g]):
  P6:=plot(RS_D(T,ag_475),T=0..500,legend="elastic respons spectra - 10% in 50 years",labels=["d* [mm]",Sa],
  color=black,grid=on):
  P7:=plot(RS(T,ag_95),T=0..4,legend="elastic response spectra - 50% in 50 years",labels=[T,Sa/g]):
  P8:=plot(RS_D(T,ag_95),T=0..500,legend="elastic respons spectra - 50% in 50 years",labels=["d* [mm]",Sa],
  color="Lime"):
  P9:=plot(RS(T,ag_2475),T=0..4,legend="elastic response spectra - 5% in 50 years",labels=[T,Sa/g]):
  P10:=plot(RS_D(T,ag_2475),T=0..500,legend="elastic respons spectra - 2% in 50 years",labels=["d* [mm]",
  Sa],color=cyan):
```

Code to determine target displacement:

```
> target_disp:=proc(F,m,T,ag,d)    #F=yield force, m=mass, T=period, ag=PGA, d=assignment value
      local q,d_et:

      d_et:=evalf(RS(T,ag)*((T/(2*Pi))^2)):     #Target displacement for unlimited elastic behavior

      if
      T<Tc                                      #Checking for short or longe structural period
      then
      if
      F/m>RS(T,ag)                              #Checking if response is elastic or inelastic
      then
      q:=1
      else
      q:=RS(T,ag)*my/Fy
      end if;

      d:=1000*d_et/q*(1+(q-1)*Tc/T);
      else
      d:=d_et;                                  #Target displacement for SDOF system
      end if;

  end proc:
```

X-Direction

```
> PX1:=plot(33000,x=0..140,linestyle=dashdot,color=black,legend="Yield Force"):
  PX2:=plot([[80,33000]],style=point,symbolsize=20,symbol=solidcircle,color=black,legend="Plastic
  Mechanism"):
  display(P1,P3,PX1,PX2);
```

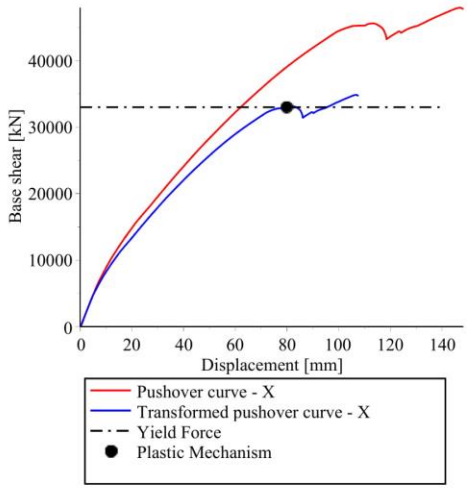

Yield strength read from graph:

```
> step:=494:
  Fy:=PX[step,4]/Gamma_x;
  dm:=PX[step,3]/Gamma_x;
```

$$Fy := 33030.19370$$

$$dm := 80.65048421 \quad (2.1)$$

Integration using trapezoidal method to find deformation energy up to formation of plastic mechanism:

```
> A:=0:
  C[1]:=0:
  i:='i':
  for i from 4 to (step-1) do
  A[i-3]:=((((PX[i,4]+PX[i+1,4])/2)/Gamma_x)*((PX[i+1,3]-PX[i,3])/Gamma_x)):
  C[i-2]:=C[i-3]+A[i-3]:
  end do:
  Em:=C[step-3];
```

$$Em := 1.674630229\ 10^{6} \quad (2.2)$$

Yield displacement

```
> dy:=2*(dm-Em/Fy);
```

$$dy := 59.9010042 \quad (2.3)$$

```
> f:=(x,y,t)->piecewise(x<=t,y*x,x>=t,y*t):
  PX3:=plot(f(x,Fy/dy,dy),x=0..100,legend="Idealized elasto-perfect plastic",color=red,labels=["Displacement
  [mm]","Base shear [kN]"]):
  PX4:=plot([dy,y,y=0..40000],linestyle=dashdot,color=black,legend="d_y*"):
  PX5:=plot([dm,y,y=0..40000],linestyle=dashdot,color=grey,legend="d_m*"):
  PX6:=plot(Fy,x=0..100,linestyle=dashdot,color=red,legend="F_y*"):
  display(P3,PX3,PX4,PX5,PX6);
```

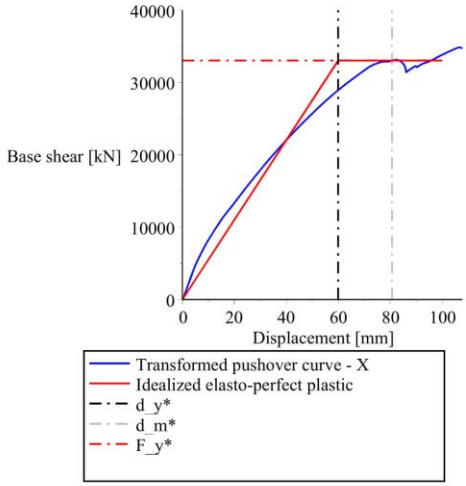

Period of idealized equivalent SDOF:

```
> T:=evalf(2*Pi*sqrt(mx*(dy/1000)/Fy));
```

$$T := 0.3437333704 \tag{2.4}$$

The target displacement (SDOF) for 95- and 475-year return period is found by the function:

```
> target_disp(Fy,mx,T,ag_2475,d_t_x_2475);
  target_disp(Fy,mx,T,ag_475,d_t_x_475);
  target_disp(Fy,mx,T,ag_95,d_t_x_95);
```

69.13827257
41.36057733
21.94642879 (2.5)

```
> T:='T':
  RESP_X:=T->piecewise(T<=1000*(Fy/mx)/(RS(0.34,ag_475)/(RS(0.34,ag_475)*(0.34/(2*3.14))^2)),0.001*RS(0.34,
  ag)/(RS(0.34,ag)*(0.34/(2*3.14))^2)*T,T>=(Fy/mx)/(RS(0.34,ag)/(RS(0.34,ag)*(0.34/(2*3.14))^2)),Fy/mx):
  PX9:=plot([d_t_x_475,y,y=0..25],color=black,linestyle=dashdot,legend="d_t_475*"):
  PX10:=plot([d_t_x_95,y,y=0..25],color=green,linestyle=dashdot,legend="d_t_95*"):
  PX10:=plot([d_t_x_2475,y,y=0..25],color=orange,linestyle=dashdot,legend="d_t_2475*"):
  PX11:=plot([1000*(Fy/mx)/(RS(0.34,ag)/(RS(0.34,ag)*(0.34/(2*3.14))^2)),y,y=0..25],color=blue,linestyle=
  dashdot,legend="d_y*"):
  PX12:=plot(RESP_X(T),T=0..300,color=red,legend="idealized response"):
  PX13:=plot(Fy/mx,x=0..300,color=red,linestyle=dashdot,legend="F_y*/m*"):
  display(P6,P8,P10,PX9,PX10,PX11,PX12,PX13);
```

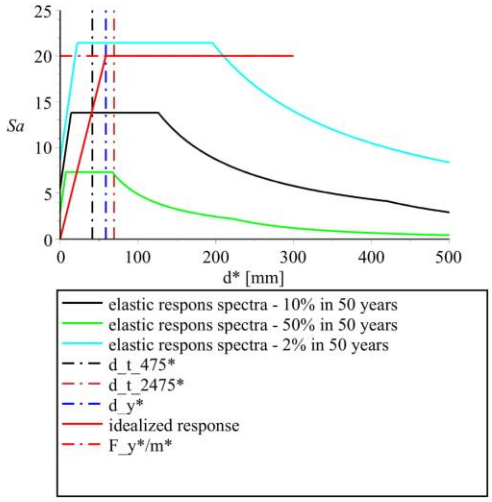

Transfer back to real pushover curve

```
> d_target_x_2475:=d_t_x_2475*Gamma_x;
  d_target_x_475:=d_t_x_475*Gamma_x;
  d_target_x_95:=d_t_x_95*Gamma_x;
  PX14:=plot([d_target_x_2475,y,y=0..50000],linestyle=dashdot,color=black,legend="Target displacement - 2%
  in 50 years"):
  PX15:=plot([d_target_x_475,y,y=0..50000],linestyle=dashdot,color=blue,legend="Target displacement - 10% in
  50 years"):
  PX16:=plot([d_target_x_95,y,y=0..50000],linestyle=dashdot,color=green,legend="Target displacement - 50% in
  50 years"):


  display(P1,PX14,PX15,PX16);
```

$d\_target\_x\_2475 := 95.13799618$

$d\_target\_x\_475 := 56.91438767$

$d\_target\_x\_95 := 30.19947101$

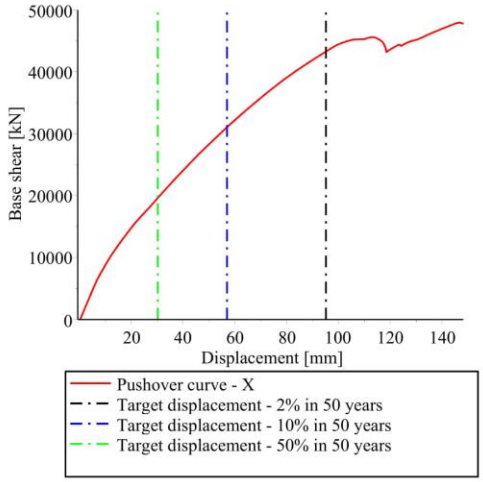

Y-Direction

```
> PY1:=plot(26300,x=0..110,linestyle=dashdot,color=black,legend="Yield Force"):
  PY2:=plot([[53,26300]],style=point,symbolsize=20,symbol=solidcircle,color=black,legend="Plastic
  Mechanism"):
  display(P2,P4,PY1,PY2);
```

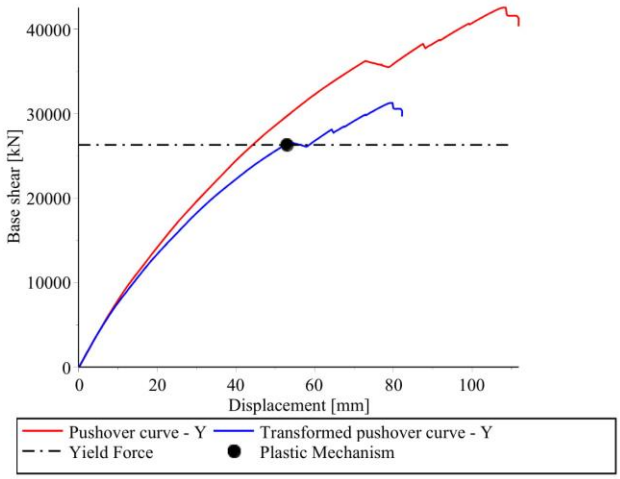

Yield strength read from graph:

```
> step:=410:
  Fy:=PY[step,4]/Gamma_y;
  dm:=PY[step,3]/Gamma_y;
```

$$Fy := 26611.03445$$

$$dm := 53.82990429 \quad (3.1)$$

Integration using trapezoidal method to find deformation energy up to formation of plastic mechanism:

```
> A:=0:
  C[1]:=0:
  i:='i':
  for i from 4 to (step-1) do
  A[i-3]:=((((PY[i,4]+PY[i+1,4])/2)/Gamma_x)*((PY[i+1,3]-PY[i,3])/Gamma_x)):
  C[i-2]:=C[i-3]+A[i-3]:
  end do:
  Em:=C[step-3];
```

$$Em := 8.278379471\ 10^{5} \quad (3.2)$$

Yield displacement

```
> dy:=2*(dm-Em/Fy);
```

$$dy := 45.44216362 \quad (3.3)$$

```
> f:=(x,y,t)->piecewise(x<=t,y*x,x>=t,y*t):
  PY3:=plot(f(x,Fy/dy,dy),x=0..100,legend="Idealized elasto-perfect plastic",color=red,labels=["Displacement
  [mm]","Base shear [kN]"]):
  PY4:=plot([dy,y,y=0..40000],linestyle=dashdot,color=black,legend="d_y*"):
  PY5:=plot([dm,y,y=0..40000],linestyle=dashdot,color=grey,legend="d_m*"):
  PY6:=plot(Fy,x=0..100,linestyle=dashdot,color=red,legend="F_y*"):
  display(P4,PY3,PY4,PY5,PY6);
```

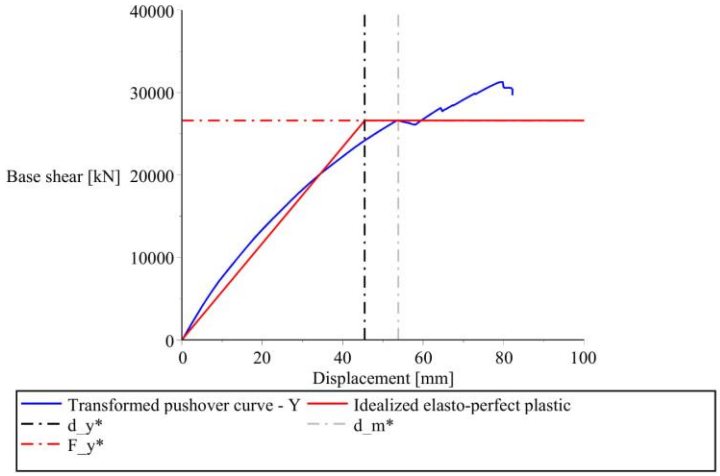

Period of idealized equivalent SDOF:

```
> T:=evalf(2*Pi*sqrt(mx*(dy/1000)/Fy));
```

$$T := 0.3335483732 \quad (3.4)$$

The target displacement (SDOF) for 95- and 475-year return period is found by the function:

```
> target_disp(Fy,my,T,ag_2475,d_t_y_2475);
  target_disp(Fy,my,T,ag_475,d_t_y_475);
  target_disp(Fy,my,T,ag_95,d_t_y_95);
```

73.83750555
38.94582009
20.66512903 (3.5)

```
> T:='T':
  RESP_Y:=T->piecewise(T<=1000*(Fy/my)/(RS(0.33,ag)/(RS(0.33,ag)*(0.33/(2*3.14))^2)),0.001*RS(0.33,ag)/(RS
  (0.33,ag)*(0.33/(2*3.14))^2)*T,T>=(Fy/my)/(RS(0.33,ag)/(RS(0.33,ag)*(0.33/(2*3.14))^2)),Fy/my):
  PER_Y:=T->0.001*RS(0.33,ag)/(RS(0.33,ag)*(0.33/(2*3.14))^2)*T:
  PY8:=plot([d_t_y_2475,y,y=0..25],color=black,linestyle=dashdot,legend="d_t_y_2475*"):
  PY9:=plot([d_t_y_475,y,y=0..25],color=blue,linestyle=dashdot,legend="d_t_y_475*"):
  PY10:=plot([d_t_y_95,y,y=0..25],color=green,linestyle=dashdot,legend="d_t_y_95*"):
  PY12:=plot(RESP_Y(T),T=0..300,color=red,legend="idealized response"):
  PY13:=plot(Fy/my,x=0..300,color=red,linestyle=dashdot,legend="Fy*/m*"):
  PY14:=plot(PER_Y(T),T=0..70,color=red,linestyle=dot,legend="T=0.33s"):

  display(P6,P8,P10,PY8,PY9,PY10,PY12,PY13,PY14);
```

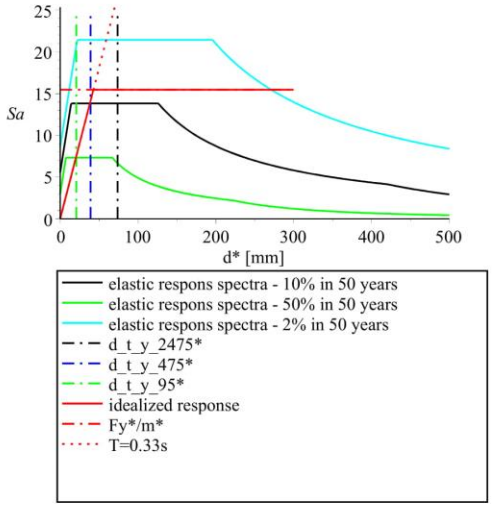

Transfer back to real pushover curve.

```
> d_target_y_2475:=d_t_y_2475*Gamma_y;
  d_target_y_475:=d_t_y_475*Gamma_y;
  d_target_y_95:=d_t_y_95*Gamma_y;
  PY15:=plot([d_target_y_475,y,y=0..50000],color=green,linestyle=dashdot,legend="Target displacement - 10%
  in 50 years"):
  PY16:=plot([d_target_y_95,y,y=0..50000],color=blue,linestyle=dashdot,legend="Target displacement - 50% in
  50 years"):
  PY17:=plot([d_target_y_2475,y,y=0..50000],color=black,linestyle=dashdot,legend="Target displacement - 2%
  in 50 years"):
  display(P2,PY15,PY16,PY17);
```

$$d\_target\_y\_2475 := 100.4600512$$
$$d\_target\_y\_475 := 52.98796394$$
$$d\_target\_y\_95 := 28.11606250$$

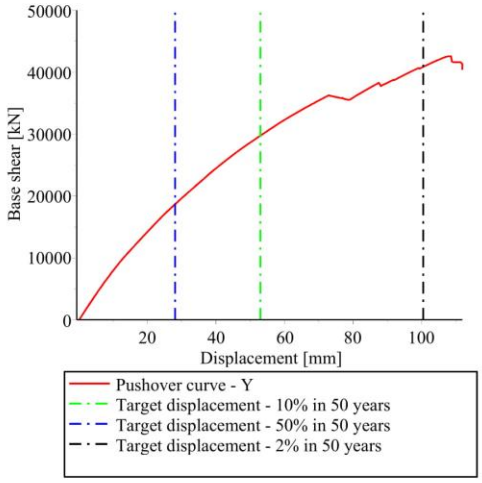

Appendix D – Analysis Results
D-1:Linear Modal Time History – 50% probability in 50 years

	Cape Mendocino			*Iwate*			*Chuetsu*			*SMART1*			*Chichi*			*Northridge*			*Loma Prieta*			***Mean***		
Base reactions 95																								
Base shear X [kN]			13870			10041			9732			13761			12061			12671			11991			12018
Base shear Y [kN]			9867			13214			9143			10625			9834			9697			13553			10848
Base force Z [kN]			31519			32845			31949			35062			31376			32319			34804			32839
Mx [MNm]			440			498			417			474			455			459			495			463
My [MNm]			448			396			415			423			414			419			419			419
Mz [MNm]			135			196			122			217			170			129			188			165
Interstory drift gravity																								
	X	Y	Tr	X	Y	Tr	X	Y	Tr	X	Y	Tr	X	Y	Tr	X	Y	Tr	X	Y	Tr	**X**	**Y**	**Tr**
Base	0.00%	0.00%	0.00%	0.00%	0.00%	0.00%	0.00%	0.00%	0.00%	0.00%	0.00%	0.00%	0.00%	0.00%	0.00%	0.00%	0.00%	0.00%	0.00%	0.00%	0.00%	**0.00%**	**0.00%**	**0.00%**
Story 2	0.06%	0.05%	0.06%	0.05%	0.07%	0.07%	0.05%	0.06%	0.07%	0.06%	0.07%	0.08%	0.05%	0.07%	0.07%	0.06%	0.06%	0.07%	0.05%	0.09%	0.09%	**0.06%**	**0.07%**	**0.07%**
Story 3	0.12%	0.10%	0.13%	0.11%	0.13%	0.15%	0.11%	0.13%	0.14%	0.13%	0.15%	0.16%	0.11%	0.15%	0.15%	0.12%	0.13%	0.14%	0.11%	0.18%	0.18%	**0.12%**	**0.14%**	**0.15%**
Story 4	0.15%	0.12%	0.16%	0.14%	0.15%	0.17%	0.14%	0.16%	0.17%	0.16%	0.18%	0.19%	0.14%	0.18%	0.18%	0.15%	0.16%	0.18%	0.14%	0.22%	0.22%	**0.14%**	**0.17%**	**0.18%**
Roof	0.16%	0.12%	0.16%	0.14%	0.15%	0.17%	0.15%	0.17%	0.18%	0.17%	0.19%	0.20%	0.15%	0.19%	0.19%	0.16%	0.17%	0.18%	0.14%	0.22%	0.22%	**0.15%**	**0.17%**	**0.19%**
Interstory drift stairway																								
	X	Y	Tr	X	Y	Tr	X	Y	Tr	X	Y	Tr	X	Y	Tr	X	Y	Tr	X	Y	Tr	**X**	**Y**	**Tr**
Base	0.00%	0.00%	0.00%	0.00%	0.00%	0.00%	0.00%	0.00%	0.00%	0.00%	0.00%	0.00%	0.00%	0.00%	0.00%	0.00%	0.00%	0.00%	0.00%	0.00%	0.00%	**0.00%**	**0.00%**	**0.00%**
Story 2	0.08%	0.04%	0.08%	0.10%	0.06%	0.10%	0.08%	0.04%	0.08%	0.12%	0.08%	0.14%	0.09%	0.06%	0.10%	0.11%	0.07%	0.11%	0.17%	0.10%	0.18%	**0.11%**	**0.07%**	**0.11%**
Story 3	0.13%	0.07%	0.14%	0.18%	0.11%	0.18%	0.15%	0.08%	0.15%	0.23%	0.15%	0.24%	0.16%	0.11%	0.18%	0.18%	0.13%	0.18%	0.27%	0.17%	0.29%	**0.19%**	**0.12%**	**0.19%**
Story 4	0.16%	0.08%	0.16%	0.22%	0.13%	0.22%	0.19%	0.09%	0.19%	0.29%	0.18%	0.29%	0.18%	0.13%	0.21%	0.21%	0.15%	0.23%	0.31%	0.20%	0.34%	**0.22%**	**0.14%**	**0.23%**
Roof	0.35%	0.08%	0.35%	0.45%	0.14%	0.45%	0.35%	0.09%	0.35%	0.59%	0.19%	0.59%	0.33%	0.13%	0.33%	0.42%	0.16%	0.43%	0.54%	0.20%	0.54%	**0.43%**	**0.14%**	**0.44%**
Mumty	0.44%	0.17%	0.45%	0.54%	0.25%	0.55%	0.42%	0.18%	0.43%	0.72%	0.30%	0.73%	0.41%	0.19%	0.41%	0.52%	0.27%	0.53%	0.63%	0.30%	0.63%	**0.53%**	**0.24%**	**0.53%**

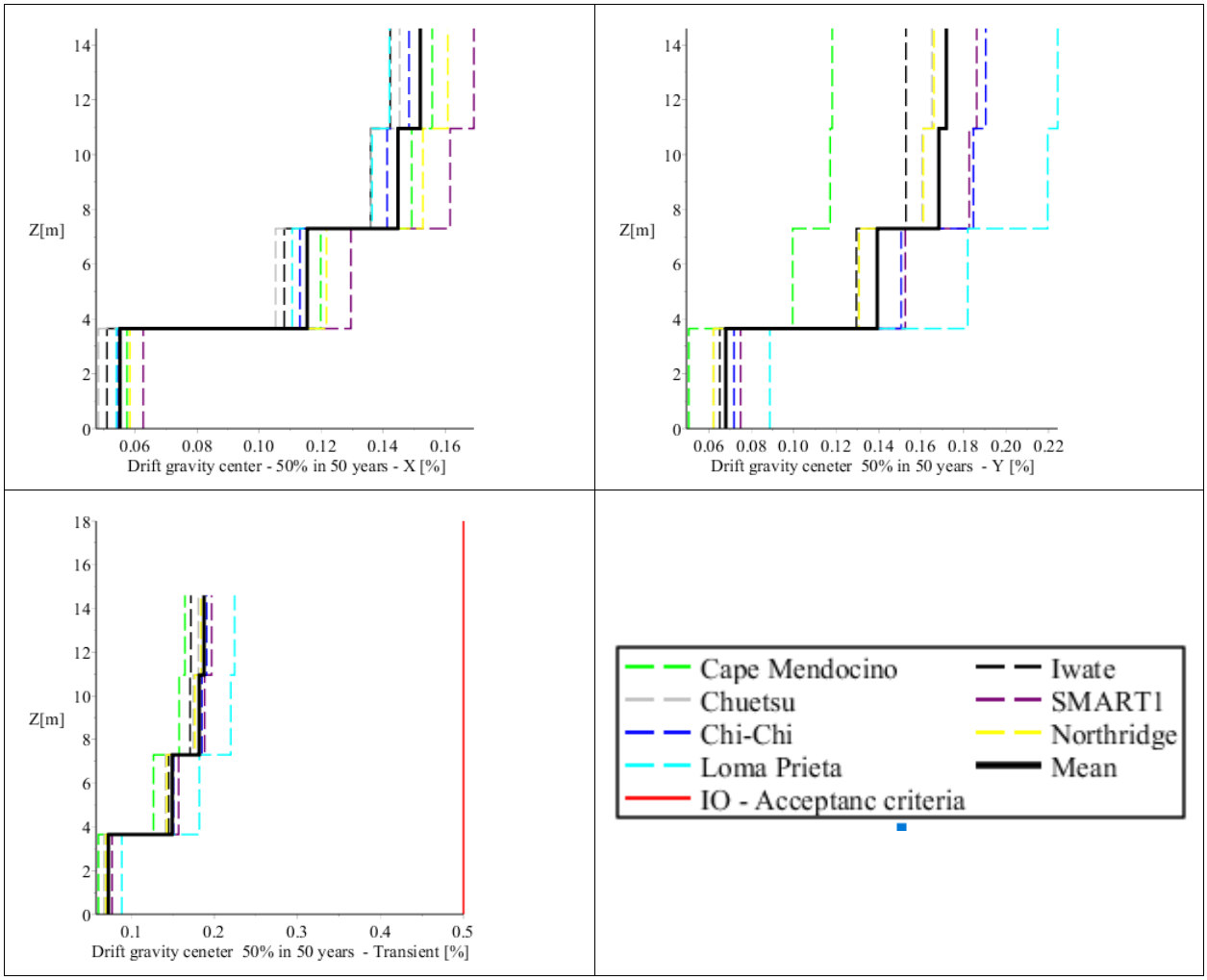
Z[m]
Drift gravity center - 50% in 50 years - X [%]
Drift gravity ceneter 50% in 50 years - Y [%]
Drift gravity ceneter 50% in 50 years - Transient [%]
Cape Mendocino
Chuetsu
Chi-Chi
Loma Prieta
IO - Acceptanc criteria
Iwate
SMART1
Northridge
Mean

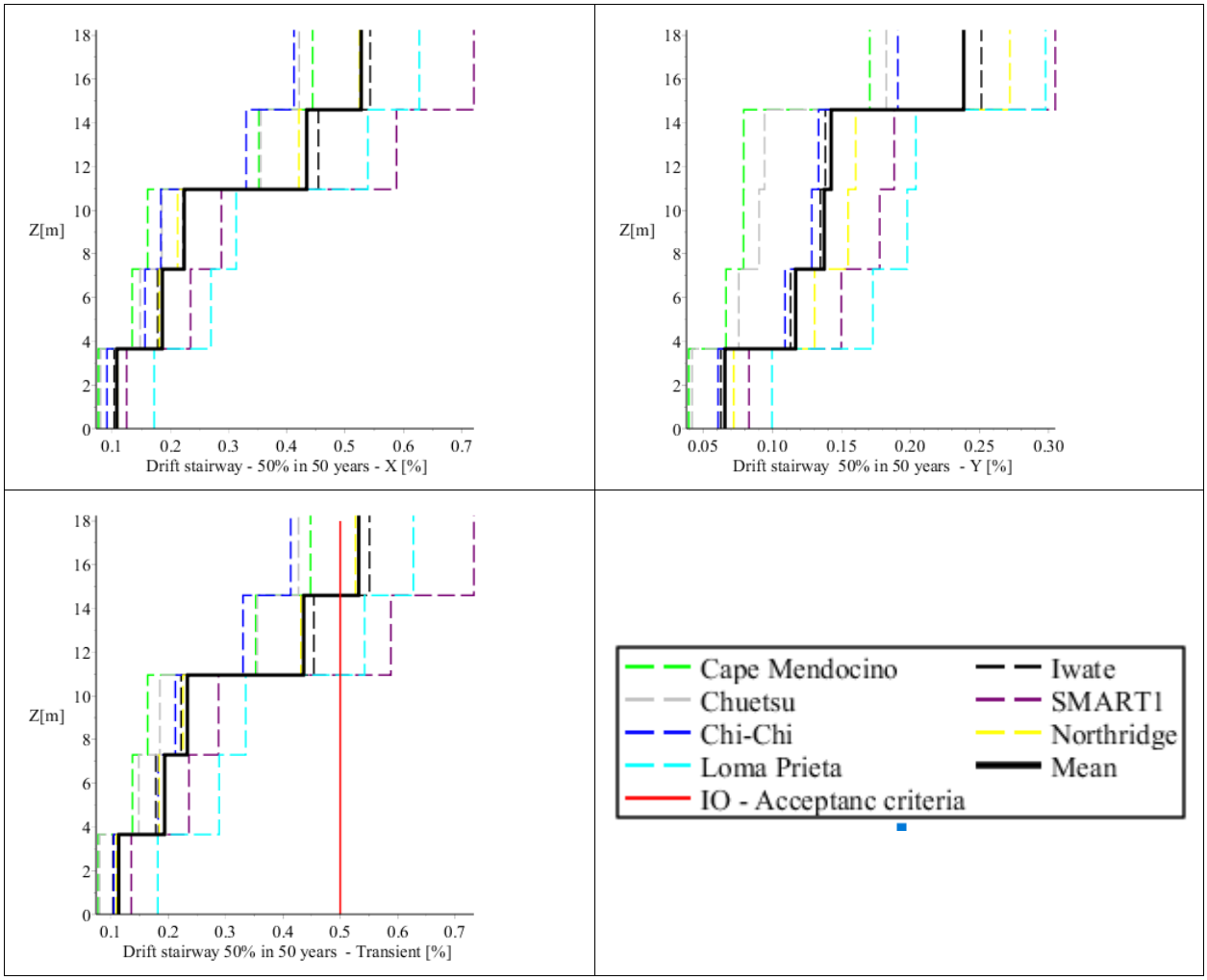
Z[m]
Drift stairway - 50% in 50 years - X [%]
Drift stairway 50% in 50 years - Y [%]
Drift stairway 50% in 50 years - Transient [%]
Cape Mendocino
Chuetsu
Chi-Chi
Loma Prieta
IO - Acceptanc criteria
Iwate
SMART1
Northridge
Mean

D-2:Nonlinear Modal Time History Analysis – 10% probability in 50 years

	Cape Mendocino			*Iwate*			*Chuetsu*			*SMART1*			*Chichi*			*Northridge*			*Loma Prieta*			***Mean***		
	Base reactions 10% probability in 50 years																							
Base shear X [kN]	23082			23246			20234			21554			20353			21468			17745			**21097**		
Base shear Y [kN]	17867			18980			16877			20134			22178			21107			22999			**20020**		
Base force Z [kN]	33746			35934			33733			39644			32489			34690			38761			**35571**		
Mx [MNm]	505			558			542			548			566			587			515			**546**		
My [MNm]	475			490			517			517			499			517			467			**497**		
Mz [MNm]	281			285			253			260			291			292			358			**289**		
	Interstory drift gravity center 10% probability in 50 years																							
	X	Y	Tr	X	Y	Tr	X	Y	Tr	X	Y	Tr	X	Y	Tr	X	Y	Tr	X	Y	Tr	**X**	**Y**	**Tr**
Base	0.00%	0.00%	0.00%	0.00%	0.00%	0.00%	0.00%	0.00%	0.00%	0.00%	0.00%	0.00%	0.00%	0.00%	0.00%	0.00%	0.00%	0.00%	0.00%	0.00%	0.00%	**0.00%**	**0.00%**	**0.00%**
Story 2	0.03%	0.04%	0.04%	0.03%	0.04%	0.04%	0.03%	0.04%	0.04%	0.03%	0.05%	0.05%	0.03%	0.05%	0.05%	0.03%	0.05%	0.05%	0.03%	0.05%	0.05%	**0.03%**	**0.05%**	**0.05%**
Story 3	0.11%	0.13%	0.13%	0.12%	0.13%	0.13%	0.12%	0.12%	0.13%	0.11%	0.14%	0.15%	0.09%	0.15%	0.16%	0.10%	0.15%	0.15%	0.09%	0.15%	0.16%	**0.11%**	**0.14%**	**0.14%**
Story 4	0.10%	0.17%	0.18%	0.16%	0.16%	0.17%	0.16%	0.15%	0.17%	0.14%	0.19%	0.19%	0.12%	0.20%	0.20%	0.13%	0.19%	0.19%	0.12%	0.19%	0.21%	**0.13%**	**0.18%**	**0.19%**
Roof	0.15%	0.18%	0.19%	0.17%	0.17%	0.19%	0.17%	0.16%	0.18%	0.15%	0.19%	0.20%	0.12%	0.21%	0.21%	0.14%	0.20%	0.20%	0.13%	0.20%	0.21%	**0.15%**	**0.19%**	**0.20%**
	Interstory drift stairway 10% probability in 50 years																							
	X	Y	Tr	X	Y	Tr	X	Y	Tr	X	Y	Tr	X	Y	Tr	X	Y	Tr	X	Y	Tr	**X**	**Y**	**Tr**
Base	0.00%	0.00%	0.00%	0.00%	0.00%	0.00%	0.00%	0.00%	0.00%	0.00%	0.00%	0.00%	0.00%	0.00%	0.00%	0.00%	0.00%	0.00%	0.00%	0.00%	0.00%	**0.00%**	**0.00%**	**0.00%**
Story 2	0.08%	0.04%	0.08%	0.07%	0.04%	0.08%	0.08%	0.03%	0.08%	0.07%	0.04%	0.07%	0.09%	0.04%	0.09%	0.08%	0.04%	0.08%	0.08%	0.05%	0.08%	**0.08%**	**0.04%**	**0.08%**
Story 3	0.16%	0.09%	0.18%	0.16%	0.10%	0.17%	0.14%	0.09%	0.15%	0.13%	0.10%	0.14%	0.14%	0.09%	0.14%	0.16%	0.11%	0.16%	0.14%	0.12%	0.17%	**0.15%**	**0.10%**	**0.16%**
Story 4	0.21%	0.13%	0.22%	0.21%	0.14%	0.22%	0.18%	0.13%	0.18%	0.17%	0.13%	0.17%	0.18%	0.12%	0.18%	0.21%	0.14%	0.22%	0.18%	0.15%	0.21%	**0.19%**	**0.13%**	**0.20%**
Roof	0.78%	0.13%	0.78%	0.72%	0.15%	0.72%	0.72%	0.14%	0.72%	0.61%	0.15%	0.61%	0.68%	0.13%	0.68%	0.72%	0.16%	0.72%	0.72%	0.17%	0.62%	**0.71%**	**0.15%**	**0.69%**
Mumty	1.17%	0.38%	1.19%	1.08%	0.42%	1.09%	1.08%	0.50%	1.08%	0.89%	0.44%	0.90%	0.97%	0.35%	0.98%	1.03%	0.45%	1.03%	0.85%	0.34%	0.86%	**1.01%**	**0.41%**	**1.02%**

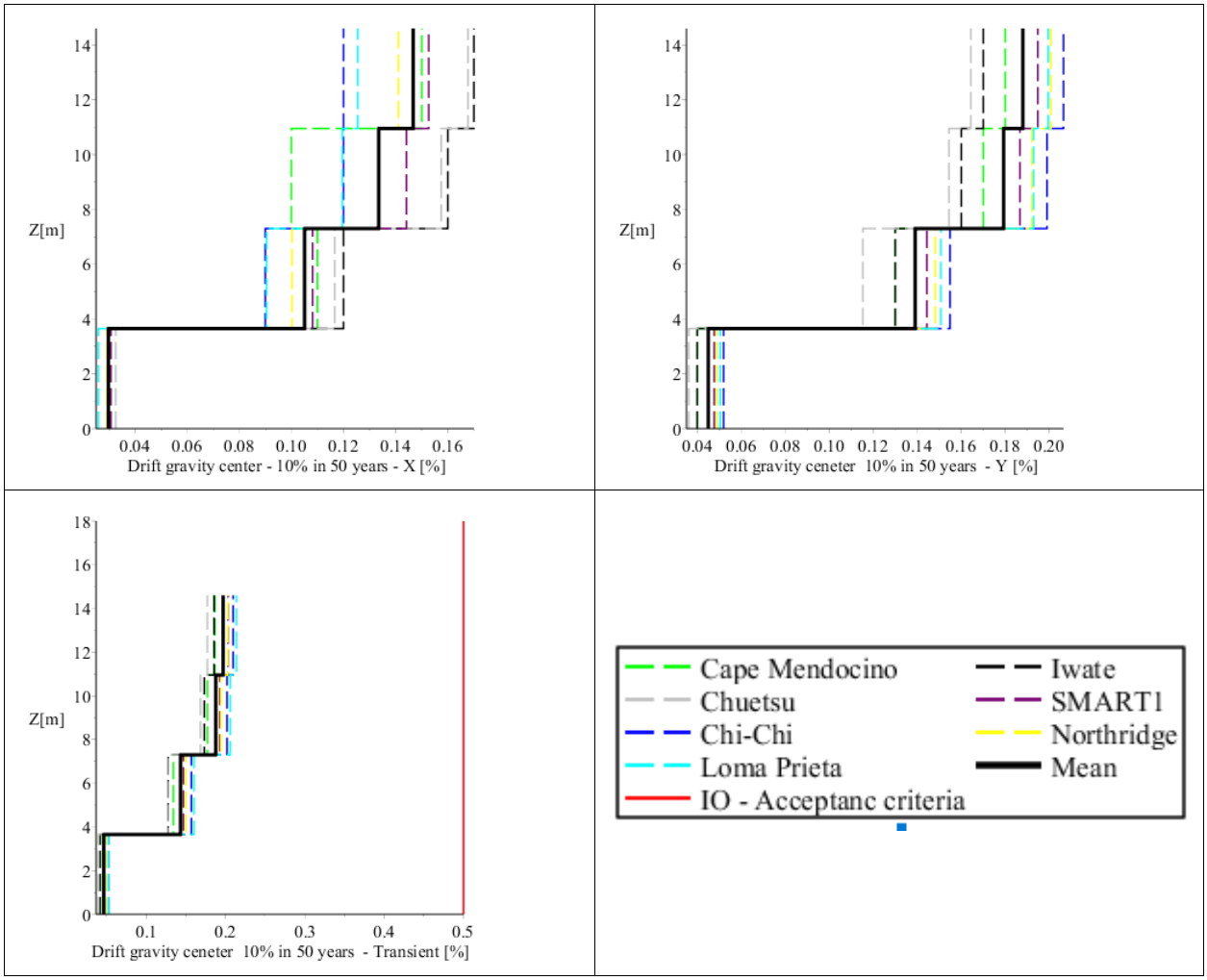
Z[m]
Drift gravity center - 10% in 50 years - X [%]
Drift gravity ceneter 10% in 50 years - Y [%]
Drift gravity ceneter 10% in 50 years - Transient [%]
Cape Mendocino
Chuetsu
Chi-Chi
Loma Prieta
IO - Acceptanc criteria
Iwate
SMART1
Northridge
Mean

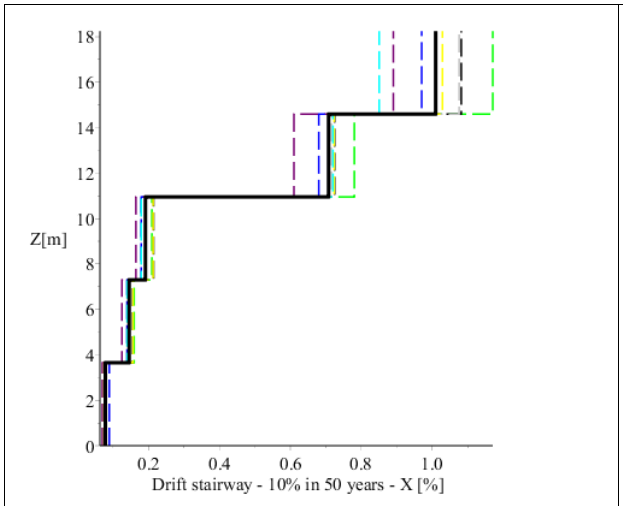
Z[m]
Drift stairway - 10% in 50 years - X [%]

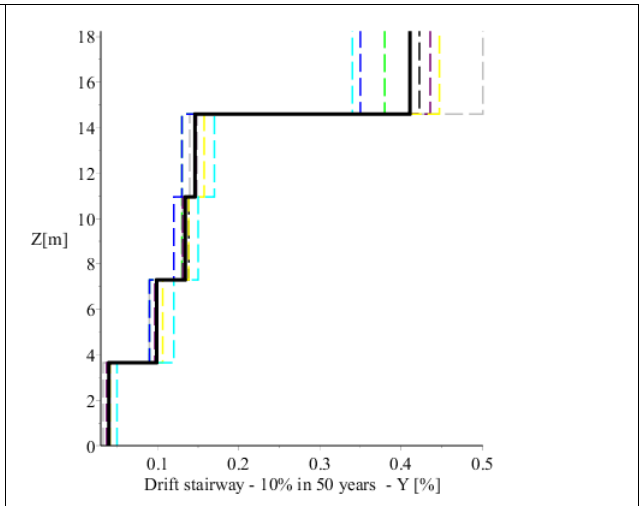
Z[m]
Drift stairway - 10% in 50 years - Y [%]

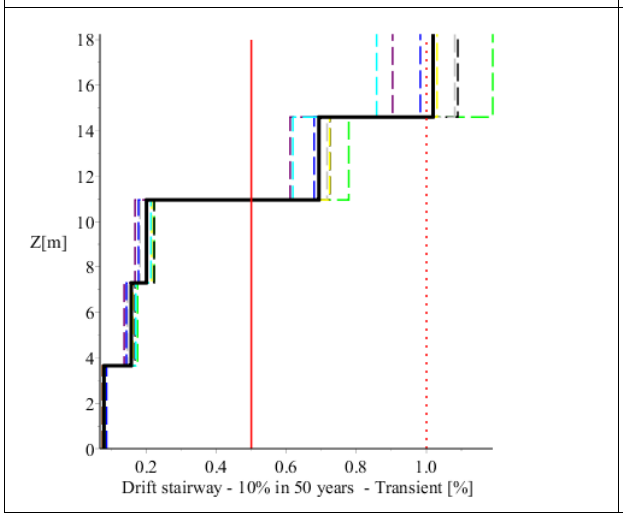
Z[m]
Drift stairway - 10% in 50 years - Transient [%]

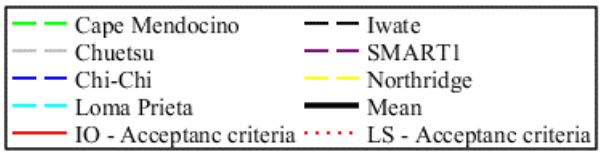
Cape Mendocino
Iwate
Chuetsu
SMART1
Chi-Chi
Northridge
Loma Prieta
Mean
IO - Acceptanc criteria
LS - Acceptanc criteria

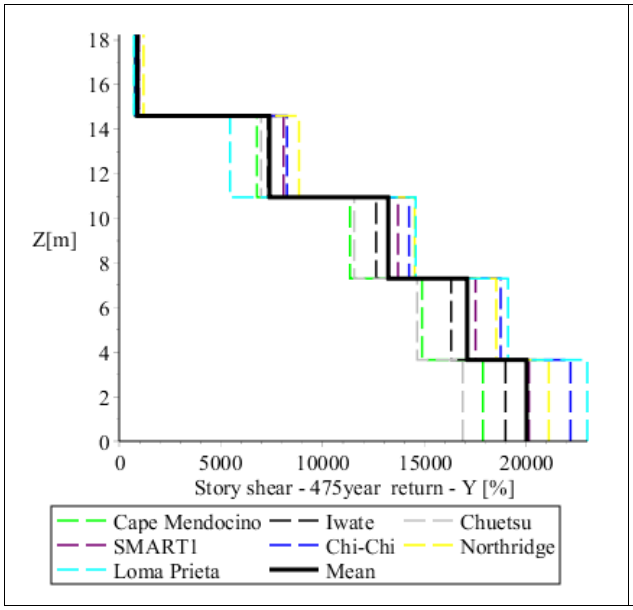
Z[m]
Story shear - 475year return - Y [%]
Cape Mendocino
Iwate
Chuetsu
SMART1
Chi-Chi
Northridge
Loma Prieta
Mean

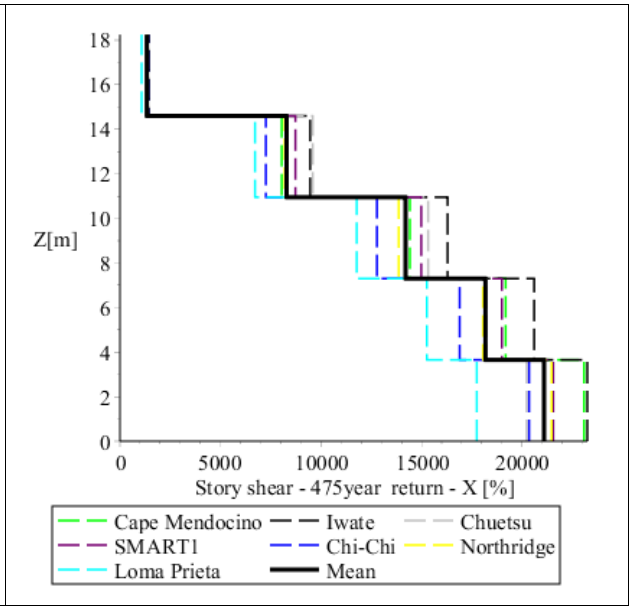
Z[m]
Story shear - 475year return - X [%]
Cape Mendocino
Iwate
Chuetsu
SMART1
Chi-Chi
Northridge
Loma Prieta
Mean

D-3: Nonlinear Modal Time History Analysis – 2% probability in 50 years

	Cape Mendocino			*Iwate*			*Chuetsu*			*SMART1*			*Chichi*			*Northridge*			*Loma Prieta*			***Mean***		
	Base reactions 2% probability in 50 years																							
Base shear X [kN]	34532			32321			29478			30890			33808			31892			26851			31396		
Base shear Y [kN]	27505			26353			24430			29609			32527			31170			33586			29311		
Base force Z [kN]	32550			38839			35787			44053			33807			37104			43281			37917		
Mx [MNm]	599			646			635			646			671			706			516			631		
My [MNm]	557			683			623			617			598			632			554			609		
Mz [MNm]	407			351			366			381			425			415			529			411		
	Interstory drift gravity center 2% probability in 50 years																							
	X	Y	Tr	X	Y	Tr	X	Y	Tr	X	Y	Tr	X	Y	Tr	X	Y	Tr	X	Y	Tr	X	Y	Tr
Base	0.00%	0.00%	0.00%	0.00%	0.00%	0.00%	0.00%	0.00%	0.00%	0.00%	0.00%	0.00%	0.00%	0.00%	0.00%	0.00%	0.00%	0.00%	0.00%	0.00%	0.00%	0.00%	0.00%	0.00%
Story 2	0.05%	0.06%	0.06%	0.05%	0.06%	0.06%	0.05%	0.05%	0.06%	0.04%	0.07%	0.07%	0.03%	0.08%	0.08%	0.04%	0.07%	0.07%	0.04%	0.07%	0.08%	0.04%	0.07%	0.07%
Story 3	0.17%	0.19%	0.20%	0.17%	0.17%	0.18%	0.17%	0.17%	0.18%	0.16%	0.21%	0.21%	0.09%	0.23%	0.23%	0.15%	0.22%	0.22%	0.13%	0.22%	0.24%	0.15%	0.20%	0.21%
Story 4	0.22%	0.25%	0.27%	0.22%	0.23%	0.24%	0.23%	0.23%	0.24%	0.21%	0.28%	0.28%	0.12%	0.29%	0.30%	0.20%	0.28%	0.29%	0.18%	0.28%	0.30%	0.20%	0.26%	0.27%
Roof	0.23%	0.26%	0.28%	0.23%	0.24%	0.25%	0.24%	0.24%	0.25%	0.22%	0.29%	0.29%	0.13%	0.31%	0.31%	0.21%	0.30%	0.30%	0.18%	0.29%	0.32%	0.21%	0.28%	0.29%
	Interstory drift stairway 2% probability in 50 years																							
	X	Y	Tr	X	Y	Tr	X	Y	Tr	X	Y	Tr	X	Y	Tr	X	Y	Tr	X	Y	Tr	X	Y	Tr
Base	0.00%	0.00%	0.00%	0.00%	0.00%	0.00%	0.00%	0.00%	0.00%	0.00%	0.00%	0.00%	0.00%	0.00%	0.00%	0.00%	0.00%	0.00%	0.00%	0.00%	0.00%	0.00%	0.00%	0.00%
Story 2	0.11%	0.06%	0.12%	0.10%	0.05%	0.10%	0.12%	0.05%	0.12%	0.10%	0.05%	0.11%	0.13%	0.06%	0.13%	0.11%	0.06%	0.11%	0.11%	0.07%	0.12%	0.11%	0.06%	0.11%
Story 3	0.24%	0.14%	0.26%	0.21%	0.13%	0.22%	0.21%	0.13%	0.21%	0.18%	0.14%	0.20%	0.20%	0.14%	0.21%	0.23%	0.16%	0.23%	0.20%	0.18%	0.25%	0.21%	0.15%	0.23%
Story 4	0.30%	0.20%	0.32%	0.28%	0.18%	0.29%	0.26%	0.20%	0.26%	0.23%	0.19%	0.25%	0.26%	0.18%	0.27%	0.31%	0.21%	0.31%	0.25%	0.22%	0.32%	0.27%	0.20%	0.29%
Roof	1.16%	0.20%	1.16%	1.04%	0.19%	1.04%	1.10%	0.21%	1.10%	0.96%	0.22%	0.96%	1.01%	0.19%	1.01%	1.09%	0.23%	1.09%	0.94%	0.25%	0.94%	1.04%	0.21%	1.04%
Mumty	1.83%	0.60%	1.85%	1.32%	0.56%	1.36%	1.73%	0.78%	1.73%	1.46%	0.66%	1.47%	1.46%	0.52%	1.48%	1.57%	0.68%	1.57%	1.31%	0.52%	1.33%	1.52%	0.62%	1.54%

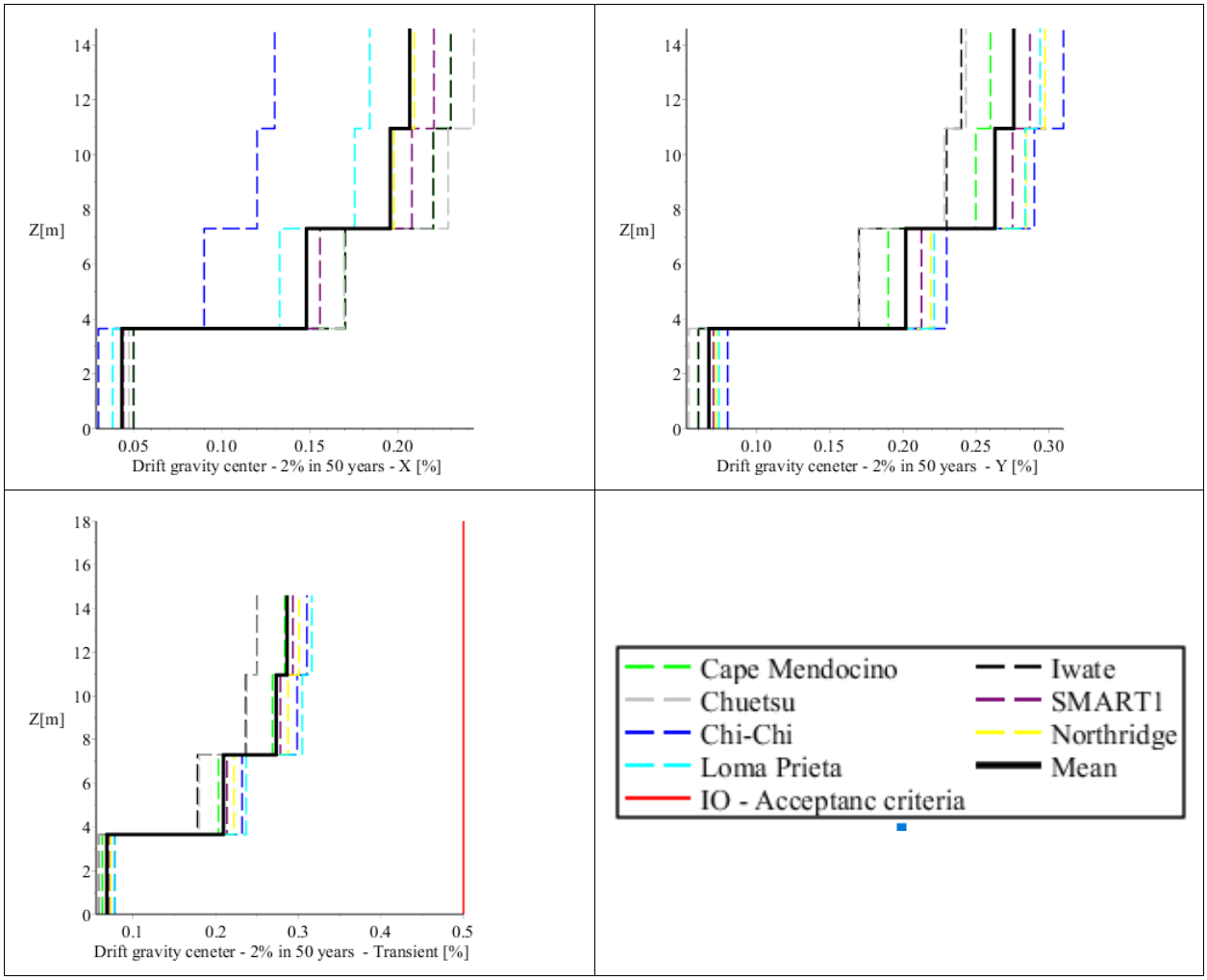
Z[m]
Drift gravity center - 2% in 50 years - X [%]
Drift gravity ceneter - 2% in 50 years - Y [%]
Drift gravity ceneter - 2% in 50 years - Transient [%]
Cape Mendocino
Chuetsu
Chi-Chi
Loma Prieta
IO - Acceptanc criteria
Iwate
SMART1
Northridge
Mean

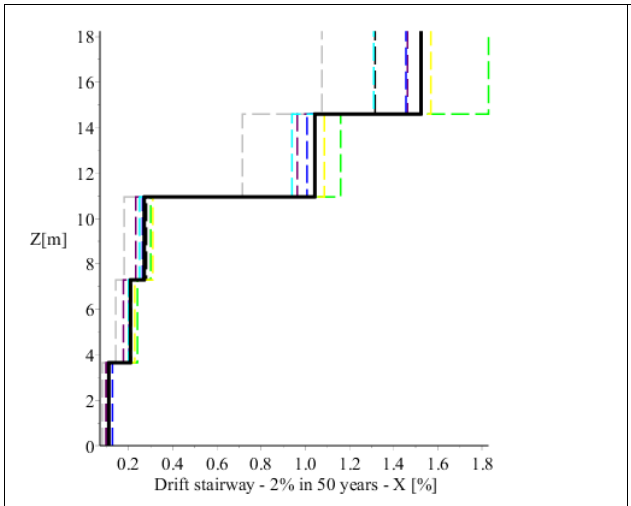
Z[m]
Drift stairway - 2% in 50 years - X [%]

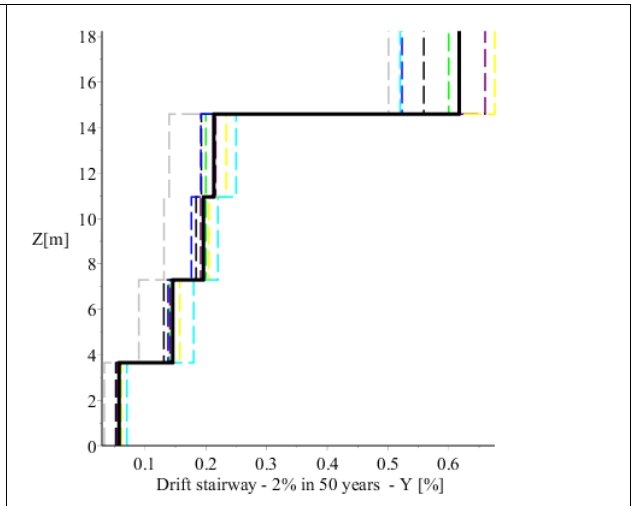
Z[m]
Drift stairway - 2% in 50 years - Y [%]

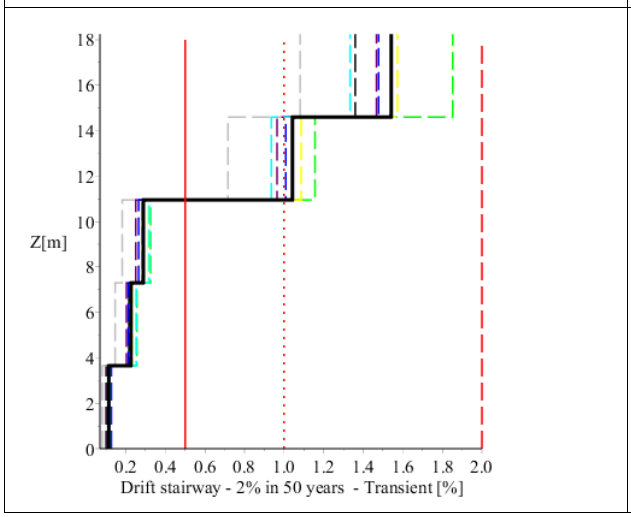
Z[m]
Drift stairway - 2% in 50 years - Transient [%]

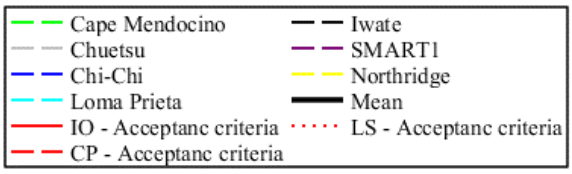
Cape Mendocino
Iwate
Chuetsu
SMART1
Chi-Chi
Northridge
Loma Prieta
Mean
IO - Acceptanc criteria
LS - Acceptanc criteria
CP - Acceptanc criteria

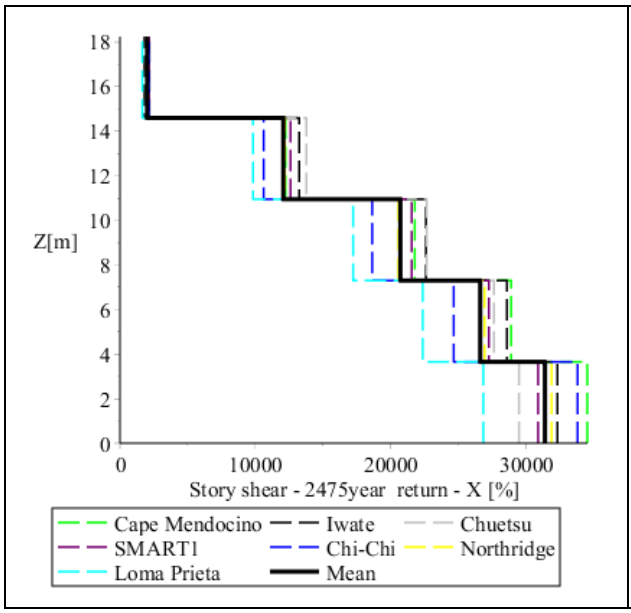
Z[m]
Story shear - 2475year return - X [%]
Cape Mendocino
Iwate
Chuetsu
SMART1
Chi-Chi
Northridge
Loma Prieta
Mean

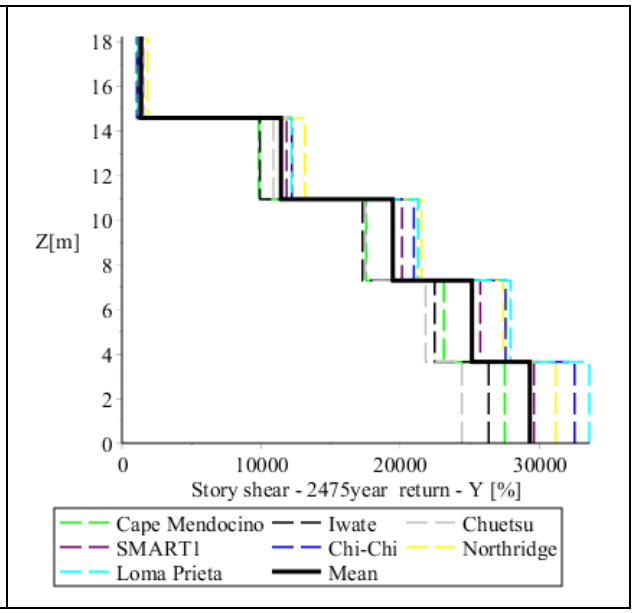
Z[m]
Story shear - 2475year return - Y [%]
Cape Mendocino
Iwate
Chuetsu
SMART1
Chi-Chi
Northridge
Loma Prieta
Mean

D-4:Nonlinear Direct Integration Time History – 10% probability in 50 years

Table 7-2 - Results from direct integration analysis with 10% probability of occurrence in 50 years

	Cape Mendocino			*Iwate*			*Northridge*			*Least favorable*		
					Base reactions 10% in 50years							
Base shear X [kN]			13579			21571			16725			**21571**
Base shear Y [kN]			15987			23285			13845			**23285**
Base force Z [kN]			36167			30822			35983			**36167**
Mx [MNm]			555			574			515			**574**
My [MNm]			466			497			474			**497**
Mz [MNm]			200			304			188			**304**
					Interstory drift gravity center 10% in 50 years							
	X	Y	Trans	X	Y	Trans	X	Y	Trans	**X**	**Y**	**Trans**
Base	0.00%	0.00%	0.00%	0.00%	0.00%	0.00%	0.00%	0.00%	0.00%	**0.00%**	**0.00%**	**0.00%**
Story 2	0.10%	0.15%	0.15%	0.16%	0.20%	0.20%	0.12%	0.12%	0.13%	**0.16%**	**0.20%**	**0.20%**
Story 3	0.21%	0.30%	0.30%	0.30%	0.41%	0.41%	0.25%	0.25%	0.27%	**0.30%**	**0.41%**	**0.41%**
Story 4	0.25%	0.33%	0.33%	0.32%	0.47%	0.47%	0.29%	0.29%	0.32%	**0.32%**	**0.47%**	**0.47%**
Roof	0.26%	0.32%	0.32%	0.32%	0.46%	0.46%	0.29%	0.28%	0.32%	**0.32%**	**0.46%**	**0.46%**
					Interstory drift stairway 10%in 50 years							
	X	Y		X	Y		X	Y		**X**	**Y**	**Trans**
Base	0.00%	0.00%	0.00%	0.00%	0.00%	0.00%	0.00%	0.00%	0.00%	**0.00%**	**0.00%**	**0.00%**
Story 2	0.13%	0.08%	0.15%	0.23%	0.15%	0.26%	0.15%	0.10%	0.15%	**0.23%**	**0.15%**	**0.26%**
Story 3	0.22%	0.14%	0.26%	0.40%	0.25%	0.44%	0.24%	0.19%	0.24%	**0.40%**	**0.25%**	**0.44%**
Story 4	0.25%	0.16%	0.29%	0.43%	0.28%	0.48%	0.27%	0.21%	0.27%	**0.43%**	**0.28%**	**0.48%**
Roof	0.47%	0.17%	0.48%	0.75%	0.30%	0.77%	0.58%	0.21%	0.58%	**0.75%**	**0.30%**	**0.77%**
Mumty	0.54%	0.30%	0.56%	0.97%	0.36%	0.97%	0.81%	0.38%	0.83%	**0.97%**	**0.38%**	**0.97%**

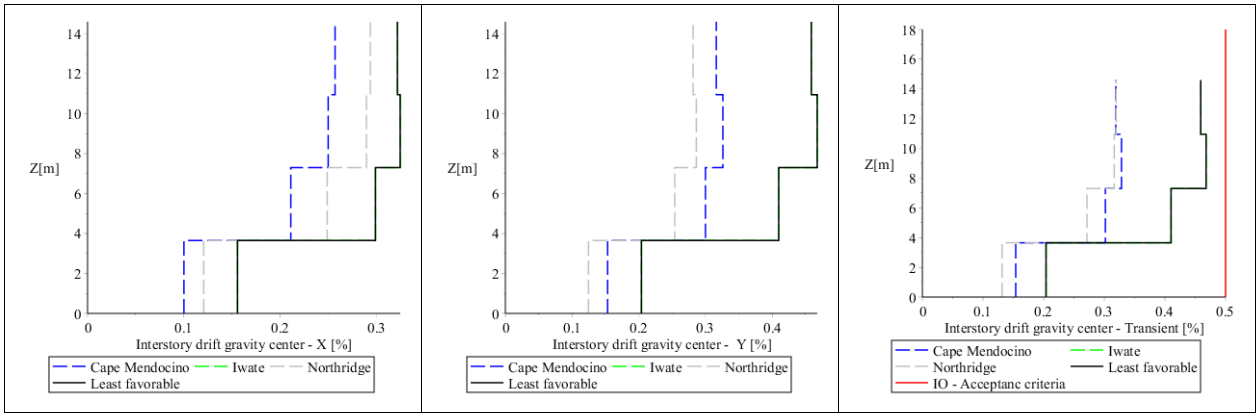

Figure 7-1 - Interstory drift at gravity center - 10% probability in 50 years

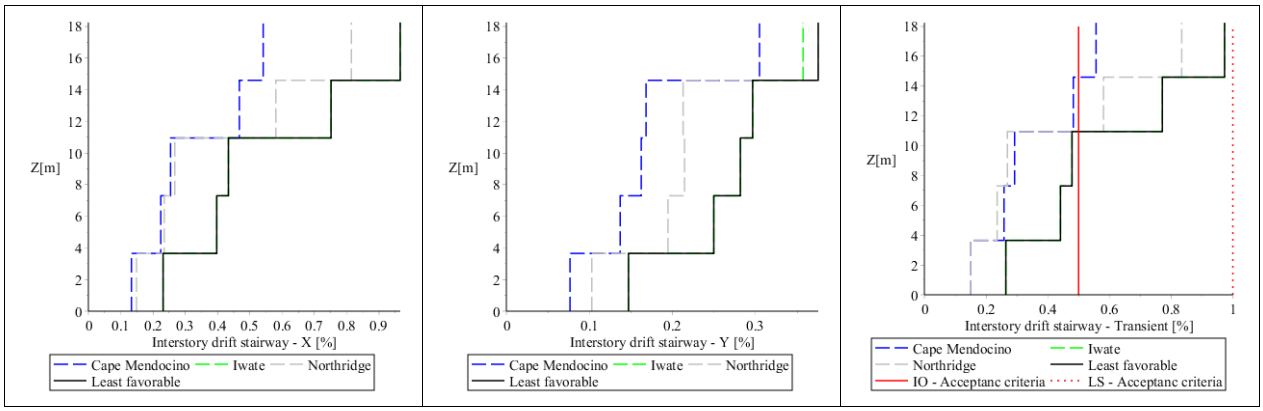

Figure 7-2 - Interstory drift at stairway - 10% probability in 50 years

D-5:Nonlinear Direct Integration Time History – 2% probability in 50 years

	Cape Mendocino	*Iwate*	*Chuetsu*	*SMART1*	*Chichi*	*Northridge*	*Loma Prieta*	***Mean***
Base shear X [kN]	21875	29404	19289	28831	19288	19258	31369	**24188**
Base shear Y [kN]	22681	25279	22570	21484	22570	19145	29222	**23279**
Base force Z [kN]	39504	54942	40831	61336	40831	39209	47957	**46373**
Mx [MNm]	644	958	675	1142	675	623	845	**795**
My [MNm]	529	584	465	645	464	518	602	**544**
Mz [MNm]	271	361	300	518	304	247	400	**343**

Interstory drift – Gravity Center

	X	Y	Tr	X	Y	Tr	X	Y	Tr	X	Y	Tr	X	Y	Tr	X	Y	Tr	X	Y	Tr	**X**	**Y**	**Tr**
Base	0.00%	0.00%	0.00%	0.00%	0.00%	0.00%	0.00%	0.00%	0.00%	0.00%	0.00%	0.00%	0.00%	0.00%	0.00%	0.00%	0.00%	0.00%	0.00%	0.00%	0.00%	**0.00%**	**0.00%**	**0.00%**
Story 2	0.17%	0.25%	0.25%	0.23%	0.20%	0.24%	0.12%	0.17%	0.17%	0.27%	0.23%	0.28%	0.12%	0.17%	0.17%	0.16%	0.19%	0.19%	0.27%	0.27%	0.27%	**0.19%**	**0.21%**	**0.22%**
Story 3	0.34%	0.50%	0.51%	0.45%	0.39%	0.46%	0.24%	0.34%	0.34%	0.59%	0.46%	0.60%	0.25%	0.34%	0.34%	0.33%	0.38%	0.39%	0.53%	0.53%	0.54%	**0.39%**	**0.42%**	**0.45%**
Story 4	0.40%	0.56%	0.56%	0.49%	0.43%	0.49%	0.29%	0.39%	0.39%	0.70%	0.51%	0.72%	0.30%	0.39%	0.39%	0.39%	0.43%	0.44%	0.58%	0.61%	0.62%	**0.45%**	**0.48%**	**0.52%**
Roof	0.41%	0.55%	0.55%	0.48%	0.42%	0.49%	0.31%	0.38%	0.39%	0.72%	0.51%	0.73%	0.31%	0.38%	0.39%	0.40%	0.43%	0.43%	0.56%	0.59%	0.61%	**0.45%**	**0.47%**	**0.51%**

Interstory drift – Stairway

	X	Y	Tr	X	Y	Tr	X	Y	Tr	X	Y	Tr	X	Y	Tr	X	Y	Tr	X	Y	Tr	**X**	**Y**	**Tr**
Base	0.00%	0.00%	0.00%	0.00%	0.00%	0.00%	0.00%	0.00%	0.00%	0.00%	0.00%	0.00%	0.00%	0.00%	0.00%	0.00%	0.00%	0.00%	0.00%	0.00%	0.00%	**0.00%**	**0.00%**	**0.00%**
Story 2	0.21%	0.20%	0.27%	0.29%	0.17%	0.29%	0.21%	0.15%	0.22%	0.39%	0.20%	0.41%	0.21%	0.15%	0.22%	0.23%	0.16%	0.23%	0.33%	0.21%	0.36%	**0.27%**	**0.18%**	**0.29%**
Story 3	0.35%	0.35%	0.48%	0.44%	0.28%	0.45%	0.33%	0.25%	0.35%	0.57%	0.37%	0.62%	0.33%	0.25%	0.35%	0.36%	0.30%	0.38%	0.50%	0.39%	0.59%	**0.41%**	**0.31%**	**0.46%**
Story 4	0.40%	0.42%	0.55%	0.48%	0.31%	0.48%	0.36%	0.29%	0.39%	0.63%	0.44%	0.69%	0.36%	0.29%	0.39%	0.40%	0.33%	0.42%	0.58%	0.43%	0.66%	**0.46%**	**0.36%**	**0.51%**
Roof	0.87%	0.43%	0.87%	0.66%	0.32%	0.66%	0.86%	0.31%	0.86%	1.11%	0.47%	1.14%	0.86%	0.31%	0.86%	0.82%	0.33%	0.82%	1.15%	0.44%	1.15%	**0.90%**	**0.37%**	**0.91%**
Mumty	1.31%	0.54%	1.32%	0.80%	0.51%	0.80%	1.29%	0.54%	1.32%	1.22%	0.73%	1.25%	1.29%	0.54%	1.32%	1.21%	0.56%	1.23%	1.72%	0.58%	1.72%	**1.26%**	**0.57%**	**1.28%**

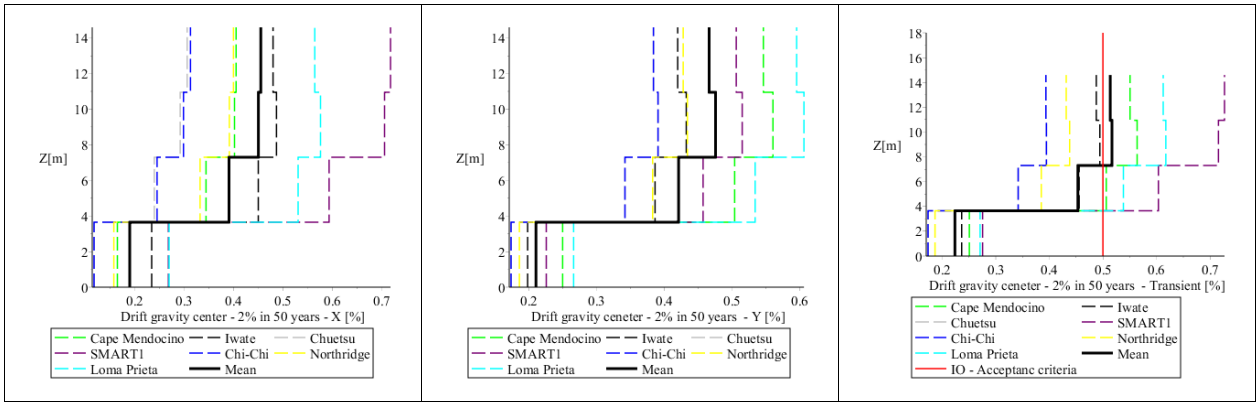

Figure 7-3 - Interstory drift at gravity center - 2% probability in 50 years

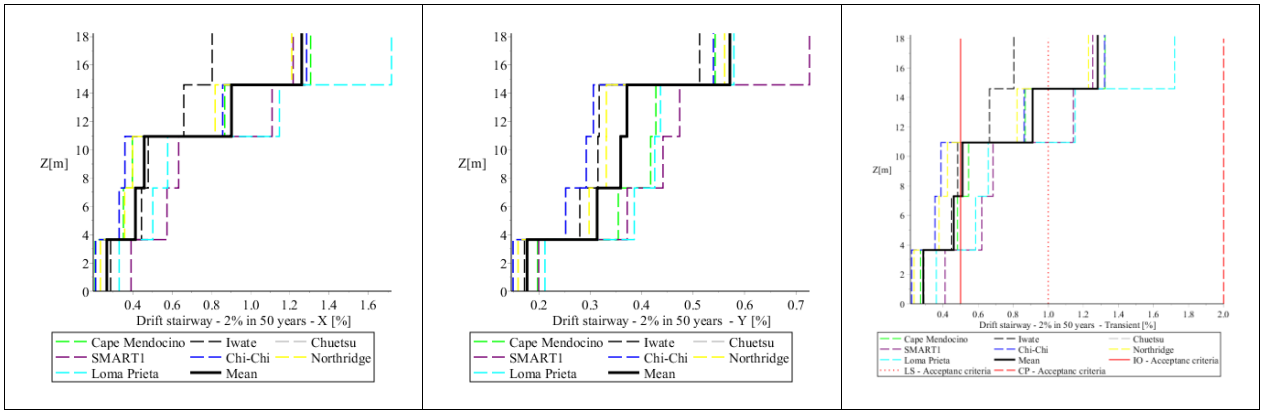

Figure 7-4 - Interstory drift at stairway - 2% probability in 50 years

D-6: Gorkha Earthquake – Direct integration time history analysis

Gorkha Earthquake

Base shear X [kN]	9 863
Base shear Y [kN]	8 360
Base force Z [kN]	34 095
Mx [MNm]	410
My [MNm]	393
Mz [MNm]	140

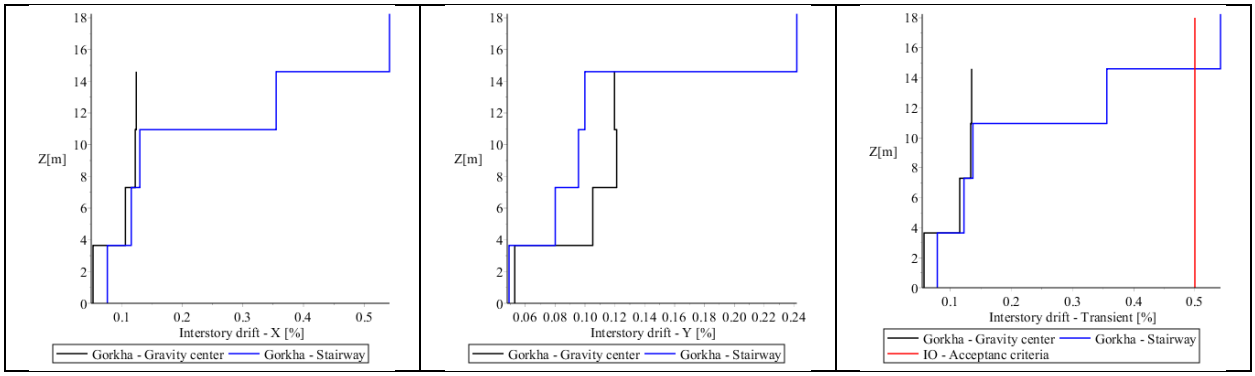

D-7:Hinge Performance – 10% in 50 years

Hinge performance for beams and columns with performance level *IO* or lower:

Beam performance:

Beam	Pushover		Nonlinear Direct Integration Time-History			Least favorable
	X-direction	Y-direction	Iwate	Northridge	Cape Mendocino	
B-5-4 – C-5-4	O	O	IO	IO	IO	IO
D-1-2 – F-1-2	IO	O	O	O	O	IO
F-1-1 – F-2-1	O	O	IO	O	O	IO
F-1-2 – F-2-2	O	IO	IO	O	O	IO
F-1-3 – F-2-3	O	IO	IO	O	O	IO
F-1-4 – F-2-4	O	IO	IO	O	O	IO

Column performance

Column	Pushover		Nonlinear Direct Integration Time-History			Least favorable
	X-direction	Y-direction	Iwate	Northridge	Cape Mendocino	
B-4-2	O	O	IO	O	O	IO
C-1-4	O	O	O	O	O	IO
D-1-2	O	O	O	O	O	IO
D-1-4	IO	O	O	O	IO	IO
F-2-2	O	O	IO	O	O	IO
F-2-3	O	O	IO	O	O	IO
F-2-4	O	O	IO	O	O	IO
F-3-1	O	O	O	O	O	IO

D-8:Hinge Performance – 2% in 50 years

Beam performance:

	Pushover		Nonlinear Direct Integration Time-History							
Beam	X-direction	Y-direction	Iwate	Northridge	Cape Mendocino	Chuetsu	Loma Prieta	Chi-chi	Smart1	Least favorable
B-3-2 – B-4-2	O	IO	O	O	O	O	IO	O	IO	**IO**
B-5-3.5 – C-5-3.5	O	O	IO	IO	IO	IO	IO	IO	IO	**IO**
B-5-4 – C-5-4	IO	O	O	IO	IO	IO	LS	IO	IO	**LS**
C-4-2 – C-5-2	O	O	O	O	O	O	IO	O	O	**IO**
C-4-3 – C-5-3	O	O	O	O	O	O	IO	O	O	**IO**
D-1-1 – F-1-1	IO	O	O	O	IO	O	O	O	IO	**IO**
D-1-2 – F-1-2	IO	O	O	IO	IO	O	IO	O	LS	**LS**
D-1-3 – F-1-3	IO	O	O	IO	IO	O	IO	O	LS	**IO**
D-1-4 – F-1-4	IO	O	O	IO	IO	O	IO	O	LS	**IO**
D-3-1 – F-3-1	IO	O	O	O	O	O	O	O	O	**IO**
D-3-2 – F-3-2	IO	O	O	O	O	O	O	O	IO	**IO**
E-3-3 – E-4-3	O	IO	O	O	O	O	O	O	O	**IO**
E-3-4 – E-4-4	O	IO	O	O	O	O	O	O	O	**IO**
F-1-1 – F-2-1	O	IO	O	O	IO	O	IO	O	IO	**IO**
F-1-2 – F-2-2	O	IO	O	IO	IO	IO	IO	IO	IO	**IO**
F-1-3 – F-2-3	O	IO	O	IO	IO	IO	IO	IO	IO	**IO**
F-1-4 – F-2-4	O	IO	O	O	IO	IO	IO	IO	IO	**IO**

Column performance:

	Pushover		Nonlinear Direct Integration Time History							
Column	X-direction	Y-direction	Iwate	Northridge	Cape Mendocino	Chuetsu	Loma Prieta	Chi-chi	Smart1	Least favorable
A-3-1	LS	O	O	O	O	O	O	O	O	LS
B-4-2	O	O	IO	IO	IO	O	IO	IO	IO	IO
B-4-4	O	O	O	IO	IO	IO	IO	IO	IO	IO
B-5-0.5	O	LS	O	O	O	O	IO	O	IO	LS
B-5-1	O	O	O	O	O	O	IO	O	IO	IO
B-5-1.5	O	LS	O	O	O	O	IO	O	IO	LS
B-5-2	O	O	O	O	O	O	IO	O	IO	IO
B-5-2.5	O	O	O	O	O	O	IO	O	IO	IO
B-5-3	O	O	O	O	O	O	IO	O	IO	IO
B-5-3.5	O	O	O	O	O	O	IO	O	IO	IO
B-5-4	O	O	O	IO	O	O	IO	O	NC	NC
B-5-5	O	O	IO	O	O	O	IO	O	NC	NC
C-1-4	IO	O	O	O	O	O	O	O	IO	IO
C-2-4	O	IO	O	O	O	O	IO	O	IO	IO
C-3-1	IO	O	O	O	O	O	O	O	O	IO
C-4-2	O	O	O	IO	O	IO	IO	IO	IO	IO
C-4-4	O	O	O	IO	IO	IO	IO	IO	IO	IO
C-5-0.5	O	LS	O	O	O	O	IO	O	IO	LS
C-5-1	O	O	O	O	O	O	IO	O	IO	IO
C-5-1.5	O	O	O	O	O	O	IO	O	IO	IO
C-5-2	O	O	O	O	O	O	IO	O	IO	IO

C-5-2.5	O	O	O	O	O	O	IO	O	IO	**IO**
C-5-3	O	O	O	O	O	O	IO	O	IO	**IO**
C-5-3.5	O	O	O	O	O	O	IO	O	IO	**IO**
C-5-4	O	O	O	O	O	O	IO	O	IO	**IO**
C-5-5	O	O	IO	O	IO	IO	NC	IO	NC	**NC**
D-1-1	O	O	O	O	O	O	IO	O	IO	**O**
D-1-2	IO	O	O	IO	O	O	IO	O	IO	**IO**
D-1-3	IO	O	O	IO	IO	O	IO	O	IO	**IO**
D-1-4	IO	IO	IO	IO	IO	IO	IO	IO	IO	**IO**
D-2-2	O	LS	O	O	O	O	O	O	IO	**LS**
D-2-3	LS	LS	O	O	O	O	IO	O	IO	**LS**
D-2-4	IO	LS	O	O	O	O	IO	O	IO	**LS**
D-3-2	LS	O	IO	O	O	O	IO	O	IO	**LS**
D-3-3	LS	O	IO	O	O	O	IO	O	IO	**LS**
D-3-4	IO	O	IO	IO	IO	O	IO	O	IO	**IO**
D-4-4	O	IO	O	O	O	O	IO	O	IO	**IO**
E-4-4	O	IO	O	O	O	O	IO	O	IO	**IO**
F-1-1	LS	LS	O	O	O	O	IO	O	IO	**LS**
F-2-1	O	IO	O	O	O	O	IO	O	IO	**IO**
F-2-2	O	LS	O	IO	IO	IO	IO	IO	IO	**LS**
F-2-3	O	LS	O	O	IO	IO	IO	IO	IO	**LS**
F-2-4	O	LS	IO	IO	IO	IO	IO	IO	IO	**LS**
F-3-1	IO	O	O	O	O	O	O	O	O	**IO**